TECHNICAL NOTES

NATIONAL ADVISORY COMMITTEE FOR AERONAUTICS

No. 894

THE EXACT SOLUTION OF SHEAR-LAG PROBLEMS IN FLAT PANELS AND BOX BEAMS ASSUMED RIGID IN THE TRANSVERSE DIRECTION

By Francis B. Hildebrand
Massachusetts Institute of Technology

Washington
June 1943

NATIONAL ADVISORY COMMITTEE FOR AERONAUTICS

TECHNICAL NOTE NO. 894

THE EXACT SOLUTION OF SHEAR-LAG PROBLEMS IN FLAT PANELS AND BOX BEAMS ASSUMED RIGID IN THE TRANSVERSE DIRECTION

By Francis B. Hildebrand

SUMMARY

A mathematical procedure is herein developed for obtaining exact solutions of shear-lag problems in flat panels and box beams: the method is based on the assumption that the amount of stretching of the sheets in the direction perpendicular to the direction of essential normal stresses is negligible. Explicit solutions, including the treatment of cut-outs, are given for several cases and numerical results are presented in graphic and tabular form. The general theory is presented in a form from which further solutions can be readily obtained. The extension of the theory to cover certain cases of non-uniform cross section is indicated. Although the solutions are obtained in terms of infinite series, the present developments differ from those previously given in that, in practical cases, the series usually converge so rapidly that sufficient accuracy is afforded by a small number of terms. Comparisons are made in several cases between the present results and the corresponding solutions obtained by approximate procedures devised by Reissner and by Kuhn and Chiarito.

INTRODUCTION

The theory given in this paper is to be considered as a refinement of approximate methods devised by Reissner in reference 1 and by Kuhn and Chiarito in reference 2 for the analysis of shear-lag problems and may thus serve as a check on the accuracy of those methods. Such problems concern the effect of shear deformation on the state of stress in thin sheets which are analyzed in the elementary theory of the strength of materials without regard to shear deformability. Examples with which this paper is concerned are: (1) the introduction of concentrated forces into flat

sheets by means of stiffeners, where the forces act in the plane of the sheet, and (2) the distribution of stress in the cover sheets of rectangular box beams subjected to bending loads: that is, in particular, the determination of the effective width of such cover sheets.

One of the assumptions made in the above-mentioned theories, which is retained in the following developments, is that stretching of the sheets in the direction perpendicular to the direction of essential normal stresses can be neglected. This assumption, which is made plausible by elastic energy considerations (reference 1), is essential for the application of the mathematical methods employed in most of this paper.

No further simplifying assumption, however, is made here and the problems considered are then solved in an exact manner, as boundary-value problems in the theory of plane stress. This work is in contrast with that of Reissner, who obtains approximate solutions in substantially simpler form of a more extensive class of problems than the problems considered in the present analysis by an application of the principle of least work, and with that of Kuhn and Chiarito, who further simplify the problems by incorporating the resistivity of the sheets in the direction of the essential normal stresses into the effects of stiffeners in this direction by increasing the actual areas of the stiffeners by an amount representing an estimated effective sheet width. Kuhn and Chiarito then have to deal with sheets that are rigid in the transverse direction and offer no resistance in the longitudinal direction but possess finite shear rigidity.

The following investigation will include the analysis of beams with and without cut-outs, and, in this connection, it is remarked that while the way was known in which series solutions could be obtained for certain problems concerning beams without cut-outs, in terms of assumed trigonometric developments in the spanwise direction (references 3 and 4), a new type of series development is obtained herein which makes possible the treatment of both types of problem in an analogous way and, in addition, possesses the advantage of being much more adaptable to computation than the known type of series solution for the problem of the beam without cut-out.

This investigation, conducted at the Massachusetts Institute of Technology, was sponsored by, and conducted with, financial assistance from the National Advisory

Committee for Aeronautics. Thanks are due to Professor E. Reissner of the Massachusetts Institute of Technology for valuable suggestions and criticisms.

SYMBOLS

l	length of panel or beam
w	one-half width of panel or beam
x	spanwise distance $\left(x_1 = \sqrt{\frac{G}{E}}\, x\right)$
A	cross-sectional area
y	transverse distance
F	externally applied concentrated force
t	sheet thickness
h	height of box beam
I_w	principal moment of inertia of cross section of two side webs, including corner flanges
σ	normal stress
τ	shear stress
ϵ	normal strain
u	displacement component in x direction
v	displacement component in y direction
E	Young's modulus $(E = E_x)$
ν	Poisson's ratio
γ	shear strain
G	shear modulus
H	stress function
c	constant

H^* modified stress function $[H + Gv(x)]$

α ratio of flange and sheet areas $\left(\frac{A_e}{tw}\right)$

$\alpha_m = \frac{A_m}{2tw}$

n positive integer

λ auxiliary parameter

ξ dimensionless span coordinate $\left(\sqrt{\frac{G}{E}}\frac{\pi x}{w}\right)$

η dimensionless transverse coordinate $\left(\frac{\pi y}{w}\right)$

β ratio of moments of inertia of web and sheet about transverse principal axis of beam (I_w/I_s)

I_s moment of inertia of cross section of two cover sheets about transverse principal beam axis (twh^2)

μ auxiliary parameter $\left(\sqrt{\frac{G}{E}}\frac{l}{w}\lambda\right)$

p_o uniformly distributed load

σ_o maximum elementary spanwise normal stress $[\sigma_b(l)]$

δ angle between x-axis and normal to edge of sheet

$$\left[\delta_n = \frac{(2n-1)\pi}{2}\sqrt{\frac{E}{G}}\frac{w}{l}\right]$$

I total principal moment of inertia of beam section $(I_s + I_w + \frac{1}{2}A_m h^2)$

p particular solution of differential equation

k constant $\left(\sqrt{\frac{G}{E}}\right)$

M moment of applied bending loads

P particular solution of differential equation

Φ stress function

X, Y separation functions in solution of differential equation

K dimensionless constant occurring in Kuhn theory (with subscript R, occurring in Reissner theory)

κ auxiliary parameter

Subscripts:

e	edge
m	middle
eff	effective
x	spanwise
y	transverse
n	corresponding to n
b	bending
a	average

DEFINITION OF THE PROBLEMS

The first problem treated concerns the stress distribution in a flat panel of length l and width $2w$ loaded at one end ($x = 0$) by concentrated axial forces introduced into flanges of cross-sectional area A_e attached to the longitudinal edges ($y = \pm w$) and by a concentrated axial force introduced into a longitudinal stiffener of area A_m along the axis of symmetry ($y = 0$). (See fig. 1.) Suitable conditions are to be prescribed along the edge $x = l$. For example, (1) the panel may be completely clamped along this edge, (2) the flanges and the longitudinal may be fixed at $x = l$ with the sheet subject to displacement, or (3) the flanges may be fixed while both the sheet and the stiffener are not attached to a support. It will be convenient to consider separately loadings that are symmetrical and antisymmetrical with respect to the longitudinal axis of the panel (fig. 1) and to obtain solutions for arbitrary loadings by superposition.

The second problem deals with the stress distribution in the cover sheets of a doubly symmetrical box beam, supported in a prescribed manner at one end ($x = l$) and unsupported at the other end ($x = 0$) and subjected to a given distribution of bending loads applied symmetrically at the sheet-web junctions (fig. 2). There may be flanges at the junctions of the cover sheets and side webs and a longitudinal stiffener along the center line ($y = 0$) of the cover sheets. The procedure will be outlined for a rather general class of end-support conditions, while explicit solutions will be obtained for the cases when (1) the structure is completely clamped along the edge at $x = l$ (fig. 2(a)), and (2) the side webs are fixed at $x = l$,

but the cover sheets are not attached to a support (fig. 2(b)), as would be the case at the outboard edge of a cut-out.

Finally, the stress distribution is determined in an infinite half-sheet rigid in the direction parallel to its straight-edge and loaded by a concentrated force, in the plane of the sheet and normal to the straight-edge, introduced into a stiffener attached to the sheet in the direction of the applied force (fig. 3(a)). While the solution in this case is probably of slight practical interest in itself, it was felt that it might serve as an indication of the limiting behavior of solutions to other related problems.

BASIC EQUATIONS IN THE THEORY OF PLANE STRESS FOR AN ORTHOTROPIC MATERIAL RIGID IN ONE DIRECTION

The following equations must be satisfied for a state of plane stress in an orthotropic medium of uniform thickness:

(a) The equilibrium conditions for an element of the sheet

$$\frac{\partial \sigma_x}{\partial x} + \frac{\partial \tau}{\partial y} = 0 \tag{1a}$$

$$\frac{\partial \tau}{\partial x} + \frac{\partial \sigma_y}{\partial y} = 0 \tag{1b}$$

(b) The stress-strain relationships

$$\epsilon_x = \frac{\partial u}{\partial x} = \frac{1}{E_x}(\sigma_x - \nu_x \sigma_y) \tag{2a}$$

$$\epsilon_y = \frac{\partial v}{\partial y} = \frac{1}{E_y}(\sigma_y - \nu_y \sigma_x) \tag{2b}$$

$$\gamma = \frac{\partial u}{\partial y} + \frac{\partial v}{\partial x} = \frac{1}{G}\tau \tag{2c}$$

For a medium rigid in the y-direction

$$\left.\begin{aligned} E_y &= \infty \\ \nu_x &= 0 \end{aligned}\right\} \tag{3}$$

and, from equation (2b), it then follows that

$$\left.\begin{aligned} \frac{\partial v}{\partial y} &= 0 \\ v &= v(x) \end{aligned}\right\} \tag{4}$$

If E is written for E_x, equations (2a) and (2c) take the form

$$E \frac{\partial u}{\partial x} = \sigma_x \tag{5a}$$

$$G \frac{\partial u}{\partial y} = \tau - G\, v'(x) \tag{5b}$$

From equation (5) it follows by differentiation that

$$\frac{1}{E} \frac{\partial \sigma_x}{\partial y} - \frac{1}{G} \frac{\partial \tau}{\partial x} = -v''(x) \tag{6}$$

If the equilibrium condition of equation (1a) is satisfied by means of a stress function H, in terms of which

$$\sigma_x = \frac{\partial H}{\partial y} \tag{7a}$$

$$\tau = -\frac{\partial H}{\partial x} \tag{7b}$$

it follows from equation (6) that H must satisfy the equation

$$\frac{\partial^2 H}{\partial x^2} + \frac{G}{E} \frac{\partial^2 H}{\partial y^2} = -G\, v''(x) \tag{8}$$

The solution of any plane stress problem in such an orthotropic medium is thus reduced to the formulation of boundary conditions relative to the function H and to the solution of the differential equation (8) subject to those boundary conditions.

With H determined, the stress σ_y is found from equation (1b) as follows:

$$\frac{\partial \sigma_y}{\partial y} = -\frac{\partial \tau}{\partial x} = \frac{\partial^2 H}{\partial x^2} = \frac{G}{E}\frac{\partial^2 H}{\partial y^2} - G\,v''(x)$$

$$\sigma_y = -\frac{G}{E}\frac{\partial H}{\partial y} - G\,y\,v''(x) + f(x) \tag{9}$$

while from equation (5) there follows for the displacement component u,

$$u = \frac{1}{E}\int \frac{\partial H}{\partial y}\,dx + c \tag{10}$$

An interesting relationship between u and H can be established by means of complex variables. If a new variable

$$x_1 = \sqrt{\frac{G}{E}}\,x \tag{11}$$

is introduced, equation (8) transforms into

$$\frac{\partial^2 H}{\partial x_1^2} + \frac{\partial^2 H}{\partial y^2} = -G\frac{d^2 v}{dx_1^2} \tag{12}$$

and equations (5) and (7) give

$$\left.\begin{aligned} \frac{\partial H}{\partial y} &= \sqrt{EG}\,\frac{\partial u}{\partial x_1} \\ \frac{\partial H}{\partial x_1} + G\frac{dv}{dx_1} &= -\sqrt{EG}\,\frac{\partial u}{\partial y} \end{aligned}\right\} \tag{13}$$

If the function

$$H^* = H + G\,v(x) \tag{14}$$

is defined, equations (12) and (13) become

$$\frac{\partial^2 H^*}{\partial x_1^2} + \frac{\partial^2 H^*}{\partial y^2} = 0 \tag{15}$$

$$\left.\begin{aligned} \frac{\partial H^*}{\partial y} &= \sqrt{EG}\,\frac{\partial u}{\partial x_1} \\ \frac{\partial H^*}{\partial x_1} &= -\sqrt{EG}\,\frac{\partial u}{\partial y} \end{aligned}\right\} \tag{16}$$

From equations (15) and (16), it may be concluded that

$$H^* + i\sqrt{EG}\,u = F(x_1 + iy) \tag{17}$$

that is, $H + Gv(x)$ and $\sqrt{EG}\,u$ are the real and the imaginary parts, respectively, of a function of the complex variable $\sqrt{\frac{G}{E}}\,x + iy$.

SUMMARY AND DISCUSSION OF EXPLICIT SOLUTIONS

In this section are presented explicit solutions of certain problems, the mathematical derivations of which are given in the two sections that follow. Solutions of a large class of related problems can be obtained directly from the analysis included in those sections.

Although the results with regard to panels are presented in this section only for the limiting case in which $l = \infty$, the corresponding solutions for panels clamped at the end $x = l$ can be obtained in all cases by replacing $e^{-\sqrt{\frac{G}{E}}\lambda_n \frac{x}{w}}$ by $\cosh\sqrt{\frac{G}{E}}\lambda_n \frac{l-x}{w} \Big/ \cosh\sqrt{\frac{E}{G}}\lambda_n \frac{l}{w}$ in the given expressions for the stress functions.

Unless otherwise specified, the ratio G/E is assigned the value $3/8$ in the numerical calculations of this paper. In case the loading is such that the sheet becomes wrinkled, a smaller value of the shear modulus must be taken. The nature of the solutions for large values of the span-width ratio is such, however, that a change in the value of G merely involves magnification of the $\frac{x}{w}$ scale in the ratio $\sqrt{\frac{G}{G_{eff}}}$, together with a

multiplication of the shear stress values by the reciprocal ratio.

Stresses in a Long Symmetrically Loaded Flanged Panel without Central Stiffener

[Panel 1]

A long panel of width $2w$ is clamped along one end ($x = \infty$) and is loaded at the end $x = 0$ by axial forces F acting on flanges of equal cross-sectional area A attached to the edges ($y = \pm w$) of the sheet (fig. 4(a)). The stress function is determined in the form

$$H = \frac{F}{t}\left\{\frac{1}{\alpha + 1}\frac{y}{w} + 2\sum_{n=1}^{\infty}\frac{\cos\lambda_n \sin\lambda_n\frac{y}{w}}{\lambda_n(1 + \alpha\cos^2\lambda_n)}\, e^{-\sqrt{\frac{G}{E}}\lambda_n\frac{x}{w}}\right\} \quad (18)$$

where α represents the ratio of the flange and sheet areas and is given as

$$\alpha = \frac{A}{tw} \quad (19)$$

and the parameters λ_n are the positive solutions of the equation

$$\tan\lambda_n + \alpha\lambda_n = 0 \quad (20)$$

the first 15 of which are listed for $\alpha = 1$ and $\alpha = 5$ in table 1. The expressions for the spanwise normal stress $\sigma_x = \frac{\partial H}{\partial y}$ and the shear stress $\tau = -\frac{\partial H}{\partial x}$ follow in the form

$$\sigma_x = \frac{F}{tw}\left\{\frac{1}{\alpha + 1} + 2\sum_{n=1}^{\infty}\frac{\cos\lambda_n \cos\lambda_n\frac{y}{w}}{1 + \alpha\cos^2\lambda_n}\, e^{-\sqrt{\frac{G}{E}}\lambda_n\frac{x}{w}}\right\} \quad (21)$$

$$\tau = 2\sqrt{\frac{G}{E}}\frac{F}{tw}\sum_{n=1}^{\infty}\frac{\cos\lambda_n \sin\lambda_n\frac{y}{w}}{1 + \alpha\cos^2\lambda_n}\, e^{-\sqrt{\frac{G}{E}}\lambda_n\frac{x}{w}} \quad (22)$$

In the case of an unflanged panel, for which $\alpha = 0$, the series become Fourier series and can be summed in closed form, giving

$$H = \frac{2F}{\pi t} \tan^{-1}\left(\tanh\frac{\xi}{2} \tan\frac{\eta}{2}\right) \qquad (23)$$

$$\sigma_x = \frac{F}{tw} \frac{\sinh\xi}{\cosh\xi + \cos\eta}$$

$$\tau = -\frac{F}{tw}\sqrt{\frac{G}{E}} \frac{\sin\eta}{\cosh\xi + \cos\eta}$$

where

$$\xi = \sqrt{\frac{G}{E}}\frac{\pi x}{w}$$

and

$$\eta = \frac{\pi y}{w}$$

The flange normal and shear stresses, as well as the normal stresses along the center line of the panel, for the cases $\alpha = 1$ and $\alpha = 5$, are plotted in figure 5(a), while the normal stress distributions along an edge and along the center line for an unflanged panel ($\alpha = 0$) are given in figure 5(b). (See table 2.) It is seen that for $\alpha = 1$ the shear-lag function $\sigma_x(x,w) - \sigma_x(x,o)$ becomes negligible at a distance from the end section equal to about $2\frac{1}{2}$ times the width of the panel ($x = 5w$), while if $\alpha = 5$ appreciable shear lag is present up to a distance of about 3 times the width of the panel. If no flanges are present, the normal stress becomes infinite at the point of load application; at a distance of about $1\frac{1}{2}$ times the width of the panel, however, the spanwise normal stress becomes practically constant over the cross section.

Stresses in a Long Antisymmetrically Loaded Flanged Panel without Central Stiffeners

[Panel 2]

If equal and opposite forces $\pm F$ are acting on the flanges of a symmetrical panel (fig. 4(b)), the stresses

are determined from the stress function[1]

$$H = \frac{F}{t}\left\{\frac{3}{2(3\alpha+1)}\left[\left(\frac{y}{w}\right)^2 - \frac{1}{3}\right] - 2\sum_{n=1}^{\infty}\frac{\sin\lambda_n\left(\cos\lambda_n\frac{y}{w} - \frac{\sin\lambda_n}{\lambda_n}\right)}{\lambda_n\left[1+\alpha\sin^2\lambda_n - \left(\frac{\sin\lambda_n}{\lambda_n}\right)^2\right]}e^{-\sqrt{\frac{G}{E}}\lambda_n\frac{x}{w}}\right\} \quad (24)$$

where again $\alpha = \frac{A}{tw}$ and the parameters λ_n satisfy the equation

$$\tan\lambda_n = \frac{\lambda_n}{\alpha\lambda_n^2 + 1} \quad (25)$$

The first 15 of these parameters are listed for $\alpha = 0$, $\alpha = 1$, and $\alpha = 5$ in table 3.

The expression for the spanwise normal and shear stresses in the panel follow from equation (24) by differentiation,

$$\sigma_x = \frac{F}{tw}\left\{\frac{3}{2\alpha+1}\frac{y}{w} + 2\sum_{n=1}^{\infty}\frac{\sin\lambda_n\sin\lambda_n\frac{y}{w}}{1+\alpha\sin^2\lambda_n - \left(\frac{\sin\lambda_n}{\lambda_n}\right)^2}e^{-\sqrt{\frac{G}{E}}\lambda_n\frac{x}{w}}\right\} \quad (26)$$

$$\tau = -2\sqrt{\frac{G}{E}}\frac{F}{tw}\sum_{n=1}^{\infty}\frac{\sin\lambda_n\left(\cos\lambda_n\frac{y}{w} - \frac{\sin\lambda_n}{\lambda_n}\right)}{1+\alpha\sin^2\lambda_n - \left(\frac{\sin\lambda_n}{\lambda_n}\right)^2}e^{-\sqrt{\frac{G}{E}}\lambda_n\frac{x}{w}} \quad (27)$$

If no flanges are present, the expression for the stress function reduces to

$$H = \frac{F}{t}\left\{\frac{3}{2}\left[\left(\frac{y}{w}\right)^2 - \frac{1}{3}\right] - 2\sum_{n=1}^{\infty}\frac{\cos\lambda_n\frac{y}{w} - \cos\lambda_n}{\lambda_n\sin\lambda_n}e^{-\sqrt{\frac{G}{E}}\lambda_n\frac{x}{w}}\right\} \quad (28)$$

[1]The irrelevant added constants present in equation (24) and in the expressions for certain of the other stress functions in the following problems are due to the convention that $H(o,o) = 0$.

where

$$\tan \lambda_n = \lambda_n \qquad (29)$$

The flange normal stress, as well as the shear stress at the flange and along the center line, is plotted for $\alpha = 1$ and $\alpha = 5$ in figure 6(a), while for an unflanged panel the normal stress along the edge and the shear stress at the center line are shown in figure 6(b). (See table 4.) It is seen that in all cases the normal stresses closely approach their limiting values at a distance from the end which is less than the width of the panel.

Stresses in a Long Flanged Panel without Central Stiffener Subjected to Asymmetrical Concentrated Loadings

If unequal loads are acting on the flanges of a symmetrical panel, the corresponding stress function can be obtained by superimposing proper multiples of the symmetrical and antisymmetrical stress functions (18) and (24).

For example, if, as in panel 3, a force F is acting upon the flange along the edge $y = w$, the other flange being unloaded (fig. 4(c)), the relevant stress function is given by one-half the sum of the functions (18) and (24). The corresponding stress distribution is indicated for $\alpha = 1$ in figure 7.

Stesses in a Long Symmetrical Flanged Panel with Central Stiffener

[Panels 4 and 5]

If arbitrary concentrated loads are introduced into the two flanges and into the central stiffener of a long symmetrical panel, the loading may be considered as the superposition of two loadings: (1) equal loads F_e acting on the two flanges and a load F_m acting on the stiffener, and (2) equal and opposite loads $\pm F$ introduced into the flanges, no load acting on the stiffener. In the second case (fig. 4(e)), the stiffener is ineffective and the stress distribution is obtained from equations (24) to (27). That the stiffener is ineffective follows from the convention that the stiffener is concentrated along a line. If the width of the stiffener is small in compari-

son with the width of the panel, the effects actually present would in any case be negligible.

In the case of a symmetrical loading (fig. 4(d)) consideration of the shearing action along the two edges of the central stiffener indicates that the shear stress is discontinuous at the stiffener. As a result, it is found that the stress function has different analytical expressions in the two sections of the panel. Because of the symmetry, however, it is sufficient to determine the state of stress in one-half the panel. In the positive half of the panel $(o < y \leq w)$ the stress function is obtained in the form

$$H = \frac{1}{t(\alpha + \alpha_m + 1)} \left\{ \frac{F_m}{2}\left(\frac{y}{w} - \alpha - 1\right) + F_e\left(\frac{y}{w} + \alpha_m\right) - \sum_{n=1}^{\infty} \kappa_n \gamma_n^2 \left(\frac{1}{\lambda_n} \sin \lambda_n \frac{y}{w} + \alpha_m \cos \lambda_n \frac{y}{w}\right) e^{-\sqrt{\frac{G}{E}}\lambda_n \frac{x}{w}} \right\} \quad (30)$$

where the constants are defined as

$$\left.\begin{aligned} \alpha &= \frac{A_e}{tw} \\ \alpha_m &= \frac{A_m}{2tw} \end{aligned}\right\} \quad (31)$$

$$\gamma_n^2 = \left[\int_o^w \left\{ \frac{1}{\lambda_n} \sin \lambda_n \frac{y}{w} + \alpha_m \cos \lambda_n \frac{y}{w} \right\}^2 dy \right]^{-1} \quad (32)$$

$$\kappa_n = \int_o^w \left\{ \frac{F_m}{2}\left(\frac{y}{w} - \alpha - 1\right) + F_e\left(\frac{y}{w} + \alpha_m\right) \right\} \left\{ \frac{1}{\lambda_n} \sin \lambda_n \frac{y}{w} + \alpha_m \cos \lambda_n \frac{y}{w} \right\} dy \quad (33)$$

and the parameters λ_n are the positive solutions of the equation

$$\alpha\, \alpha_m\, \lambda_n \tan \lambda_n - \frac{\tan \lambda_n}{\lambda_n} = \alpha + \alpha_m \quad (34)$$

The stresses σ_x and τ follow from equation (30) by differentiation in accordance with equation (7). Although the expression in equation (30) is somewhat complicated, it is found that, except in the immediate neighborhood of the end $x = 0$ where the stresses are already known, the presence of the exponential factor in the series brings about such rapid convergence in practical cases that very few terms of the series are needed for ordinary accuracy. In a later section the stress distribution associated with equation (30) is evaluated numerically for the case of an actual test panel (panel 10) considered previously in reference 3.

Panels 6 to 9 represent a special case in which $A_m = 2 A_e$. If the area of the central stiffener is just twice the area of each flange, the expressions involved in the solution are considerably simplified. In this case a general symmetrical loading can be treated by superimposing two basic loadings: (1) equal loads F acting on the flanges and a load $2F$ acting on the stiffener (panel 6), and (2) equal loads F acting on the flanges and a load $-2F$ acting on the stiffener (panel 7). Again, because of symmetry, it is sufficient in each case to consider the positive half of the panel.

For panel 6 (fig. 4(f)), each half of the panel behaves in the same way as panel 1. The stress function is obtained by replacing w by $\frac{w}{2}$ and y by $\left(2\frac{y}{w} - 1\right)$ in the expression for the stress function for the complete panel, so that, for $0 < y \leq w$,

$$H = \frac{F}{t}\left\{\frac{1}{2\alpha+1}\left(2\frac{y}{w} - 1\right) + 2\sum_{n=1}^{\infty} \frac{\cos \lambda_n \sin \lambda_n\left(2\frac{y}{w} - 1\right)}{\lambda_n(1 + 2\alpha \cos^2 \lambda_n)} e^{-2\sqrt{\frac{G}{E}}\lambda_n \frac{x}{w}}\right\} \quad (35)$$

$$\sigma_x = \frac{F}{tw}\left\{\frac{2}{2\alpha+1} + 4\sum_{n=1}^{\infty} \frac{\cos \lambda_n \cos \lambda_n\left(2\frac{y}{w} - 1\right)}{1 + 2\alpha \cos^2 \lambda_n} e^{-2\sqrt{\frac{G}{E}}\lambda_n \frac{x}{w}}\right\} \quad (36)$$

and

$$\tau = 4\sqrt{\frac{G}{E}}\frac{F}{tw}\sum_{n=1}^{\infty} \frac{\cos \lambda_n \sin \lambda_n\left(2\frac{y}{w} - 1\right)}{1 + 2\alpha \cos^2 \lambda_n} e^{-2\sqrt{\frac{G}{E}}\lambda_n \frac{x}{w}} \quad (37)$$

where $\alpha = \frac{A_e}{tw}$ and the constants λ_n are now the positive solutions of the equation

$$\tan \lambda_n + 2\alpha \lambda_n = 0 \tag{38}$$

The stress function corresponding to panel 7 (fig. 4(g)) is obtained by using $F_e = -\frac{F_m}{2} = F$ and $A_m = 2 A_e$ in equation (30). After some simplification there follows, for $0 < y \leq w$,

$$H = \frac{F}{t}\left\{1 - 2 \sum_{n=1}^{\infty} \frac{\sin \lambda_n \cos \lambda_n\left(2 \frac{y}{w} - 1\right)}{\lambda_n(1 + 2\alpha \sin^2 \lambda_n)} e^{-2\sqrt{\frac{G}{E}} \lambda_n \frac{x}{w}}\right\} \tag{39}$$

$$\sigma_x = 4 \frac{F}{tw} \sum_{n=1}^{\infty} \frac{\sin \lambda_n \sin \lambda_n \left(2 \frac{y}{w} - 1\right)}{1 + 2\alpha \sin^2 \lambda_n} e^{-2\sqrt{\frac{G}{E}} \lambda_n \frac{x}{w}} \tag{40}$$

and

$$\tau = -4\sqrt{\frac{G}{E}} \frac{F}{tw} \sum_{n=1}^{\infty} \frac{\sin \lambda_n \cos \lambda_n \left(2 \frac{y}{w} - 1\right)}{1 + 2\alpha \sin^2 \lambda_n} e^{-2\sqrt{\frac{G}{E}} \lambda_n \frac{x}{w}} \tag{41}$$

where

$$\alpha = \frac{A_e}{tw}$$

and

$$\cot \lambda_n - 2\alpha \lambda_n = 0 \tag{42}$$

The first 15 of the solutions of equation (42), for $\alpha = \frac{1}{2}$ and $\alpha = \frac{5}{2}$, are given in table 5.

The spanwise normal stresses and the shear stresses at a flange and at a quarter section $\left(y = \frac{w}{2}\right)$ are plotted for panel 6 in figure 8(a) and in table 6, for $\alpha = \frac{1}{2}$ and $\alpha = \frac{5}{2}$, while in figure 8(b) and in table 7 are presented curves representing the flange normal and shear stresses for panel 7. It is to be remarked that the stress σ_x is symmetrical about the center line ($y = 0$) in both cases, symmetrical about the quarter section $\left(y = \frac{w}{2}\right)$ for panel 6 and antisymmetrical about that line for panel 7.

By combining suitable multiples of the stress functions given in equations (24), (36), and (39), solutions

may be obtained for an arbitrary set of three concentrated loads introduced into the flanges and the stiffener for the case in which $A_m = 2A_e$. In particular, if equal loads F are acting on the flanges, while no load acts on the stiffener (panel 8, fig. 4(h)), the relevant stress function is given by one-half the sum of the functions given in equations (36) and (39). The normal stresses in a flange, in the stiffener, and at a quarter section, and the flange and stiffener shear stresses are presented, for $\alpha = \frac{1}{2}$ and $\alpha = \frac{5}{2}$, in figures 9(a) and 9(b), respectively, and in table 8. If a load 2F is acting on the stiffener, while no loads are introduced into the flanges (fig. 4(i)), the stress function is given by one-half the difference between the functions of equations (36) and (39). In the present case, however, it is seen that the expressions for the flange and stiffener stresses, respectively, in panel 9, are obtained by interchanging the corresponding expressions for panel 8.

For the purpose of comparison there are included in figure 10 curves representing the normal stresses along the longitudinal edges of unflanged panels subjected to (1) equal concentrated axial forces F acting at the corners of the free edge and a force 2F acting at the center of that edge, (2) equal forces F acting at the corners and a force −2F at the center, and (3) equal and opposite forces ±F acting at the corners. (See table 9.)

Panels 6 and 7 can be considered sections of a semi-infinite sheet stiffened by a series of equally spaced longitudinals of area $2A_e$ and constant separation w. where, for panel 6, equal axial loads 2F are acting on successive stiffeners, while, for panel 7, successive loadings are of magnitude 2F but are alternately compressive and tensile. By superposition the stress distribution is obtained for an arbitrary pair of concentrated loads repeated periodically along the edge of the sheet. For example, the stresses given for panel 8 (or panel 9) can be interpreted as the stresses in a section of a sheet of this type where alternate stiffeners are not loaded. Similar statements apply to the curves presented in figure 10.

Stresses in a Doubly Symmetrical Rectangular Box Beam Clamped at One End and Subjected to Concentrated Bending Loads Applied at the Free End

The rectangular box beam shown in figure 2(a) is subjected to concentrated bending loads applied at the free end. It is here supposed that no longitudinal center stiffener is present, although the analysis of a later section includes also the theory in the more general case.

The stress function is determined in the form

$$H = w\sigma_o\left\{\frac{x}{l}\,\frac{y}{w} + 2(\beta+1)\sqrt{\frac{E}{G}}\,\frac{w}{l}\sum_{n=1}^{\infty}\frac{\cos\lambda_n \sin\lambda_n \frac{y}{w} \quad \sinh\mu_n \frac{x}{l}}{\lambda_n^2(1+\beta\cos^2\lambda_n) \quad \cosh\mu_n}\right\} \tag{43}$$

where σ_o is the maximum elementary spanwise normal stress,

$$\sigma_o = \frac{M(l)}{I}\,\frac{h}{2} = \frac{Flh}{2I} \tag{44}$$

β is a dimensionless parameter representing the ratio of the moments of inertia of the web and the sheet about the transverse principal axis of the beam and is given as

$$\beta = \frac{I_w}{I_s} = \frac{A_r}{A_s} \tag{45}$$

the parameters λ_n are the positive solutions of the equation

$$\tan\lambda_n + \beta\lambda_n = 0 \tag{46}$$

which is of the same form as equation (20), and μ_n is defined by the relationship

$$\mu_n = \sqrt{\frac{G}{E}}\,\frac{l}{w}\,\lambda_n \tag{47}$$

The stresses σ_x and τ follow from equation (43) by differentiation

$$\sigma_x = \sigma_o\left\{\frac{x}{l} + 2(\beta+1)\sqrt{\frac{E}{G}}\,\frac{w}{l}\sum_{n=1}^{\infty}\frac{\cos\lambda_n\cos\lambda_n\frac{y}{w}}{\lambda_n(1+\beta\cos^2\lambda_n)}\,\frac{\sinh\mu_n\frac{x}{l}}{\cosh\mu_n}\right\} \quad (48)$$

$$\tau = -\sigma_o\,\frac{w}{l}\left\{\frac{y}{w} + 2(\beta+1)\sum_{n=1}^{\infty}\frac{\cos\lambda_n\sin\lambda_n\frac{y}{w}}{\lambda_n(1+\beta\cos^2\lambda_n)}\,\frac{\cosh\mu_n\frac{x}{l}}{\cosh\mu_n}\right\} \quad (49)$$

It is seen that the series parts of equations (48) and (49) are of the nature of corrections to the linear stresses predicted by the elementary theory. For span-width ratios in the practical range the parameters μ_n are of such a magnitude that, except in the immediate neighborhood of the fixed end ($x = l$), sufficient accuracy is obtained by retaining only a small number of the terms in the series.

An alternative expansion for the stress function can be obtained by conventional methods, which are somewhat simpler than those employed here, in the form

$$H = \frac{8w}{\pi^2}\,\frac{I}{I_s}\,\sigma_o\sum_{n=1}^{\infty}\frac{(-1)^{n+1}}{(2n-1)^2}\,\frac{\sinh\delta_n\frac{y}{w}}{\sinh\delta_n + \beta\,\delta_n\cosh\delta_n}\sin\frac{(2n-1)\pi}{2}\,\frac{x}{l} \quad (50)$$

where

$$\left.\begin{aligned}\delta_n &= \frac{(2n-1)\pi}{2}\sqrt{\frac{E}{G}}\,\frac{w}{l}\\ \beta &= \frac{I_w}{I_s}\end{aligned}\right\} \quad (51)$$

from which there is obtained

$$\sigma_x = \frac{4}{\pi}\,\frac{I}{I_s}\sqrt{\frac{E}{G}}\,\frac{w}{l}\,\sigma_o\sum_{n=1}^{\infty}\frac{(-1)^{n+1}}{2n-1}\,\frac{\cosh\delta_n\frac{y}{w}}{\sinh\delta_n + \beta\,\delta_n\cosh\delta_n}\sin\frac{(2n-1)\pi}{2}\,\frac{x}{l} \quad (52)$$

$$\tau = -\frac{4}{\pi}\,\frac{I}{I_s}\,\frac{w}{l}\,\sigma_o\sum_{n=1}^{\infty}\frac{(-1)^{n+1}}{2n-1}\,\frac{\sinh\delta_n\frac{y}{w}}{\sinh\delta_n + \beta\,\delta_n\cosh\delta_n}\cos\frac{(2n-1)\pi}{2}\,\frac{x}{l} \quad (53)$$

This form of the solution has the disadvantage that the

series, instead of being of the nature of end corrections, serve to determine completely the stresses. Moreover, the convergence is least rapid in the neighborhood of the flanges ($y = \pm w$) where the magnitude of the stresses is generally of greatest interest. Finally, the procedure leading to equation (50) cannot be directly employed in dealing with beams with cut-outs while, as will be shown, the present methods apply without modification.

The normal stresses in the flanges and along the center line of the sheet for a beam with length-width ratio $\frac{l}{2w} = 2.5$ are shown as the solid curves in figure 11(a) for $\beta = 1$ and in figure 11(b) for the limiting case $\beta = 0$. (See table 10.) The solutions obtained by Reissner and by Kuhn and Chiarito for the former case will later be compared with the present results.

The transverse distribution of normal stress at the root is presented for $\beta = 1$ and $\beta = 0$ in figure 12 and in table 11. The parabolic distribution predicted by Reissner's solution for the case $\beta = 1$ is shown as a broken-line curve. The fact that the stresses in the flanges and in the central fibers of the beam, as predicted by the Reissner solution and by the present solution, agree almost exactly along the entire span except for small deviations at the root, as is shown in a later section, indicates that the parabolic approximation is extremely accurate except in the immediate vicinity of the root. In the limiting case $\beta = 0$ theoretically infinite stresses are predicted at the root corners.

The so-called effective width of the cover sheets, defined by the relationship

$$w_{eff}\,\sigma_x(x,w) = \int_0^w \sigma_x(x,y)\,dy \tag{54}$$

can be expressed as follows in terms of the flange stress and the elementary linear stress

$$\frac{w_{eff}}{w} = 1 - (\beta + 1)\left[1 - \frac{\sigma_o \frac{x}{l}}{\sigma_x(x,w)}\right] \tag{55}$$

The solid curves of figure 13 represent the ratio of the

effective width to the actual width of the cover sheet as a function of distance from the free end for $\beta = 1$ and $\beta = 0$. (See table 12.) For $\beta = 1$, the effective root width is found to be 78.6 percent of the actual width as compared with the value of 80.1 percent obtained by Reissner. In the limiting case $\beta = 0$, the sheet is over 90 percent efficient at distances from the root greater than one-fourth the width of the sheet, but the effective width rapidly decreases to zero as the root is approached.

Effect of a Cut-Out on the Stress Distribution in a Rectangular Box Beam Subjected to Concentrated Free-End Bending Loads

If a section of the cover sheet is removed at $x = l$ (fig. 2(b)) and no sheet stiffener is present, the stress distribution in that part of the sheet between the free end and the cut-out is derived from the stress function

$$H = w\,\sigma_o\left\{\frac{x}{l}\,\frac{y}{w} + 2(\beta+1)\sum_{n=1}^{\infty}\frac{\cos\lambda_n \sin\lambda_n\frac{y}{w}}{\lambda_n(1+\beta\cos^2\lambda_n)}\,\frac{\sinh\mu_n\frac{x}{l}}{\sinh\mu_n}\right\} \quad (56)$$

where the constants are defined as in equation (43). It follows that

$$\sigma_x = \sigma_o\left\{\frac{x}{l} + 2(\beta+1)\sum_{n=1}^{\infty}\frac{\cos\lambda_n\cos\lambda_n\frac{y}{w}}{1+\beta\cos^2\lambda_n}\,\frac{\sinh\mu_n\frac{x}{l}}{\sinh\mu_n}\right\} \quad (57)$$

$$\tau = -\sigma_o\,\frac{w}{l}\left\{\frac{y}{w} + 2(\beta+1)\sqrt{\frac{G}{E}}\,\frac{l}{w}\sum_{n=1}^{\infty}\frac{\cos\lambda_n\sin\lambda_n\frac{y}{w}}{1+\beta\cos^2\lambda_n}\,\frac{\cosh\mu_n\frac{x}{l}}{\sinh\mu_n}\right\} \quad (58)$$

The spanwise normal stress distributions in a flange and along the central line of the sheet for the span-width ratio $\frac{l}{2w} = 2.5$ are shown as broken-line curves in figure 11 for $\beta = 1$ and $\beta = 0$, while the variation of the effective width along the span as computed from equation (55) is presented for $\beta = 1$ and $\beta = 0$ in figure 13. (See tables 12 and 13.) A discussion of the results is

postponed until a later section in which a comparison is made with the solution given by the procedure of reference 2.

Stress Distribution in a Semi-Infinite Sheet with One Stiffener

If a load F is introduced through a stiffener of cross section A into the straight-edge of an infinite half-sheet assumed rigid in the direction parallel to the straight-edge (fig. 3(a)), the stress distribution is derivable from the stress function

$$H = -\frac{2F}{\pi A}\int_0^\infty e^{-y\,p}\,\frac{\sin k\,x\,p}{p\left(p+\frac{2t}{A}\right)}\,dp \qquad (59)$$

where

$$k = \sqrt{\frac{G}{E}} \qquad (60)$$

so that, in particular, the expressions for the normal stress in the direction of the stiffener and for the shear stress take the form

$$\sigma_x = \frac{2F}{\pi A}\int_0^\infty e^{-y\,p}\,\frac{\sin k\,p\,x}{p+\frac{2t}{A}}\,d\,p \qquad (61)$$

$$\tau = \frac{2kF}{\pi A}\int_0^\infty e^{-y\,p}\,\frac{\cos k\,p\,x}{p+\frac{2t}{A}}\,d\,p \qquad (62)$$

Along the stiffener ($y = 0$) these expressions can be written in terms of tabulated functions as

$$\sigma_x(x,o) = \frac{2F}{\pi A}\left\{\cos\frac{2ktx}{A}\left[\frac{\pi}{2} - \mathrm{Si}\,\frac{2ktx}{A}\right] + \sin\frac{2ktx}{A}\,\mathrm{Ci}\,\frac{2ktx}{A}\right\} \qquad (63)$$

$$\tau(x,o) = \frac{2kF}{\pi A}\left\{\sin\frac{2ktx}{A}\left[\frac{\pi}{2} - \mathrm{Si}\,\frac{2ktx}{A}\right] - \cos\frac{2ktx}{A}\,\mathrm{Ci}\,\frac{2ktx}{A}\right\} \qquad (64)$$

with the conventional abbreviations

$$\left.\begin{aligned} \mathrm{Si}\ x &= \int_0^x \frac{\sin u\ du}{u} \\ \mathrm{Ci}\ x &= -\int_x^\infty \frac{\cos u\ du}{u} \end{aligned}\right\} \tag{65}$$

In the limiting case $A = 0$, when the sheet is unstiffened,

$$H = -\frac{F}{\pi t}\int_0^\infty e^{-yp}\,\frac{\sin k\,x\,p}{p}\,dp = -\frac{F}{\pi t}\tan^{-1}\frac{kx}{y} \tag{66}$$

$$\left.\begin{aligned} \sigma_x &= \frac{F}{\pi t}\,\frac{kx}{y^2 + k^2x^2} \\ \tau &= \frac{kF}{\pi t}\,\frac{y}{y^2 + k^2x^2} \end{aligned}\right\} \tag{67}$$

and, in particular, the normal stress in the direction of the applied load is given by

$$\sigma_x(x,o) = \frac{F}{\pi t k x} \tag{68}$$

The corresponding stresses in an unstiffened isotropic sheet are known to be of the form

$$\left.\begin{aligned} \sigma_x &= \frac{2Fx^3}{\pi t(x^2 + y^2)^2} \\ \tau &= \frac{2Fx^2y}{\pi t(x^2 + y^2)^2} \\ \sigma_x(x,o) &= \frac{2F}{\pi t x} \end{aligned}\right\} \tag{69}$$

It seems of some interest to compare the stress distributions just obtained with that associated with a load uniformly distributed over a small area at the margin of

the sheet. In particular, if the load F is uniformly distributed over an area t^2 (fig. 3(b)), the stress function takes the form

$$H = \frac{F}{\pi t^2}\int_0^\infty e^{-kxp}\frac{\sin pt}{p^2}\sin py\,dp \tag{70}$$

and the normal stress along the line of symmetry follows by differentiation,

$$\sigma_x(x,0) = \frac{\partial H(x,0)}{\partial y} = \frac{F}{\pi t^2}\tan^{-1}\left(\frac{t}{kx}\right) \tag{71}$$

The corresponding stress for an isotropic material is given by the expression

$$\sigma_x(x,0) = \frac{F}{\pi t^2}\left\{\tan^{-1}\frac{t}{x} + \frac{\frac{x}{t}}{1+\left(\frac{x}{t}\right)^2}\right\} \tag{72}$$

In figure 14 the stiffener shear and normal stresses are represented in their dependence upon the ratios $\sqrt{\frac{G}{E}}\frac{A}{t^2}$ and $\frac{F}{A}$, while in figure 15 the flange normal stresses corresponding to equations (71), (72), and (63) are compared. (See tables 14 and 15.)

MATHEMATICAL FORMULATION OF THE BOUNDARY-VALUE PROBLEMS

Stresses in Axially Loaded Symmetrical Panels

Symmetrical loading.- The notations and dimensions assumed in this section are indicated in figure 1(a).

Because of the symmetry the transverse displacement must vanish along the line $y = 0$ and hence, from equation (4), must vanish everywhere. Thus the differential equation (8) for the stress function H takes the form

$$\frac{\partial^2 H}{\partial x^2} + \frac{G}{E}\frac{\partial^2 H}{\partial y^2} = 0 \tag{73}$$

At the free end ($x = 0$) the spanwise normal stress

$\sigma_x = \frac{\partial H}{\partial y}$ must vanish except at $y = 0$ and at $y = \pm w$ and is finite at those points, so that $H(o,y)$ must be constant. Since, according to equation (7), the stresses remain unchanged if H is increased by a constant, it is permissible to require that

$$H(o,y) = 0 \tag{74}$$

Because of continuity of the spanwise strain ϵ_x, it follows that the spanwise stress $\sigma_x = \frac{\partial H}{\partial y}$ is continuous at $y = 0$ and the condition of equilibrium between the sheet and stiffener along the line $y = 0$ can be written in the form

$$A_m \frac{\partial \sigma_x(x,o)}{\partial x} = -t\,[\tau(x,o+) - \tau(x,o-)] \tag{75}$$

If equation (75) is written in terms of the stress function H and if the fact that τ is an odd function of y is used, this condition becomes

$$\left.\begin{aligned} &\frac{\partial}{\partial x}\left[H(x,o+) - \frac{A_m}{2t}\frac{\partial H(x,o)}{\partial y}\right] = 0 \\ &H(x,o+) - \frac{A_m}{2t}\frac{\partial H(x,o)}{\partial y} = \text{constant} \end{aligned}\right\} \tag{76}$$

It now follows from the end condition

$$A_m\,\sigma_x(o,o) \equiv A_m \frac{\partial H(o+,o)}{\partial y} = F_m \tag{77}$$

and from equation (74) that the constant in equation (76) has the value of $-\frac{F_m}{2t}$, and the condition along the positive side of the line $y = o$ takes the form

$$2tH(x,o+) - A_m \frac{\partial H(x,o)}{\partial y} = -F_m \tag{78}$$

Since H and $\frac{\partial H}{\partial x}$ are odd functions of y, it is seen that they are discontinuous at the line $y = 0$ (except at $x = 0$) unless $A_m = F_m = 0$. Also, from equations (74) and (78), it follows that

$$\left.\begin{aligned} \lim_{y \to 0} \frac{\partial H(o,y)}{\partial y} &= 0 \\ \lim_{x \to 0} \frac{\partial H(x,o)}{\partial y} &= \frac{F_m}{A_m} \end{aligned}\right\} \tag{79}$$

The condition along the line $y = w$ can be obtained from the spanwise condition of equilibrium

$$2t \int_0^w \sigma_x \, dy + 2 A_e \sigma_x(x,w) + A_m \sigma_x(x,o) = 2F_e + F_m \tag{80}$$

If $\sigma_x = \frac{\partial H}{\partial y}$ is introduced into equation (80) and if equation (78) is taken into account, this condition reduces to

$$t H(x,w) + A_e \frac{\partial H(x,w)}{\partial y} = F_e \tag{81}$$

At the end $x = l$ a condition of the form

$$\left.\begin{aligned} a_o H(l,y) + a_1 \frac{\partial H(l,y)}{\partial x} &= f(y) \\ y &> 0 \end{aligned}\right\} \tag{82}$$

is assumed. Among the situations in which equation (82) applies, the following cases may be noted:

1. If the end $x = l$ is clamped so that the spanwise displacement u vanishes, it follows from equation (5b) that

$$\frac{\partial H(l,y)}{\partial x} = 0 \tag{82a}$$

2. If a section of the panel, including the central stiffener, is removed at $x = l$, it follows that

$\sigma_x(l,y) = 0$ if $y \neq \pm w$ so that $H(l,y) =$ constant. Equation (78) then requires that $H(l,o) = -\frac{F_m}{2t}$ and the condition at $x = l$ becomes

$$\left.\begin{aligned} H(l,y) &= -\frac{F_m}{2t} \\ y &> 0 \end{aligned}\right\} \tag{82b}$$

It should be noticed that, since H is an odd function of y

$$\left.\begin{aligned} H(l,y) &= +\frac{F_m}{2t} \\ y &< 0 \end{aligned}\right\}$$

so that $H(l,y)$ is discontinuous at $y = 0$ unless $F_m = 0$. If $F_m = 0$, it follows from symmetry that the panel can be considered as clamped along the line $x = \frac{l}{2}$, so that this case is then reduced to case (1).

3. If a section of the sheet is removed at $x = l$ but the central stiffener is built in, it again follows that

$$\left.\begin{aligned} H(l,y) &= c \\ y &> 0 \end{aligned}\right\} \tag{82c}$$

Although constant c cannot in this case be determined from static considerations, if the stress function is determined in terms of c, the additional condition

$$u(l,w) = u(l,o)$$

which becomes, from equation (56),

$$\int_o^w \frac{\partial H(l,y)}{\partial x}\, dy = 0$$

is sufficient for the determination of the constant.

4. If the end $x = l$ is subjected to an axial loading distribution $g(y)$ which is statically equivalent to the loading at the end $x = 0$, so that

$$\sigma_x(l,y) \equiv \frac{\partial H(l,y)}{\partial y} = -g(y)$$

it follows from equation (78) that

$$\left.\begin{aligned} H(l,y) &= -\int_0^y g(u)\,du + \frac{A_m}{2t}\,g(0) - \frac{F_m}{2t} \\ & \\ & y > 0 \end{aligned}\right\} \qquad (82d)$$

If the preceding results are summarized, the stress function H is completely determined in the region $[0 \leq x \leq l, \quad 0 < y \leq w]$ and hence, by symmetry, over the entire panel, by the following set of equations:

$$\frac{\partial^2 H}{\partial x^2} + \frac{G}{E}\frac{\partial^2 H}{\partial y^2} = 0 \qquad (A1)$$

$$H(0,y) = 0 \qquad (A2)$$

$$a_0 H(l,y) + a_1 \frac{\partial H(l,y)}{\partial x} = f(y) \qquad (A3)$$

$$2tH(x,0+) - A_m \frac{\partial H(x,0)}{\partial y} = -F_m \qquad (A4)$$

$$tH(x,w) + A_e \frac{\partial H(x,w)}{\partial y} = F_e \qquad (A5)$$

Antisymmetrical loading.- The notations and dimensions assumed in this section are indicated in figure 1(b).

Since the transverse displacement v does not vanish in this case, the stress function is governed by the more general differential equation (8) which can be written in the form

$$\frac{\partial}{\partial y}\left(\frac{\partial^2 H}{\partial x^2} + \frac{G}{E}\frac{\partial^2 H}{\partial y^2}\right) = 0 \qquad (83)$$

The conditions along the lines $x = o$, $x = l$, and $y = w$ are identical with those in the preceding section and are given in equations (74), (81), and (82). Since $\sigma_x(x,o) = 0$ from symmetry, equation (78) is replaced by the condition

$$\frac{\partial H(x,o)}{\partial y} = 0 \tag{84}$$

An additional condition is obtained from the equation of moment equilibrium which can be written in the form

$$t \int_o^w y\, \sigma_x\, dy + w\, A\, \sigma_x(x,w) = w\, F \tag{85}$$

If $\sigma_x = \frac{\partial H}{\partial y}$ is introduced into equation (85) and the first term is integrated by parts,

$$t\, H(x,w) - \frac{t}{w} \int_o^w H\, dy + A\, \frac{\partial H(x,w)}{\partial y} = F \tag{86}$$

and equations (81) and (86) are compatible only if H satisfies the additional restriction

$$\int_o^w H(x,y)\, dy = 0 \tag{87}$$

The following set of equations then determines the stress function H in the region $[o \leq x \leq l,\ o < y \leq w]$:

$$\frac{\partial}{\partial y}\left(\frac{\partial^2 H}{\partial x^2} + \frac{G}{E}\frac{\partial^2 H}{\partial y^2}\right) = 0 \tag{B1}$$

$$H(o,y) = 0 \tag{B2}$$

$$a_o\, H(l,y) + a_1 \frac{\partial H(l,y)}{\partial x} = f(y) \tag{B3}$$

$$\frac{\partial H(x,o)}{\partial y} = 0 \tag{B4}$$

$$t\,H(x,w) + A\,\frac{\partial H(x,w)}{\partial y} = F \tag{B5}$$

$$\int_0^w H(x,y)\,dy = 0 \tag{B6}$$

Stresses in the Cover Sheets of Doubly Symmetrical Box Beams

The notations and dimensions assumed in this section are indicated in figure 2.

If it is assumed that the bending loads are applied symmetrically about the line $y = 0$, it follows as before that the transverse displacement v vanishes identically and the stress function is determined by the differential equation (73).

The conditions along the lines $x = 0$ and $x = l$ are identical with those derived in the preceding sections: namely,

$$H(o,y) = 0 \tag{74}$$

$$a_o\,H(l,y) + a_1\,\frac{\partial H(l,y)}{\partial x} = f(y) \tag{82}$$

where equation (82) includes, in particular, the case when the beam is completely clamped at $x = l$ [$a_o = 0$, $f(y) = 0$] and the case when the side structure is fixed but the sheet and longitudinal are not attached to the support [$a_1 = 0$, $f(y) = 0$].

Along the positive side of the line $y = 0$, the discussion of the preceding section again leads to equation (76). In the present case, however, the normal stress $\sigma_x = \frac{\partial H}{\partial y}$ vanishes at $x = 0$ for all y, and it follows from equation (74) that the constant of integration in equation (76) must vanish, giving the condition

$$2t\,H(x,o+) - A_m\,\frac{\partial H(x,o)}{\partial y} = 0 \tag{88}$$

The equation of moment equilibrium about the transverse principal beam axis can be written

$$2th \int_0^w \sigma_x dy + \frac{I_w}{h/2} \sigma_x(x,w) + h A_m \sigma_x(x,o) = M(x) \quad (89)$$

where $M(x)$ is the moment of the applied bending loads. If equation (89) is expressed in terms of H and if equation (88) is taken into account, the boundary condition along the line $y = w$ follows in the form

$$\frac{I_s}{w} H(x,w) + I_w \frac{\partial H(x,w)}{\partial y} = M(x) \frac{h}{2} \quad (90)$$

In summarizing these results, it may be seen that the stress function H is determined in the region $[o \leq x \leq l, \; o < y \leq w]$ by the following set of equations:

$$\frac{\partial^2 H}{\partial x^2} + \frac{G}{E} \frac{\partial^2 H}{\partial y^2} = 0 \quad (C1)$$

$$H(o,y) = 0 \quad (C2)$$

$$a_o H(l,y) + a_1 \frac{\partial H(l,y)}{\partial x} = f(y) \quad (C3)$$

$$2t \; H(x,o+) - A_m \frac{\partial H(x,o)}{\partial y} = 0 \quad (C4)$$

$$\frac{I_s}{w} H(x,w) + I_w \frac{\partial H(x,w)}{\partial y} = M(x) \frac{h}{2} \quad (C5)$$

SOLUTION OF THE PROBLEMS

One of the difficulties encountered in solving the sets of equations derived in the preceding section arises from the nonhomogeneity of the conditions at both the boundaries x = constant and y = constant. In most cases, however, the problems considered can be reduced to problems of a more convontional type by the definition

$$H = \Phi + P \quad (91)$$

where P is a particular solution of the governing differ-

ential equation (73) or (83), determined so as to satisfy either the end conditions along the boundaries x = constant or the equilibrium conditions prescribed along the boundaries y = constant, so that the corresponding conditions become homogeneous in Φ. In case both procedures are possible it is preferable to satisfy the equilibrium conditions for two reasons: (1) The function P so determined is then a stress function corresponding to the state of stress in a sheet subjected to external forces that are statically equivalent to the actual forces and, according to Saint Venant's principle, if the length-width ratio of the sheet is sufficiently large, the two stress distributions will be nearly identical except in the regions near the ends of the sheet. Thus the function Φ, which must be expressed, in general, as an infinite series, is of the nature of an end correction. If, however, the particular solution P satisfies only the end conditions along the sections x = constant, the infinite series representing Φ will be in general significant over the entire span. (2) Certain computational advantages follow from the fact that if P is made to satisfy the equilibrium conditions the variation of Φ in the spanwise direction is expressed in terms of exponential (or hyperbolic) functions, while in the alternate procedure the reverse is true. If the condition of support at $x = l$ is such that $f(y) \equiv 0$ in equation (82), as is true in many practical cases, the first procedure is applicable with $P \equiv 0$. Certain special cases of the problems considered here have been solved by this last method (references 3 and 4), but the solutions obtained in this way are not so well adapted to numerical computation as those obtained here.

In the rest of this section the boundary value problems formulated in the preceding section are reduced to sets of ordinary differential equations with terminal conditions, all of which can be solved by elementary methods.

The Symmetrically Loaded Panel

A solution of equation (A) is assumed in the form

$$H = \sum_n X_n(x)\, Y_n(y) + p(y) \tag{91a}$$

Now the differential equation (A1) requires that X_n, Y_n and p satisfy the ordinary differential equations

$$p''(y) = 0 \tag{92}$$

$$X_n''(x) - \left(\frac{\mu_n}{l}\right)^2 X_n(x) = 0 \tag{93}$$

$$Y_n''(y) + \left(\frac{\lambda_n}{w}\right)^2 Y_n(y) = 0 \tag{94}$$

where λ_n and μ_n are arbitrary constants satisfying the relation

$$\mu_n = \sqrt{\frac{G}{E}}\,\frac{l}{w}\,\lambda_n \tag{95}$$

The boundary conditions of equations (A2) to (A5) take the form

$$\sum_n X_n(o)\,Y_n(y) = -p(y) \tag{96a}$$

$$\sum_n \left\{a_o\,X_n(l) + a_1\,X_n'(l)\right\} Y_n(y) = f(y) - a_o\,p(y) \tag{96b}$$

$$\sum_n \left\{2t\,Y_n(o) - A_m\,Y_n'(o)\right\} X_n(x) = -\left[2t\,p(o) - A_m\,p'(o) + F_m\right] \tag{96c}$$

$$\sum_n \left\{t\,Y_n(w) + A_e\,Y_n'(w)\right\} X_n(w) = -\left[t\,p(w) + A_e\,p'(w) - F_e\right] \tag{96d}$$

The equilibrium conditions equations (96c) and (96d) are satisfied and homogeneous conditions of the type required are obtained if it is required that

$$\left.\begin{aligned} 2t\,p(o) - A_m\,p'(o) &= -F_m \\ t\,p(w) + A_e\,p'(w) &= F_e \end{aligned}\right\} \tag{97}$$

and

$$\left.\begin{aligned} 2t\,Y_n(o) - A_m\,Y_n'(o) &= 0 \\ t\,Y_n(w) + A_e\,Y_n'(w) &= 0 \end{aligned}\right\} \tag{98}$$

Equations (92) and (97) are sufficient to determine the particular solution $p(y)$, while the differential equation (94) and the homogeneous boundary conditions (98) constitute a "characteristic value" problem of the Sturm-Liouville type over the interval $0 < y < w$. The constants λ_n are determined as a discrete infinite set of characteristic numbers; and, corresponding to each such λ_n,

a characteristic function Y_n satisfying the conditions of the problem is determined. It is a property of such systems that the set of characteristic functions so obtained is orthogonal over the interval involved and that any function having a continuous second derivative in that interval has a unique expansion in a series of those functions. Furthermore, if the permissible condition of normalization

$$\int_0^w Y_n^2 \, dy = 1 \tag{99}$$

is imposed, the constants in the expansion

$$\left.\begin{aligned} F(y) &= \Sigma \, c_n \, Y_n(y) \\ 0 &< y < w \end{aligned}\right\} \tag{100}$$

are determined by the formula

$$c_n = \int_0^w F(u) \, Y_n(u) \, du \tag{101}$$

With $p(y)$ determined and the relationships necessary for the determination of the orthonormal set $\{Y_n(y)\}$ known, it remains to determine $X_n(x)$ so that equations (96a) and (96b) are satisfied. If it is assumed that $f(y)$ has a continuous second derivative in (o,w), it follows from equations (96a) and (96b) that, according to equation (101) $X_n(x)$ must satisfy the conditions

$$X_n(0) = -\int_0^w p(u) \, Y_n(u) \, du \tag{102}$$

$$a_o \, X_n(l) + a_1 \, X_n'(l) = \int_0^w \{f(u) - a_o \, p(u)\} \, Y_n(u) \, du \tag{103}$$

and equations (102) and (103), together with equations (95) and (93), are sufficient to determine $X_n(x)$.

The solution of the boundary value problem of equation (A) in the region $[o \leq x \leq l, \; o < y \leq w]$ is given, as a summary, by

$$H = \sum_n X_n(x) \, Y_n(y) + p(y)$$

where

$$\left.\begin{aligned} p'' &= 0 \\ 2t\,p(o) - A_m\,p'(o) &= -F_m \\ t\,p(w) + A_e\,p'(w) &= F_e \end{aligned}\right\}$$

$$\left.\begin{aligned} Y_n'' + \left(\frac{\lambda_n}{w}\right)^2 Y_n &= 0 \\ 2t\,Y_n(o) - A_m\,Y_n'(o) &= 0 \\ t\,Y_n(w) + A_e\,Y_n'(w) &= 0 \\ \int_o^w Y_n^2\,dy &= 1 \end{aligned}\right\}$$

$$\left.\begin{aligned} X_n'' - \frac{G}{E}\left(\frac{\lambda_n}{w}\right)^2 X_n &= 0 \\ X_n(o) &= -\int_o^w p\,Y_n\,dy \\ a_o\,X_n(l) + a_1\,X_n'(l) &= \int_o^w (f - a_o\,p)Y_n\,dy \end{aligned}\right\}$$

Explicit solutions in several cases are presented in a preceding section. The determination of H is illustrated by considering the first case in that section (panel 1).

Here

$$\left.\begin{aligned} l &= \infty \qquad a_o = f(y) = A_m = F_m = 0 \\ F_e &= F \qquad A_e = A \end{aligned}\right\} \tag{104}$$

The particular solution is obtained as

$$\left.\begin{aligned} p(y) &= c_1\,y + c_2 \\ p(o) &= 0 \qquad t\,p(w) + A\,p'(w) = F \\ p(y) &= \frac{F}{t(\alpha + 1)}\,\frac{y}{w} \qquad \alpha = \frac{A}{tw} \end{aligned}\right\} \tag{105}$$

Next the functions $Y_n(y)$ satisfy the conditions

$$Y_n(y) = c_1 \sin \lambda_n \frac{y}{w} + c_2 \cos \lambda_n \frac{y}{w}$$

$$Y_n(o) = 0 \qquad t\, Y_n(w) + A\, Y_n'(w) = 0 \qquad \int_o^w Y_n^2\, dy = 1$$

from which the characteristic numbers λ_n are determined as the positive solutions of the equation

$$\tan \lambda_n + \alpha \lambda_n = 0 \tag{106}$$

with corresponding normalized characteristic functions

$$\left.\begin{aligned} Y_n(y) &= \gamma_n \sin \lambda_n \frac{y}{w} \\ \gamma_n^2 &= \frac{2}{w(1 + \alpha \cos^2 \lambda_n)} \end{aligned}\right\} \tag{107}$$

The terminal conditions governing the function $X_n(x)$, which according to equation (93) is of the form $c_1 e^{-\sqrt{\frac{G}{E}} \lambda_n \frac{x}{w}} + c_2 e^{\sqrt{\frac{G}{E}} \lambda_n \frac{x}{w}}$, follow from equations (102) and (103)

$$\left.\begin{aligned} X_n'(\infty) &= 0 \\ X_n(o) &= \frac{-\gamma_n F}{t(\alpha + 1)} \int_o^w \frac{y}{w} \sin \lambda_n \frac{y}{w}\, dy = \frac{w \gamma_n F}{t} \frac{\cos \lambda_n}{\lambda_n} \end{aligned}\right\} \tag{108}$$

from which

$$X_n(x) = \frac{w \gamma_n F}{t} \frac{\cos \lambda_n}{\lambda_n} e^{-\sqrt{\frac{G}{E}} \lambda_n \frac{x}{w}} \tag{109}$$

and the solution is obtained in the form

$$H = \frac{F}{t}\left\{\frac{1}{\alpha + 1}\frac{y}{w} + 2 \sum_{n=1}^{\infty} \frac{\cos \lambda_n \sin \lambda_n \frac{y}{w}}{\lambda_n (1 + \alpha \cos^2 \lambda_n)} e^{-\sqrt{\frac{G}{E}} \lambda_n \frac{x}{w}}\right\} \tag{110}$$

[1] See (18), page 10

where

$$\alpha = \frac{A}{tw}$$

and

$$\tan \lambda_n + \alpha \lambda_n = 0$$

The validity of this solution can be rigorously established if the fact is taken into account that, for large values of n,

$$\lambda_n \approx \frac{(2n - 1)\pi}{2}$$

$$\cos \lambda_n \approx \frac{(-)^{n+1}\, 2}{\alpha(2n - 1)\pi}$$

The Antisymmetrically Loaded Panel

A solution of equation (B) is assumed in the form

$$H = \sum_n X_n(x)\, Y_n(y) + p(y) \qquad (111)$$

where, in consequence of equation (B1), the functions X_n, Y_n, and p must satisfy the differential equations

$$p'''(y) = 0 \qquad (112)$$

$$X_n''(x) - \left(\frac{\mu_n}{l}\right)^2 X_n(x) = 0 \qquad (113)$$

$$Y_n'''(y) + \left(\frac{\lambda_n}{w}\right)^2 Y_n'(y) = 0 \qquad (114)$$

and, as before,

$$\mu_n = \sqrt{\frac{G}{E}}\, \frac{l}{w}\, \lambda_n \qquad (115)$$

Equations (B2) to (B6) are now satisfied if it is required that

$$\sum_n X_n(o)\, Y_n(y) = -\, p(y) \qquad (116a)$$

$$\sum_n \left\{ a_o\, X_n(l) + a_1\, X_n'(l) \right\} Y_n(y) = f(y) - a_o\, p(y) \qquad (116b)$$

$$\left.\begin{aligned} p'(o) &= 0 \\ t\,p(w) + A\,p'(w) &= F \\ \int_o^w p\,dy &= 0 \end{aligned}\right\} \tag{117}$$

$$\left.\begin{aligned} Y_n'(o) &= 0 \\ t\,Y_n(w) + A\,Y_n'(w) &= 0 \\ \int_o^w Y_n\,dy &= C \end{aligned}\right\} \tag{118}$$

The conditions given in equation (117) together with the differential equation (112) uniquely determine $p(y)$, while $Y_n(y)$ must satisfy the boundary value problem consisting of the differential equation (108) and the homogeneous boundary conditions of equation (118). Although this problem is not of the conventional Sturm–Liouville type, it can be shown that the characteristic functions Y_n are again orthogonal over (o,w) and that an arbitrary function $F(y)$ having a continuous second derivative and satisfying the condition $\int_o^w F(y)dy = 0$ has a unique expansion of the type of equation (100) where, if the functions Y_n are normalized,

$$\int_o^w Y_n^2\,dy = 1 \tag{119}$$

the constants are given by the formula of (101). Thus, if it is assumed that $f(y)$ satisfies the conditions mentioned, equations (116) imply equations (102) and (103).

The solution of the boundary value problem of equation (B) in the entire region $[o \le x \le l,\ |y| \le w]$ is given, as a summary, by

$$H = \sum_n X_n(x)\,Y_n(y) + p(y)$$

where

$$\left.\begin{aligned} p^{IV} &= 0 \\ p'(o) &= 0 \\ t\,p(w) + A\,p'(w) &= F \\ \int_o^w p\,dy &= 0 \end{aligned}\right\}$$

$$\left.\begin{aligned} Y_n''' + \left(\frac{\lambda_n}{w}\right)^2 Y_n' &= 0 \\ Y_n'(o) &= 0 \\ t\, Y_n(w) + A\, Y_n'(w) &= 0 \\ \int_o^w Y_n\, dy &= 0 \\ \int_o^w Y_n^2\, dy &= 1 \end{aligned}\right\}$$

$$\left.\begin{aligned} X_n'' - \frac{G}{E}\left(\frac{\lambda_n}{w}\right)^2 X_n &= 0 \\ X_n(o) &= -\int_o^w p\, Y_n\, dy \\ a_o\, X_n(l) + a_1\, X_n'(l) &= \int_o^w (f - a_o\, p) Y_n\, dy \end{aligned}\right\}$$

The explicit solution for the case $l = \infty$, $a_o = f(y) = 0$ is given in equation (24).

The Rectangular Box Beam

If the solution of equation (C) is assumed in the form

$$H = \sum_n X_n(x)\, Y_n(y) + P(x,y) \tag{120}$$

where

$$\frac{\partial^2 P}{\partial x^2} + \frac{G}{E}\frac{\partial^2 P}{\partial y^2} = 0 \tag{121}$$

and

$$l^2\, X_n'' - \mu_n^2\, X_n = 0 \tag{122a}$$

$$w^2\, Y_n'' + \lambda_n^2\, Y_n = 0 \tag{122b}$$

$$\mu_n = \sqrt{\frac{G}{E}}\,\frac{l}{w}\,\lambda_n \tag{122c}$$

equations (C2) to (C5) take the form

$$\sum_n X_n(o)\, Y_n(y) = -P(o,y) \tag{123a}$$

$$\sum_n \left\{a_o\, X_n(l)+a_1\, X_n'(l)\right\} Y_n(y) = f(y) - \left[a_o\, P(l,y)+a_1 P_x(l,y)\right] \tag{123b}$$

$$\sum_n \left\{2t\, Y_n(o) - A_m\, Y_n'(o)\right\} X_n(x) = -\left[2t\, P(x,o) - A_m\, P_y(x,o)\right] \tag{123c}$$

$$\sum_n \left\{\frac{I_s}{w}\, Y_n(w) + I_w\, Y_n'(w)\right\} X_n(x) = M(x)\,\frac{h}{2} - \left[\frac{I_s}{w}\, P(x,w) + I_w\, P_y(x,w)\right] \tag{123d}$$

It is first shown that, if $M(x)$ can be expressed as a polynomial in x, a function $P(x,y)$ satisfying equation (121) can be determined as a polynomial in x and y so that the right-hand sides of equations (123c) and (123d) vanish and

$$P(x,o) - \frac{A_m}{2t}\, P_y(x,o) = 0 \tag{124a}$$

$$\frac{I_s}{w}\, P(x,w) + I_w\, P_y(x,w) = M(x)\,\frac{h}{2} \tag{124b}$$

It can be directly verified that the expression

$$P(x,y) = \frac{h}{2I}\left\{M(x)\left[y + \frac{A_m}{2t}\right] - \frac{E}{G}\, M''(x)\left[\left(\frac{y^3}{3!} + \frac{A_m}{2t}\,\frac{y^2}{2!}\right) - k_1\left(y+\frac{A_m}{2t}\right)\right]\right.$$

$$+ \left(\frac{E}{G}\right)^2 M^{IV}(x)\left[\left(\frac{y^5}{5!} + \frac{A_m}{2t}\,\frac{y^4}{4!}\right) - k_1\left(\frac{y^3}{3!} + \frac{A_m}{2t}\,\frac{y^2}{2!}\right) + k_2\left(y + \frac{A_m}{2t}\right)\right]$$

$$- \left(\frac{E}{G}\right)^4 M^{VI}(x)\left[\left(\frac{y^7}{7!} + \frac{A_m}{2t}\,\frac{y^6}{6!}\right) - k_1\left(\frac{y^5}{5!} + \frac{A_m}{2t}\,\frac{y^4}{4!}\right) + k_2\left(\frac{y^3}{3!} + \frac{A_m}{2t}\,\frac{y^2}{2!}\right)\right.$$

$$\left.\left. - k_3\left(y + \frac{A_m}{2t}\right)\right] + \cdots\cdots\cdots\right\} \tag{125}$$

where the law of formation of the following terms is obvious, satisfies the differential equation (121) and the condition of equation (124a) for an arbitrary choice of the

constants $k_1, k_2, \ldots\ldots$ The factor $\frac{h}{2I}$, where I is the total moment of inertia of the cross section about the transverse principal axis and is given as

$$I = I_s + I_w + \frac{A_m}{2} h^2 \tag{126}$$

has been chosen so that the leading term $\frac{M(x)}{I} \frac{h}{2} \left(y + \frac{A_m}{2t} \right)$ satisfies the condition of equation (124b). The constant k_1 is then determined so that the coefficient of $M''(x)$ in equation (124b) vanishes and

$$k_1 = \frac{w^2}{6I} \left\{ (I_s + 3I_w) + \frac{3A_m}{2tw} (I_s + 2I_w) \right\} \tag{127}$$

after which the constants $k_2, k_3, \ldots\ldots$ can be determined so that the coefficients of $M^{IV}(x), M^{VI}(x), \ldots\ldots$ in equation (124b) vanish. It appears that, if $M(x)$ involves only odd powers of x, the polynomial $P(x,y)$ satisfies also equation (C3) as well as equations (C1), (C4), and (C5). It may also be noticed that the leading term $\frac{M(x)}{I} \frac{h}{2} \left(y + \frac{A_m}{2t} \right)$ corresponds to the stress distribution given by the elementary theory of the strength of materials, according to which the spanwise normal stress σ_x does not vary in the transverse direction.

The conditions of equations (123c) and (123d) are now fulfilled if $Y_n(y)$ satisfies the Sturm-Liouville problem consisting of the differential equation

$$w^2 Y_n'' + \lambda_n^2 Y_n = 0 \tag{128}$$

and the homogeneous boundary conditions

$$\left.\begin{aligned} Y_n(o) - \frac{A_m}{2t} Y_n'(o) &= 0 \\ Y_n(w) + w \frac{I_w}{I_s} Y_n'(w) &= 0 \end{aligned}\right\} \tag{129}$$

If it is assumed that $f(y)$ has a continuous second derivative in (o,w), it follows from the remarks made

in connection with equations (100) and (101) that, if condition (97) is imposed, equations (123a) and (123b) imply

$$X_n(o) = -\int_o^w P(o,y)Y_n(y)\,dy \qquad (130a)$$

$$a_o X_n(l) + a_1 X_n'(l) = \int_o^w \left\{ f(y) - a_o P(l,y) - a_1 P_x(l,y) \right\} Y_n(y)\,dy \qquad (130b)$$

and these conditions, together with equations (122a) and (122c), determine $X_n(x)$.

Hence, finally, the solution of the problem of equation (C), in case $M(x)$ can be expressed as a polynomial, is given by equation (120), where $P(x,y)$ is given in equation (125), $Y_n(y)$ is determined by equations (128) and (129), and $X_n(x)$ is determined by equations (122a) and (130).

The "effective area" of the combined cover sheet and central stiffener, defined by the relationship

$$A_{eff}\sigma_x(x,w) = (A_m + 2tw)_{eff}\sigma_x(x,w) = 2t\int_o^w \sigma_x dy + A_m\sigma_x(x,o) \qquad (131)$$

can be expressed in terms of the elementary normal stress σ_b,

$$\sigma_b(x) = \frac{M(x)}{I}\,\frac{h}{2}$$

and the actual flange and stiffener stresses as follows. If equations (7a), (88), (90), and (126) are used

$$A_{eff}\,\sigma_x(x,w) = 2t\,[H(x,w) - H(x,o+)] + A_m\,\sigma_x(x,o)$$

$$= 2tw\left[\frac{I}{I_s}\,\sigma_b(x) - \beta\,\sigma_x(x,w)\right]$$

$$= 2tw\,[(\beta + 1)\,\sigma_b(x) - \beta\,\sigma_x(x,w)]$$

and, finally,

$$A_{eff} = 2tw\left\{1 - (\beta + 1)\left[1 - \frac{\sigma_b(x)}{\sigma_x(x,w)}\right]\right\} \tag{132}$$

In particular, if no central stiffener is present, the ratio of the effective width of the cover sheet to the actual width is given by the expression

$$\frac{w_{eff}}{w} = 1 - (\beta + 1)\left[1 - \frac{\sigma_b(x)}{\sigma_x(x,w)}\right] \tag{133}$$

The evaluation of the solution may be illustrated by taking the case of a concentrated tip load F, for which

$$M(x) = Fx \tag{134}$$

and the stress function is determined for an end-support condition of the form

$$a_0 H(l,y) + a_1 \frac{\partial H(l,y)}{\partial x} = 0 \tag{135}$$

It is further assumed that no central sheet stiffener is present. First, from equation (125), it follows that

$$\left.\begin{aligned} P(x,y) &= \sigma_o \frac{x}{l} y \\ \sigma_o &= \frac{Fhl}{2I} \end{aligned}\right\} \tag{136}$$

Next, from equations (128) and (129), the constants λ_n are determined as the solutions of the equation

$$\left.\begin{aligned} \tan \lambda_n + \beta\lambda_n &= 0 \\ \beta &= \frac{I_w}{I_s} \end{aligned}\right\} \tag{137}$$

while the functions $Y_n(y)$ take the form

$$\left.\begin{aligned} Y_n(y) &= \gamma_n \sin \lambda_n \frac{y}{w} \\ \gamma_n^2 &= \frac{2}{w(1+\beta \cos^2\lambda_n)} \end{aligned}\right\} \tag{138}$$

The terminal conditions governing the functions $X_n(x)$ become, according to equation (130),

$$\left.\begin{aligned} X_n(o) &= 0 \\ a_o X_n(l)+a_1 X_n'(l) &= \frac{w^2}{l}(l\, a_o+a_1)\sigma_o \gamma_n(\beta+1)\frac{\cos \lambda_n}{\lambda_n} \end{aligned}\right\} \tag{139}$$

and hence, from equation (122)

$$X_n(x) = w^2 \sigma_o \gamma_n(\beta+1)\frac{\cos \lambda_n}{\lambda_n}\frac{(l\, a_o+a_1)\sinh \mu_n \frac{x}{l}}{l\, a_o \sinh \mu_n + a_1 \mu_n \cosh \mu_n} \tag{140}$$

If these expressions are introduced into equation (120), the stress function is determined in the form

$$H = w\sigma_o\left\{\frac{x}{l}\frac{y}{w} + 2(\beta+1)\sum_{n=1}^{\infty}\frac{\cos \lambda_n \sin \lambda_n \frac{y}{w}}{\lambda_n(1+\beta\cos^2\lambda_n)}\frac{(l\, a_o + a_1)\sinh \mu_n \frac{x}{l}}{l a_o \sinh\mu_n + a_1\mu_n \cosh\mu_n}\right\} \tag{141}$$

The stress patterns derived from equation (141) in the cases $a_o = 0$ and $a_1 = 0$ were discussed in a preceding section.

In case the sheet, the stiffener, and the side structure are rigidly clamped at $x = l$, so that $a_o = f(y) = 0$ in equations (C3) and (123a), the general solution for arbitrary $M(x)$ can also be obtained very simply by the alternate procedure mentioned at the beginning of this section. If $P(x,y) \equiv 0$, equations (123a) and (123b) are satisfied if $X_n(o) = X_n'(l) = 0$ so that, from equation (122),

$$\left.\begin{aligned} \mu_n &= \frac{(2n-1)\pi i}{2} \\ X_n(x) &= \sin \frac{(2n-1)\pi x}{2l} \end{aligned}\right\} \tag{142}$$

Equations (122) and (123c) require that

$$\left.\begin{aligned} Y_n(y) &= c_n\left(\sinh \delta_n \frac{y}{w} + \frac{A_m}{2tw}\delta_n \cosh \delta_n \frac{y}{w}\right) \\ \delta_n &= \frac{(2n-1)\pi}{2}\sqrt{\frac{E}{G}}\frac{w}{l} \end{aligned}\right\} \quad (143)$$

and, if

$$M(x)\frac{h}{2} = \sum_{n=1}^{\infty} a_n \sin\frac{(2n-1)\pi x}{2l} \quad (144)$$

equation (123d) determines H in the form

$$H = \sum_{n=1}^{\infty} \frac{a_n w}{\gamma_n}\left(\sinh\delta_n \frac{y}{w} + \frac{A_m\delta_n}{2tw}\cosh\delta_n\frac{y}{w}\right)\sin\frac{(2n-1)\pi x}{2l} \quad (145)$$

where

$$\gamma_n = I_s\left(\sinh\delta_n + \frac{A_m}{2tw}\delta_n\cosh\delta_n\right) + \delta_n I_w\left(\cosh\delta_n + \frac{A_m}{2tw}\delta_n\sinh\delta_n\right) \quad (145a)$$

This solution was given for the special case in which $A_m = 0$ and $M = M_o \sin\frac{\pi x}{2l}$ by Younger (reference 4) and for arbitrary M with $A_m = 0$ by Kuhn (reference 3).

The Semi-Infinite Sheet with One Stiffener

In order to determine the stress function corresponding to the state of stress in a semi-infinite sheet subjected to a load introduced into a stiffener normal to the straight-edge (fig. 3(a)), a different type of procedure is needed. If the y axis is taken along the straight-edge and the x axis coincides with the stiffener and if the sheet is assumed rigid in the y direction, the stress function H is determined by the differential equation

$$\frac{\partial^2 H}{\partial x^2} + \frac{G}{E}\frac{\partial^2 H}{\partial y^2} = 0 \tag{146}$$

and the boundary conditions

$$H(o,y) = 0 \tag{147a}$$

$$H(\infty,y) = 0 \tag{147b}$$

$$-2t\ H(x,o) + A\frac{\partial H(x,o)}{\partial y} = F \tag{147c}$$

$$H(x,\infty) = 0 \tag{147d}$$

If it is assumed that H is the Laplace transform of a function g to be determined, it follows that

$$H(x,y) = \int_o^\infty e^{-yp}\, g(x,p)\, dp \tag{148}$$

The differential equation (146) requires that g satisfy the equation

$$\left.\begin{aligned} \frac{\partial^2 g}{\partial x^2} + k^2 p^2 g &= 0 \\ k &= \sqrt{\frac{G}{E}} \end{aligned}\right\} \tag{149}$$

while condition (147a) is satisfied if

$$g(o,p) = 0 \tag{150}$$

so that

$$g(x,p) = h(p) \sin k\, x\, p \tag{151}$$

where h is an arbitrary function of p.

If this expression is introduced into equation (148), condition (147c) requires that $h(p)$ satisfy the integral equation

$$\int_o^\infty (2t + A\,p)\, h(p) \sin k\, x\, p\, dp = -F \tag{152}$$

which has as solution the expression

$$h(p) = -\frac{2F}{\pi}\frac{1}{p(2t + Ap)} \tag{153}$$

Thus a formal solution of the problem is determined in the form

$$H = -\frac{2F}{\pi A}\int_0^\infty e^{-yp}\frac{\sin k x p}{p\left(p + \frac{2t}{A}\right)}\,dp \tag{154}$$

It can be shown without difficulty that the conditions of equations (147b) and (147d) are satisfied and, furthermore, that the expression (154) constitutes the rigorous solution of the problem.

The stress distribution associated with equation (154) was discussed in a previous section.

COMPARISON OF APPROXIMATE PROCEDURES

Axially Loaded Panels

Although the analysis of panels is not included in reference 1, approximate solutions for most of the cases considered in the third section can be found by the procedure of reference 2. In that procedure the effect of the transverse stretching of the sheet is neglected, in accordance with the present theory. In addition, it is assumed that the resistivity of the sheet in the spanwise direction can be neglected if the sheet area is added to the area of the central longitudinal, or treated as a fictitious central stiffness in the absence of a longitudinal, and a substitute width of one-half the actual panel width is used in the subsequent calculations.

In order to investigate the agreement between the results of this procedure and the present results, panel 8 (fig. 4(h)) is considered. In this case the expressions for the flange stress $\sigma_x(x,w)$ and for the average spanwise normal stress $\sigma_a(x)$ are obtained in the form

$$\sigma_x(x,w) = \frac{2F}{A_m + 2A_e + 2t\,w}\left(1 + \frac{A_m + 2t\,w}{2A_e}e^{-K\frac{x}{w}}\right) \tag{155}$$

and

$$\sigma_a(x) = \frac{2F}{A_m + 2A_e + 2t\ w}\left(1 - e^{-K\frac{x}{w}}\right) \tag{156}$$

where K is a dimensionless constant defined by the relationship

$$K^2 = \frac{G}{E}\ t\ \frac{w}{2}\left(\frac{2}{A_m + 2t\ w} + \frac{1}{A_e}\right) \tag{157}$$

The transverse variation of the spanwise normal stress at each section is assumed in reference 2 to follow a hyperbolic-cosine law, in terms of which the stress variation in the longitudinal can be expressed.

For the numerical evaluation of the solutions two cases are chosen

(a)
$$\left.\begin{aligned} A_m &= t\ w \\ A_e &= \frac{1}{2}\ t\ w \end{aligned}\right\} \tag{158}$$

(b)
$$\left.\begin{aligned} A_m &= 5\ t\ w \\ A_e &= \frac{5}{2}\ t\ w \end{aligned}\right\} \tag{159}$$

corresponding, respectively, to the cases $\alpha = \frac{1}{2}$ and $\alpha = \frac{5}{2}$ in the third section. Figures 16(a) and 16(b) present a comparison of the results of the two procedures. It may be noticed that the Kuhn solution in general overestimates the magnitude of the flange stresses and underestimates the longitudinal stresses, with a resultant increase in the predicted shear-lag effect, which becomes smaller as the contribution of the sheet to the total area of the panel decreases.

The deviation of the Kuhn solution from the exact solution in the neighborhood of the loaded end of the panel is partly due to the fact that, in this region, the transverse variation of the normal stress cannot be satisfactorily approximated by a hyperbolic-cosine law.

Doubly Symmetrical Box Beam with Concentrated Tip Load

If it is assumed that no central sheet stiffener is present, the stresses given by the procedure in reference 1 can be written in the form

$$\sigma_x(x,o) = \sigma_o \left\{ \frac{x}{l} - \frac{7}{2} \frac{(3\beta + 1)(6\beta + 1)}{51\beta^2 + 18\beta + 2} \frac{\sinh K_R \frac{x}{l}}{K_R \cosh K_R} \right\} \tag{160}$$

$$\sigma_x(x,w) = \sigma_o \left\{ \frac{x}{l} + 7 \frac{6\beta + 1}{51\beta^2 + 18\beta + 2} \frac{\sinh K_R \frac{x}{l}}{K_R \cosh K_R} \right\} \tag{161}$$

where σ_o and β are defined by equations (44) and (45) and the parameter K_R is defined by

$$K_R^2 = 21 \frac{G}{E} \frac{(\beta + 1)(6\beta + 1)}{51\beta^2 + 18\beta + 2} \left(\frac{l}{w}\right)^2 \tag{162}$$

This solution was obtained by an application of the method of least work, under the assumption of a parabolic transverse distribution of the spanwise normal stress σ_x.

According to the procedure of reference 2, it is necessary to incorporate the sheet area $2tw$ into a fictitious central stiffness. The following expressions are then obtained for the flange stress and the average sheet stress:

$$\sigma_x(x,w) = \sigma_o \left\{ \frac{x}{l} + \frac{1}{\beta} \frac{\sinh K \frac{x}{l}}{K \cosh K} \right\} \tag{163}$$

$$\sigma_a(x) = \sigma_o \left\{ \frac{x}{l} - \frac{\sinh K \frac{x}{l}}{K \cosh K} \right\} \tag{164}$$

where

$$K^2 = 2 \frac{G}{E} \frac{\beta + 1}{\beta} \left(\frac{l}{w}\right)^2 \tag{165}$$

The stress variation along the center line of the sheet is

again determined by assuming that the sheet normal stress varies according to a hyperbolic-cosine law in the transverse direction.

For a numerical comparison of these solutions, the following values of the parameters are chosen in the same way as in the third section:

$$\left.\begin{aligned} \frac{l}{w} &= 5 \\ \beta = \frac{I_w}{I_s} &= 1 \\ \frac{G}{E} &= \frac{3}{8} \end{aligned}\right\} \tag{166}$$

The shear-lag functions $\left(\frac{\sigma_x(x,w)}{\sigma_o} - \frac{x}{l}\right)$ and $\left(\frac{\sigma_x(x,o)}{\sigma_o} - \frac{x}{l}\right)$, according to the two procedures, are compared with the corresponding functions obtained by the present procedure in figure 17. It is seen that the Reissner solution is in close agreement with the present solution, except in the immediate vicinity of the fixed end, where differences of 11 percent and 8 percent occur in the stress corrections at the center of the sheet and at the flanges, respectively, corresponding to differences of 2.7 percent and 0.8 percent, respectively, in the values of the stresses themselves. The shear-lag effect predicted by the Kuhn solution is again considerably greater than that given by the present procedure. Differences of 62 percent and 35 percent are present in the root-stress corrections at the center of the sheet and at the flanges, respectively, corresponding to differences of 15 percent and 4 percent in the actual stress values.

In view of the fact that for a uniform box beam subjected to a concentrated tip load, the shear-lag effect is comparatively small and is appreciable over only a small part of the span, it seems desirable further to compare the solutions obtained by the approximate methods and by the present procedure for other types of beam and loading where the shear-lag effects are more pronounced.

Effect of a Cut-Out in the Cover Sheet of a Box Beam

The Reissner procedure is not directly applicable to

the analysis of cover sheets with cut-outs, since in the vicinity of the cut-out the transverse distribution of σ_x is no longer approximated by a parabola. It may be pointed out that a least-work solution of the type considered in that procedure would be obtained if it were assumed that the difference between the actual normal stress σ_x and the elementary stress $\sigma_o \frac{x}{l}$ is expressible as the product of a function of x and a function of y. If then the conditions of equilibrium were satisfied and the method of least work were applied, a correction would be obtained that would be identical with the first term of the series given in equation (57). The corresponding stress pattern, for the values of the parameters listed in equation (166), is compared in figure 18 with the pattern obtained by retaining the complete series. It is seen that the first term of the series affords a reasonably accurate correction at a distance from the cut-out greater than one-half the width of the sheet.

The corresponding solution according to the Kuhn procedure can be written in the form

$$\sigma_x(x,w) = \sigma_o \left\{ \frac{x}{l} + \frac{1}{\beta} \frac{\sinh K \frac{x}{l}}{\sinh K} \right\} \tag{167}$$

$$\sigma_a(x) = \sigma_o \left\{ \frac{x}{l} - \frac{\sinh K \frac{x}{l}}{\sinh K} \right\} \tag{168}$$

where, as before, $\sigma_a(x)$ is the average sheet stress and K is defined by equation (165). The stress patterns, for the values of the parameters given in equation (166), are compared with the present results in figure 19. It is seen that the shear-lag effect is greatly overestimated by the Kuhn solution and that, except in the immediate vicinity of the cut-out where the stresses are already known, a better approximation to the actual stresses is given by the first two terms of the present solution.

NUMERICAL APPLICATION OF THE THEORY TO A TEST PANEL

In order to illustrate further the numerical evaluation of the exact theory, the panel sketched in figure 4(j) is analyzed. The results are then compared with the

experimental test results reported in reference 3 and with the approximate results presented in that paper.

If the stress function (30) is modified in accordance with the statement at the beginning of the third section and if

$$\left.\begin{aligned} F_m &= 0 \\ \alpha &= 2\alpha_m \end{aligned}\right\}$$

and

the expressions for the stiffener and flange stresses follow from equation (7a) in the form

$$\sigma_x(x,o) = \frac{F_o}{(3\alpha_m + 1)tw}\left\{1 - \sum_{n=1}^{\infty} \frac{\kappa_n}{F_o}\gamma_n^2 \frac{\cosh\sqrt{\frac{G}{E}}\lambda_n\frac{l-x}{w}}{\cosh\sqrt{\frac{G}{E}}\lambda_n\frac{l}{w}}\right\} \tag{169}$$

$$\sigma_x(x,w) = \frac{F_o}{(3\alpha_m + 1)tw}$$

$$\left\{1 - \sum_{n=1}^{\infty} \frac{\kappa_n}{F_o}\gamma_n^2(\cos\lambda_n - \alpha_m\lambda_n \sin\lambda_n)\frac{\cosh\sqrt{\frac{G}{E}}\lambda_n\frac{l-x}{w}}{\cosh\sqrt{\frac{G}{E}}\lambda_n\frac{l}{w}}\right\} \tag{170}$$

where, from equation (34), the constants λ_n are the solutions of the equation

$$\tan\lambda_n = \frac{3\alpha_m\lambda_n}{2\alpha_m^2\lambda_n^2 - 1} \tag{171}$$

and the definitions of the remaining constants, as given in equations (32) and (33), take the form

$$\frac{1}{\gamma_n^2} = \frac{w}{4\lambda_n^3}\left\{(2\lambda_n - \sin 2\lambda_n) - 2\alpha_m\lambda_n(\cos 2\lambda_n - 1) + \alpha_m^2\lambda_n^2(2\lambda_n + \sin 2\lambda_n)\right\} \tag{172}$$

$$\frac{\kappa_n}{F_E} = \frac{w}{\lambda_n^3}\left\{(\sin\lambda_n - \lambda_n\cos\lambda_n) + \alpha_m(1+\alpha_m)\lambda_n\sin\lambda_n\right\} \tag{173}$$

In accordance with the notation of the third section, the following data are to be assumed:

$$\left.\begin{aligned} F_m &= 0 \\ F_e &= 2400 \\ w &= 4.60 \\ l &= 36 \\ t &= 0.016 \\ A_m = A_e &= 0.366 \\ \frac{G}{E} &= 0.4 \end{aligned}\right\} \tag{174}$$

and hence, from equation (31),

$$\left.\begin{aligned} \alpha &= 2\alpha_m \\ \alpha_m &= 2.487 \end{aligned}\right\} \tag{175}$$

First, from equation (171), the parameters λ_n are determined readily by a method of successive approximations, after which the following table is constructed from equations (172) and (173):

n	λ_n	$\frac{\kappa_n}{F_e}\gamma_n^2$	$\cos \lambda_n - \alpha_m \lambda_n \sin \lambda_n$
1	0.7521	1.0522	−0.5478
2	3.323	−.1229	.5704
3	6.397	.0412	−.8134

(176)

The results obtained by introducing the data of equations (174), (175), and (176) into equations (169) and (170) are presented in tabular form and the computed stresses are compared with the corresponding values determined by approximate formulas given by Kuhn in reference 3, as follows:

	Solution by equation (169)					Kuhn solution	
x	First term	Second term	Third term	Fourth term	$\sigma_x(x,o)$	$\sigma_x(x,o)$	
0	3850	−4050	470	−160	110 (0)	0	
3	3850	−2970	120	−10	990	990	
5	3850	−2420	50	———	1480	1500	
8	3850	−1770	10	———	2090	2110	(177)
10	3850	−1440	———	———	2420	2420	
15	3850	−860	———	———	2990	2960	
20	3850	−530	———	———	3320	3300	
25	3850	−330	———	———	3520	3500	
30	3850	−230	———	———	3620	3600	
36	3850	−190	———	———	3660	3630	

	Solution by equation (170)					Kuhn solution	
x	First term	Second term	Third term	Fourth term	$\sigma_x(x,w)$	$\sigma_x(x,w)$	
0	3850	2220	270	130	6470 (6560)	5960	
3	3850	1630	70	10	5560	5420	
5	3850	1330	30	———	5210	5140	
8	3850	970	10	———	4830	4810	(178)
10	3850	800	———	———	4650	4640	
15	3850	480	———	———	4330	4330	
20	3850	290	———	———	4140	4160	
25	3850	190	———	———	4040	4050	
30	3850	130	———	———	3980	4000	
36	3850	110	———	———	3960	3980	

The calculated stresses, together with the test data taken from reference 3, are presented graphically in figure 20.

It is seen that the convergence of the series is sufficiently rapid that only two terms of the correction series need be retained. While the prescribed boundary values (noted in parentheses in equations (177) and (178)) are not yet attained, this fact is of no consequence since the values are known and since the calculated stress values at a distance of only 3 inches from the free end are apparently accurate to three significant figures. The Kuhn solution was calculated by associating one-half the sheet area with the longitudinal and the remainder with the two flanges, and is in very good agreement with the present solution except near the point of load application.

The discrepancies between the theoretical and the test values, as was pointed out in reference 3, can be attributed to two factors: (1) because of the magnitude of the loading, an observed tension fold was developed on each side of the panel near the loaded end, reducing the effective shear modulus in this region; and (2) the fact that the flange stress readings near the root of the panel are actually less than the statically requisite limiting values for an infinitely long panel must be accounted for by assuming an elastic deformation of the steel triangle which served as the panel support.

MISCELLANEOUS EXTENSIONS AND MODIFICATIONS OF THE THEORY

Analysis of Tapered Box Beams

The procedure given in this paper can be extended in many cases to apply to box beams or panels the cross-sectional characteristics of which vary along the span. Three explicit cases may be mentioned here.

Taper in beam height.- The basic equations (C) again apply. If it is assumed that the side-web characteristics also vary in such a way that the ratio of the contributions of the web and of the sheet to the total stiffness of the beam remains constant along the span, so that

$$\beta = \frac{I_w}{I_s} = \text{constant} \qquad (179)$$

the effect of varying height can be taken into account by merely replacing $\frac{h}{2I}\frac{d^n}{dx^n}M(x)$ by $\frac{d^n}{dx^n}\left(\frac{M(x)}{I}\frac{h}{2}\right)$ in the definition of the function $P(x,y)$ as given in equation (125).

Taper in cover-sheet thickness.- If the problem is formulated in terms of the stress resultants rather than in terms of the stresses themselves and if a stress function Φ is defined, in terms of which

$$\left.\begin{aligned} t\,\sigma_x &= \frac{\partial\Phi}{\partial y} \\ t\,\tau &= -\frac{\partial\Phi}{\partial x} \end{aligned}\right\} \tag{180}$$

it is found that Φ is determined by the differential equation

$$t\,\frac{\partial}{\partial x}\left[\frac{1}{t}\frac{\partial\Phi}{\partial x}\right] + \frac{G}{E}\frac{\partial^2\Phi}{\partial y^2} = 0 \tag{181}$$

and boundary conditions that differ from those which apply to the function H in equation (C) only by the substitution of $t\,M(x)$ for $M(x)$. If it is assumed that

$$\left.\begin{aligned} \frac{A_w}{t} &= \text{constant} \\ \frac{I_w}{I_s} &= \text{constant} \end{aligned}\right\} \tag{182}$$

the solution can be readily obtained in terms of Bessel functions, by a modification of the procedure of a preceding section, for beams in which the cover-sheet thickness varies according to a law of the form

$$t(x) = t_o(x + x_o)^n \tag{183}$$

For example, if a box beam in which the cover-sheet thickness tapers linearly to zero at the free end, so that

$$t(x) = t_R \frac{x}{l} \tag{184}$$

is subjected to a uniformly distributed load of intensity p_o, so that

$$M(x) = \frac{1}{2} p_o x^2 \tag{185}$$

and if the beam is fixed at the end $x = l$ (no central sheet stiffener being present), the stress function Φ is obtained in the form

$$\Phi = w t_R \sigma_o \frac{x}{l}\left\{\frac{x}{l}\frac{y}{w} + 4(\beta+1)\sqrt{\frac{E}{G}}\frac{w}{l}\sum_{n=1}^{\infty}\frac{\cos\lambda_n \sin\lambda_n \frac{y}{w}}{\lambda_n^2(1+\beta\cos^2\lambda_n)}\frac{I_1\left(\mu_n\frac{x}{l}\right)}{I_o(\mu_n)}\right\} \tag{186}$$

where I_o and I_1 are modified Bessel functions of the first kind, of orders zero and one, σ_o is the maximum elementary stress, and the remaining quantities are defined in equations (45) and (46). From equation (180) the stresses are given by the expressions

$$\sigma_x = \sigma_o\left\{\frac{x}{l} + 4(\beta+1)\sqrt{\frac{E}{G}}\frac{w}{l}\sum_{n=1}^{\infty}\frac{\cos\lambda_n\cos\lambda_n\frac{y}{w}}{\lambda_n(1+\beta\cos^2\lambda_n)}\frac{I_1\left(\mu_n\frac{x}{l}\right)}{I_o(\mu_n)}\right\} \tag{187}$$

$$\tau = -\sigma_o\frac{w}{l}\left\{\frac{y}{w} + 4(\beta+1)\sum_{n=1}^{\infty}\frac{\cos\lambda_n\sin\lambda_n\frac{y}{w}}{\lambda_n(1+\beta\cos^2\lambda_n)}\frac{I_o\left(\mu_n\frac{x}{l}\right)}{I_o(\mu_n)} + \frac{\sigma_x}{\sigma_o\frac{x}{l}}\right\} \tag{188}$$

An approximate solution of the same problem is given in reference 5.

Tapered cover-sheet width.- The principal modification necessary in case the width of the sheet varies in the spanwise direction arises from the fact that the normal stress in the flange can no longer be identified with the spanwise normal stress in the adjacent sheet fibers, but is related to the sheet stresses by the expression

$$[\sigma(x)]_{flange} = \sigma_x(x,w)\cos^2\delta + \sigma_y(x,w)\sin^2\delta + \tau(x,w)\sin 2\delta \quad (189)$$

where δ is the angle between the x-axis and the normal to the edge of the sheet.

A More General Class of End-Support Conditions

If equation (C3) is replaced by a condition of the more general form

$$a_0 H(l,y) + a_1 \frac{\partial H(l,y)}{\partial x} + a_2 \frac{\partial^2 H(l,y)}{\partial x^2} + a_3 \frac{\partial^3 H(l,y)}{\partial x^3} + \ldots = f(y) \quad (190)$$

equation (122) can be used to rewrite the equation replacing equation (123b) in the form

$$\sum_n \left\{ \left[a_0 + a_2 \left(\frac{\mu_n}{l}\right)^2 + \ldots \right] X_n(l) + \left[a_1 + a_3 \left(\frac{\mu_n}{l}\right)^2 + \ldots \right] X_n'(l) \right\} Y_n(y)$$

$$= f(y) - [a_0 P(l,y) + a_1 P_x(l,y) + a_2 P_{xx}(l,y) + a_3 P_{xxx}(l,y) + \ldots] \quad (191)$$

The only modification in the solution therefore consists in replacing the terminal condition of equation (130b) by the condition

$$\left[a_0 + a_2 \left(\frac{\mu_n}{l}\right)^2 + \ldots \right] X_n(l) + \left[a_1 + a_3 \left(\frac{\mu_n}{l}\right)^2 + \ldots \right] X_n'(l)$$

$$= \int_0^w \left\{ f(\mu) - a_0 P(l,u) - a_1 P_x(l,u) - a_2 P_{xx}(l,u) - \ldots \right\} Y_n(u)\,du \quad (192)$$

For example, if the box beam is attached to an elastic springlike support, the end condition is of the form

$$u(l,y) = -c\,\sigma_x(l,y) \quad (193)$$

If both sides of equation (193) are differentiated with respect to y, and if equations (5), (7), and (C1) are used, this condition can be written

$$\frac{\partial H(l,y)}{\partial x} + c\,E\,\frac{\partial^2 H(l,y)}{\partial x^2} = 0 \qquad (194)$$

For the case of a concentrated tip load, equation (139b) is now replaced, according to equation (192), by

$$c\,E\left(\frac{\mu_n}{l}\right)^2 X_n(l) + X_n'(l) = \frac{w^2}{l}\,\sigma_o\,\gamma_n(\beta+1)\,\frac{\cos\lambda_n}{\lambda_n} \qquad (195)$$

so that, in place of equation (140),

$$X_n(x) = w^2\sigma_o\gamma_n(\beta+1)\,\frac{\cos\lambda_n}{\lambda_n}\,\frac{\sinh\mu_n\frac{x}{l}}{\frac{c\,E}{l}\mu_n^2\sinh\mu_n + \mu_n\cosh\mu_n} \qquad (196)$$

and the stress function is obtained in the form

$$H = w\,\sigma_o\left\{\frac{x}{l}\,\frac{y}{w} + 2(\beta+1)\sqrt{\frac{E}{G}}\,\frac{w}{l}\sum_{n=1}^{\infty}\frac{\cos\lambda_n\sin\lambda_n\frac{y}{w}}{\lambda_n(1+\beta\cos^2\lambda_n)}\,\frac{\sinh\mu_n\frac{x}{l}}{\frac{c\,E}{l}\mu_n\sinh\mu_n+\cosh\mu_n}\right\} \qquad (197)$$

Box Beam with One Cover Sheet

If a box beam carries a cover sheet on only one side, the equation of moment equilibrium about the neutral axis becomes (see reference 6, p. 11, equation (12))

$$I_w\sigma_x(x,w) + 2t\left(d^2 + \frac{I_w}{A_w}\right)\int_o^w \sigma_x dy + A_m\left(d^2 + \frac{I_w}{A_w}\right) = M(x)d \qquad (198)$$

where, in addition to the constants previously defined, A_w is the cross-sectional area of the two side webs (including the corner flanges) and d is the distance from the plane of the cover sheet to the neutral axis. If equation (198) is expressed in terms of H and if equation (88) is taken into account, equation (90) is now replaced by the condition

$$2tw\left(d^2 + \frac{I_w}{A_w}\right)\frac{H(x,w)}{w} + I_w\,\frac{\partial H(x,w)}{\partial y} = M(x)d \qquad (199)$$

It follows that the results of the preceding sections can be applied directly to this case if I_s is replaced by $2t\,w\left(d^2 + \frac{I_w}{A_w}\right)$ and $\frac{h}{2}$ by d.

CONCLUDING REMARKS

The shear-lag analysis of the present paper presents mathematically exact solutions of several problems that have been previously treated in general by approximate methods. Although the results strictly apply only to beams and panels that are theoretically rigid in the transverse direction, it seems probable that they are applicable with reasonable accuracy in actual cases when stiff chordwise ribs are present. The solutions are obtained in the form of rapidly convergent infinite series that are much more adaptable to numerical computation than exact solutions that have been given elsewhere in certain special cases.

On the basis of comparisons of the present results with approximate solutions given by Reissner and by Kuhn and Chiarito, it appears that in cases when both the approximate solutions are applicable, for example, uniform rectangular box beams without cut-outs, the Reissner solutions are in better agreement with the exact solutions than are the solutions given by the methods of Kuhn and Chiarito. In other cases for which the Reissner procedure was not designed, for example, box beams with cut-outs and panels loaded by concentrated axial forces, the solutions given by the procedure of Kuhn and Chiarito predict shear-lag effects that are in general considerably larger than those given by the present procedure.

Department of Mathematics,
Massachusetts Institute of Technology,
Cambridge, Mass., July 1942.

REFERENCES

1. Reissner, Eric: Least Work Solutions of Shear Lag Problems. Jour. Aeron. Sci., vol. 8, no. 7, May 1941, pp. 284-291.

2. Kuhn, Paul, and Chiarito, Patrick T.: Shear Lag in Box Beams - Methods of Analysis and Experimental Investigations. Rep. No. 739 (to be issued), NACA, 1942.

3. Kuhn, Paul: Stress Analysis of Beams with Shear Deformation of the Flanges. Rep. No. 608, NACA, 1937.

4. Younger, John E.: Metal Wing Construction. Pt. II - Mathematical Investigations. A.C.T.R. ser. no. 3288, Materiel Div., Army Air Corps, 1930.

5. Hildebrand, Francis B., and Reissner, Eric: Least-Work Analysis of the Problem of Shear Lag in Box Beams. T.N. No. 893, NACA, 1943.

6. Newell, Joseph S., and Reissner, Eric: Shear Lag in Corrugated Sheets Used for the Chord Member of a Box Beam. T.N. No. 791, NACA, 1941.

Table 1.- Solutions of $\tan \lambda_n + \alpha\lambda_n = 0$.

n	λ_n	
	$\alpha = 1$	$\alpha = 5$
1	2.0288	1.6887
2	4.9132	4.7544
3	7.9787	7.8794
4	11.0855	11.0157
5	14.2074	14.1513
6	17.3364	17.2903
7	20.4692	20.4301
8	23.6043	23.5704
9	26.7409	26.7110
10	29.8786	29.8518
11	33.0170	32.9928
12	36.1560	36.1339
13	39.2954	39.2750
14	42.4351	42.4162
15	45.5750	45.5575

Table 2.- Stresses in Panel No. 1.

$\frac{x}{w}$	$\alpha = 1$			$\alpha = 5$			$\alpha = 0$	
	$\frac{A}{F}\sigma_x(x,0)$	$\frac{A}{F}\sigma_x(x,w)$	$\frac{A}{F}\tau(x,w)$	$\frac{A}{F}\sigma_x(x,0)$	$\frac{A}{F}\sigma_x(x,w)$	$\frac{A}{F}\tau(x,w)$	$\frac{tw}{F}\sigma_x(x,0)$	$\frac{tw}{F}\sigma_x(x,w)$
0	0	1.	$-\infty$	0	1.	$-\infty$	0	∞
0.1	.036	.88	-.79	.062	.97	-1.06	.096	10.43
0.2	.071	.816	-.543	.113	.951	-.806	.190	5.26
0.4	.159	.728	-.338	.213	.925	-.553	.367	2.726
0.8	.256	.628	-.172	.391	.891	-.319	.647	1.546
1.2	.343	.575	-.097	.530	.871	-.200	.819	1.221
1.6	.402	.546	-.058	.628	.858	-.129	.912	1.097
2.0	.440	.528	-.034	.697	.850	-.085	.958	1.044
3.0	.482	.508	-.010	.784	.839	-.030	.994	1.006
5.0	.499	.501	-.001	.828	.834	-.004	1.000	1.000

Table 3.- Solutions of $\tan \lambda_n = \frac{\lambda_n}{\alpha\lambda_n^2 + 1}$

n	λ_n		
	$\alpha = 0$	$\alpha = 1$	$\alpha = 5$
1	4.4934	3.4056	3.2028
2	7.7253	6.4338	6.3147
3	10.9041	9.5272	9.4459
4	14.0662	12.6448	12.5823
5	17.2208	15.7710	15.7207
6	20.3713	18.9025	18.8602
7	23.5195	22.0364	22.0002
8	26.6661	25.1724	25.1407
9	29.8116	28.3096	28.2814
10	32.9564	31.4477	31.4223
11	36.1006	34.5864	34.5633
12	39.2444	37.7256	37.7044
13	42.3879	40.8652	40.8456
14	45.5311	44.0050	43.9869
15	48.6742	47.1451	47.1281

Table 4.- Stresses in Panel No. 2.

$\frac{x}{w}$	$\alpha = 1$			$\alpha = 5$			$\alpha = 0$	
	$\frac{A}{F}\sigma_x(x,w)$	$\frac{A}{F}\tau(x,0)$	$\frac{A}{F}\tau(x,w)$	$\frac{A}{F}\sigma_x(x,w)$	$\frac{A}{F}\tau(x,0)$	$\frac{A}{F}\tau(x,w)$	$\frac{tw}{F}\sigma_x(x,w)$	$\frac{tw}{F}\tau(x,0)$
0	1.	.21	$-\infty$	1.	.259	$-\infty$	∞	∞
0.1	.911	.189	-.55	.980	.224	-.67	11.6	1.016
0.2	.867	.160	-.340	.972	.192	-.420	6.57	.722
0.4	.818	.113	-.171	.959	.140	-.225	4.225	.416
0.8	.776	.055	-.059	.944	.070	-.085	3.279	.150
1.2	.761	.026	-.024	.941	.054	-.036	3.081	.055
1.6	.755	.011	-.010	.939	.016	-.016	3.025	.018
2.0	.753	.005	-.004	.937	.007	-.007	3.008	.006
3.0	.751	.001	-.001	.936	.001	-.001	3.001	.000
5.0	.750	.000	-.000	.936	.000	-.000	3.000	.000

Table 5.- Solutions of cot $\lambda_n - 2\alpha\lambda_n = 0$.

n	λ_n	
	$\alpha = 1/2$	$\alpha = 5/2$
1	.86033	.43284
2	3.4256	3.2039
3	6.4373	6.3148
4	9.5293	9.4459
5	12.6453	12.5823
6	15.7715	15.7207
7	18.9024	18.8602
8	22.0365	22.0002
9	25.1724	25.1407
10	28.3096	28.2814
11	31.4477	31.4223
12	34.5864	34.5633
13	37.7256	37.7044
14	40.8652	40.8456
15	44.0050	43.9869

Table 6.- Stresses in Panel No. 6.

$\frac{x}{w}$	$\alpha = 1/2$			$\alpha = 5/2$		
	$\frac{A_e}{F}\sigma_x(x,\frac{w}{2})$	$\frac{A_e}{F}\sigma_x(x,w)$	$\frac{A_e}{F}\tau(x,w)$	$\frac{A_e}{F}\sigma_x(x,\frac{w}{2})$	$\frac{A_e}{F}\sigma_x(x,w)$	$\frac{A_e}{F}\tau(x,w)$
0	0	1.	$-\infty$	0	1.	$-\infty$
0.05	.036	.88	-.79	.062	.97	-1.08
0.1	.071	.816	-.543	.113	.951	-.806
0.15	.106	.766	-.419	.164	.937	-.657
0.2	.139	.728	-.338	.213	.925	-.553
0.4	.256	.628	-.172	.391	.891	-.319
0.6	.343	.576	-.097	.530	.871	-.200
0.8	.402	.546	-.058	.628	.858	-.129
1.0	.440	.528	-.034	.697	.850	-.085
1.5	.482	.508	-.010	.784	.839	-.050
2.5	.499	.501	-.001	.828	.834	-.004

Table 7.- Stresses in Panel No. 7.

$\frac{x}{w}$	$\alpha = 1/2$		$\alpha = 5/2$	
	$\frac{A_e}{F}\sigma_x(x,w)$	$\frac{A_e}{F}\tau(x,w)$	$\frac{A_e}{F}\sigma_x(x,w)$	$\frac{A_e}{F}\tau(x,w)$
0	1.	$-\infty$	1.	$-\infty$
0.05	.867	-.954	.955	-1.86
0.1	.785	-.716	.920	-1.606
0.2	.667	-.500	.862	-1.347
0.4	.508	-.319	.766	-1.091
0.6	.400	-.231	.685	-.940
0.8	.319	-.177	.614	-.828
1.0	.257	-.159	.552	-.738
1.5	.151	-.060	.423	-.561
2.5	.052	-.028	.249	-.330
5.0	.004	-.002	.005	-.006

Table 8a.- Stresses in Panel No. 8. $(\alpha = \frac{1}{2})$

$\frac{x}{w}$	$\frac{A_e}{F}\sigma_x(x,0)$	$\frac{A_e}{F}\sigma_x(x,\frac{w}{2})$	$\frac{A_e}{F}\sigma_x(x,w)$	$\frac{A_e}{F}\tau(x,0)$	$\frac{A_e}{F}\tau(x,w)$
0	0	0	1.	.09	$-\infty$
0.05	.008	.018	.876	.09	-.869
0.1	.015	.035	.800	.087	-.629
0.15	.022	.055	.744	.084	-.503
0.2	.030	.069	.697	.082	-.419
0.3	.045	.101	.625	.077	-.312
0.4	.061	.128	.569	.074	-.245
0.6	.088	.178	.488	.067	-.164
0.8	.113	.201	.452	.060	-.117
1.0	.135	.220	.392	.052	-.087
2.0	.207	.248	.296	.022	-.025
5.0	.248	.250	.252	.001	-.001

Table 8b.- Stresses in Panel No. 9. ($\alpha = \frac{5}{2}$)

$\frac{x}{w}$	$\frac{A_9}{F}\sigma_x(x,0)$	$\frac{A_9}{F}\sigma_x(x,\frac{w}{2})$	$\frac{A_9}{F}\sigma_x(x,w)$	$\frac{A_9}{F}\tau(x,0)$	$\frac{A_9}{F}\tau(x,w)$
0	0	0	1.	.40	
0.05	.007	.031	.965	.40	-1.46
0.1	.016	.056	.935	.400	-1.206
0.15	.024	.082	.913	.399	-1.056
0.2	.032	.106	.895	.397	-.950
0.3	.048	.154	.858	.392	-.805
0.4	.062	.195	.829	.386	-.705
0.6	.093	.265	.778	.370	-.570
0.8	.122	.314	.736	.350	-.479
1.0	.149	.349	.701	.326	-.411
2.0	.256	.408	.580	.210	-.221
5.0	.383	.416	.450	.043	-.044

Table 9.- Edge Stresses in Unstiffened Panels. ($\alpha = 0$)

$\frac{x}{w}$	$\frac{tw}{F}\sigma_x(x,w)$		
	Panel No. 7	Panel No. 8	Panel No. 2
0	--	--	--
0.1	10.524	10.330	11.612
0.2	5.452	5.072	6.572
0.3	3.842	3.280	4.975
0.4	3.092	2.358	4.225
0.6	2.442	1.400	3.554
0.8	2.194	.900	3.279
1.0	2.088	.596	3.148
1.25	2.032	.364	3.071
1.50	2.012	.224	3.034
2.0	2.002	.086	3.008
2.5	2.000	.032	3.002

Table 10.- Stresses in Cover Sheet of Box Beam Without Cutout.

$\frac{x}{l}$	$\beta = 1$		$\beta = 0$	
	$\sigma_x(x\rho)/\sigma_0$	$\sigma_x(x,w)/\sigma_0$	$\sigma_x(x\rho)/\sigma_0$	$\sigma_x(xw)/\sigma_0$
0	0	0	0	0
0.1	.099	.100	.100	.100
0.2	.199	.201	.200	.200
0.3	.297	.301	.300	.300
0.4	.394	.403	.400	.401
0.5	.489	.505	.499	.502
0.6	.580	.609	.596	.605
0.7	.664	.716	.689	.712
0.8	.734	.831	.772	.833
0.9	.782	.959	.833	1.000
0.95	.795	1.033	.850	1.150
0.97	- - - -	- - - -	- - - -	1.258
0.99	- - - -	- - - -	- - - -	1.487
1.00	.800	1.120	.856	∞

Table 11.- Transverse Distribution of Root Normal Stress in Cover Sheet of Box Beam Without Cutout.

$\frac{y}{w}$	$\sigma_x(l,y)/\sigma_0$	
	$\beta = 1$	$\beta = 0$
0	.800	.856
0.1	.801	.858
0.2	.807	.866
0.3	.817	.880
0.4	.831	.900
0.5	.851	.928
0.6	.876	.966
0.7	.908	1.020
0.8	.951	1.100
0.9	1.011	1.242
0.99	- - - -	1.720
0.999	- - - -	2.198
1.000	1.120	--

Table 12.- Spanwise Variation of Cover-sheet Effective Width.

$\frac{x}{l}$ \ $\frac{w_{eff}}{w}$	Fixed sheet		Free sheet	
	$\beta = 1$	$\beta = 0$	$\beta = 1$	$\beta = 0$
0	1.	1.	1.	1.
0.1	.994	1.000	.997	.997
0.2	.993	1.000	.971	.996
0.3	.991	.999	.950	.992
0.4	.988	.998	.926	.985
0.5	.981	.996	.889	.968
0.6	.971	.992	.833	.932
0.7	.954	.983	.743	.856
0.8	.926	.960	.605	.701
0.9	.877	.900	.393	.421
0.95	.859	.826	.242	.227
0.97	-	.771	-	-
0.99	-	.666	-	-
1.00	.786	0	0	0

Table 13.- Stresses in Cover Sheet of Box Beam With Cutout.

$\frac{x}{l}$	$\beta = 1$		$\beta = 0$	
	$\sigma_x(x,\rho)/\sigma_0$	$\sigma_x(x,w)/\sigma_0$	$\sigma_x(x,0)/\sigma_0$	$\sigma_x(x,w)/\sigma_0$
0	0	0	0	0
0.1	.096	.101	.100	.100
0.2	.191	.204	.199	.201
0.3	.281	.308	.298	.302
0.4	.365	.416	.394	.406
0.5	.434	.529	.484	.516
0.6	.479	.655	.558	.644
0.7	.479	.803	.594	.818
0.8	.408	.997	.545	1.142
0.9	.242	1.292	.347	2.137
0.95	.127	1.53	.186	4.188
1.00	0	2.000	0	-

Table 14.

Stresses in stiffened half-sheet.			Stresses in unstiffened half-sheet.	
$\sqrt{\frac{G}{E}}\frac{tx}{A}$	$\frac{A}{F}\sigma_x(x,0)$	$\sqrt{\frac{E}{G}}\frac{A}{F}\tau(x,0)$	$\sqrt{\frac{G}{E}}\frac{x}{t}$	$\frac{t^2}{F}\sigma_x(x,0)$
0	1.	-	0	-
0.01	.968	2.574	0.01	63.66
0.10	.822	1.188	0.10	6.366
0.25	.685	.717	0.25	2.547
0.50	.548	.428	0.50	1.273
1.	.396	.219	1.	.637
2.	.254	.092	2.	.318
5.	.120	.022	5.	.127
10.	.063	.006	10.	.064

Table 15.- Comparison of values of $\frac{t^2}{F}\sigma_x(x,0)$ according to equations (71), (72), and (63).

$\frac{x}{t}$ \ $\frac{t^2}{F}\sigma_x(x,0)$	Distributed load		($A = t^2$) Concentrated load
	$E_y = \infty$	$E_x = E_y$	
0	1.	1.	1.
0.016	.994	1.	.968
0.163	.938	.998	.822
0.408	.844	.976	.685
0.817	.705	.888	.548
1.633	.500	.635	.396
3.266	.294	.369	.254
8.165	.125	.155	.120
16.330	.064	.078	.063

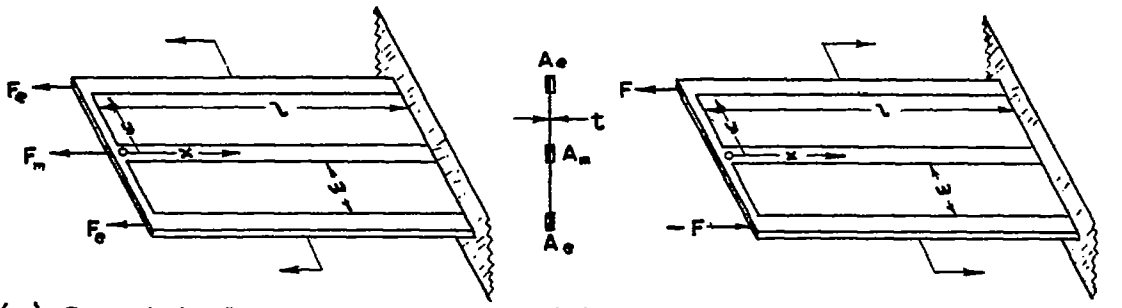

(a) Symmetrical axial loading. (b) Antisymmetrical axial loading.

Figure 1.- Sketches of panels indicating the notation used.

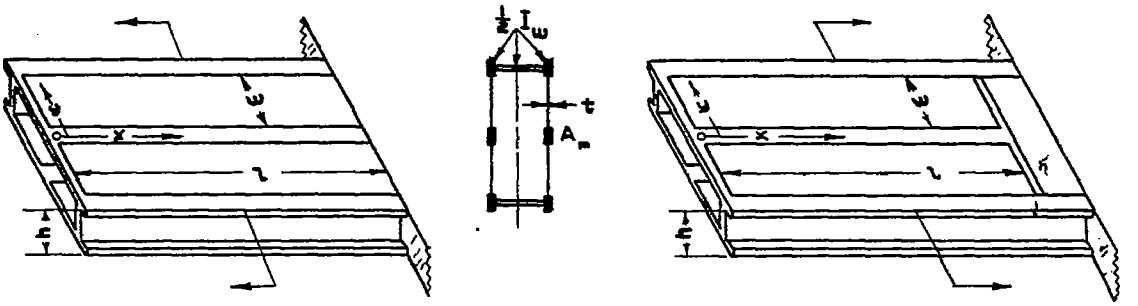

(a) Completely clamped along edge at $x = l$.

(b) Cover sheets not attached to support.

Figure 2.- Sketches of cantilever box beams.

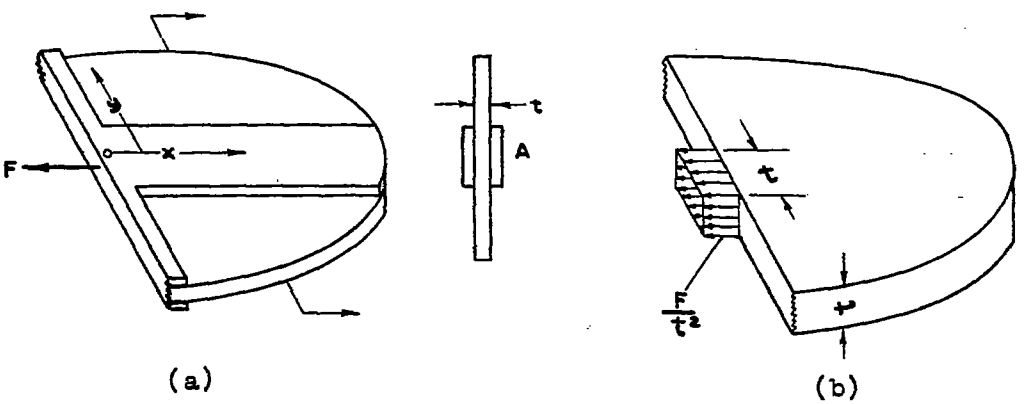

(a) (b)

Figure 3.- Sketches of half-sheets loaded by concentrated and distributed forces.

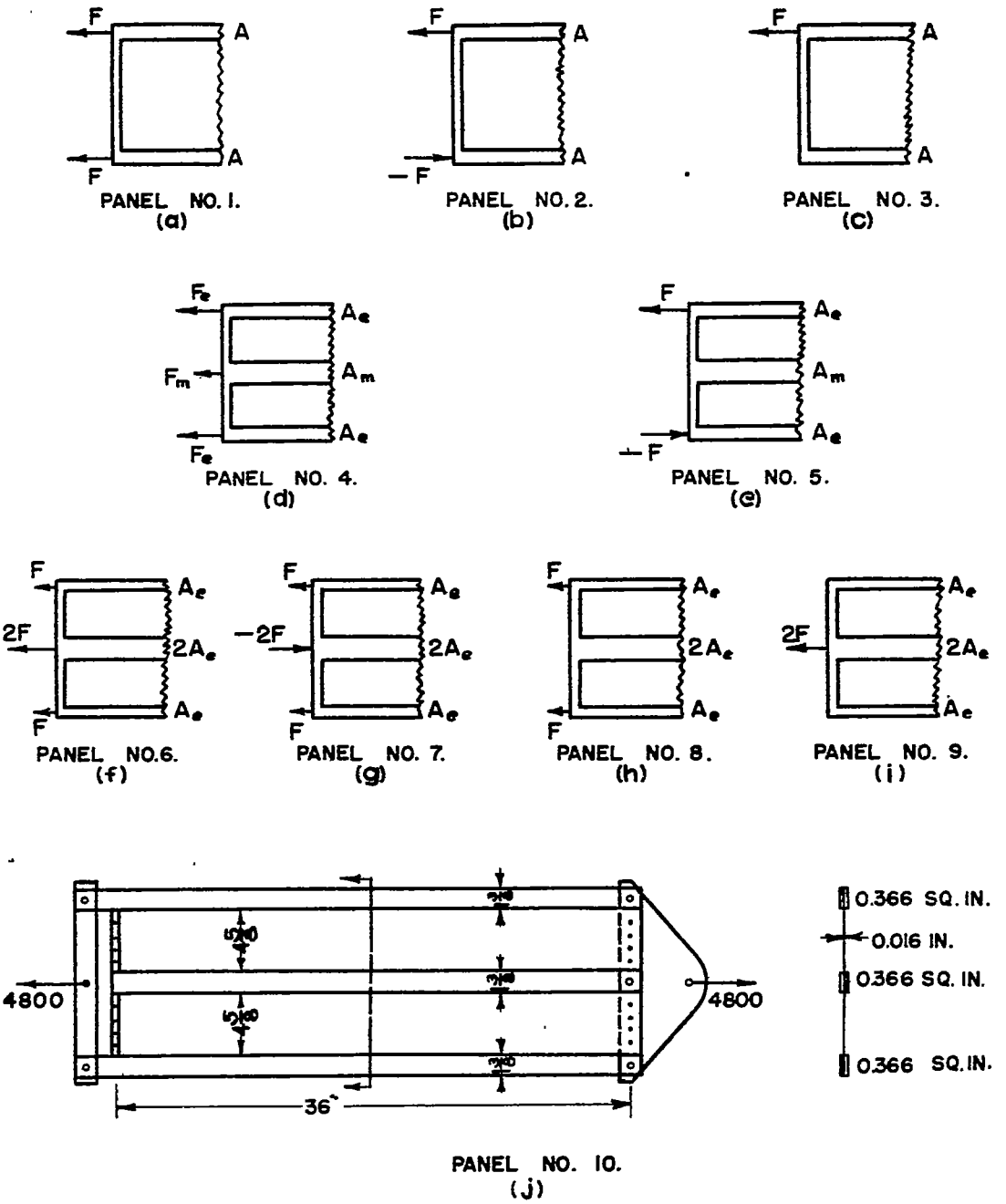

Figure 4.- Sketches of panels showing notation and dimensions.

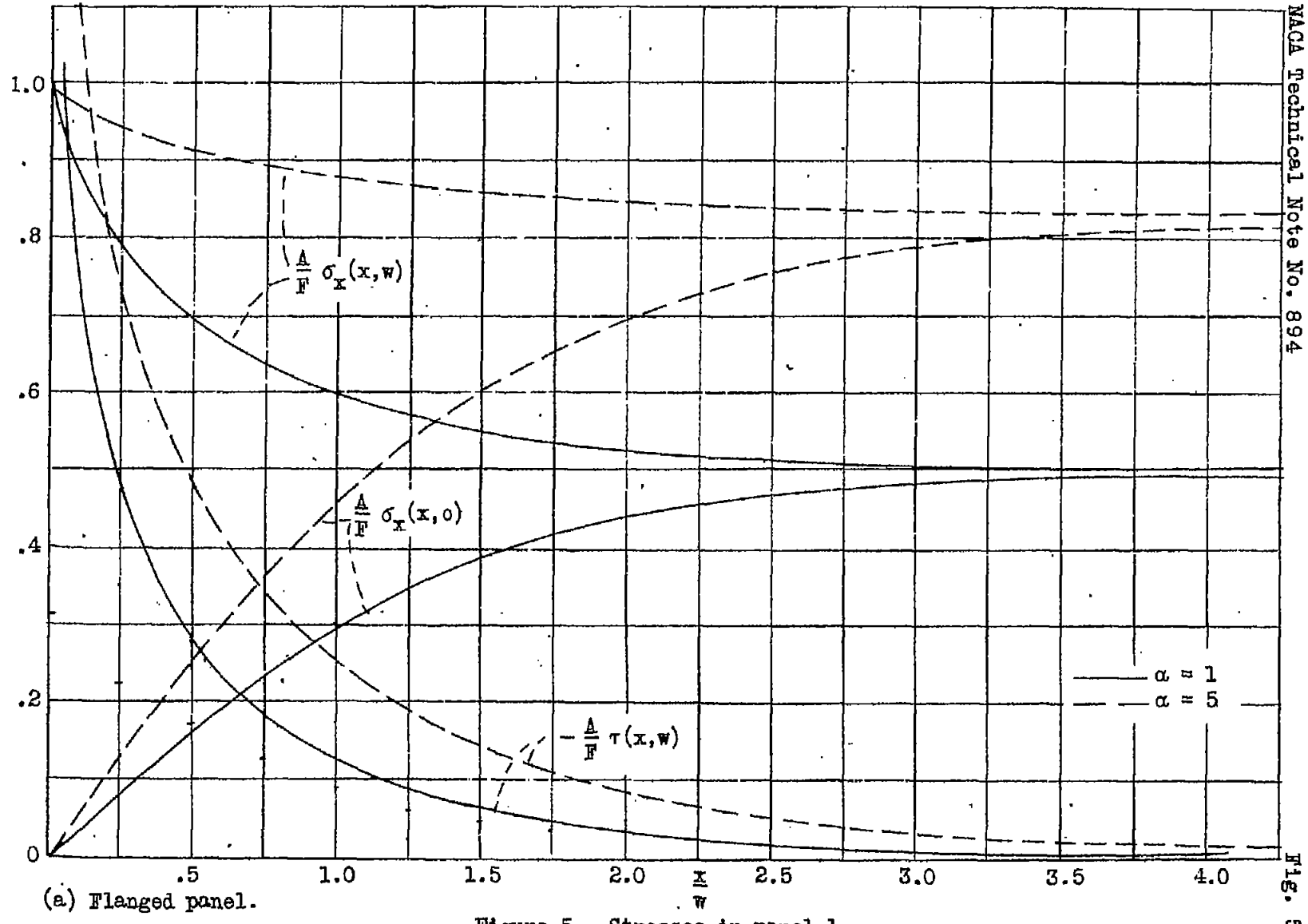

(a) Flanged panel.

Figure 5.- Stresses in panel 1.

Fig. 5a

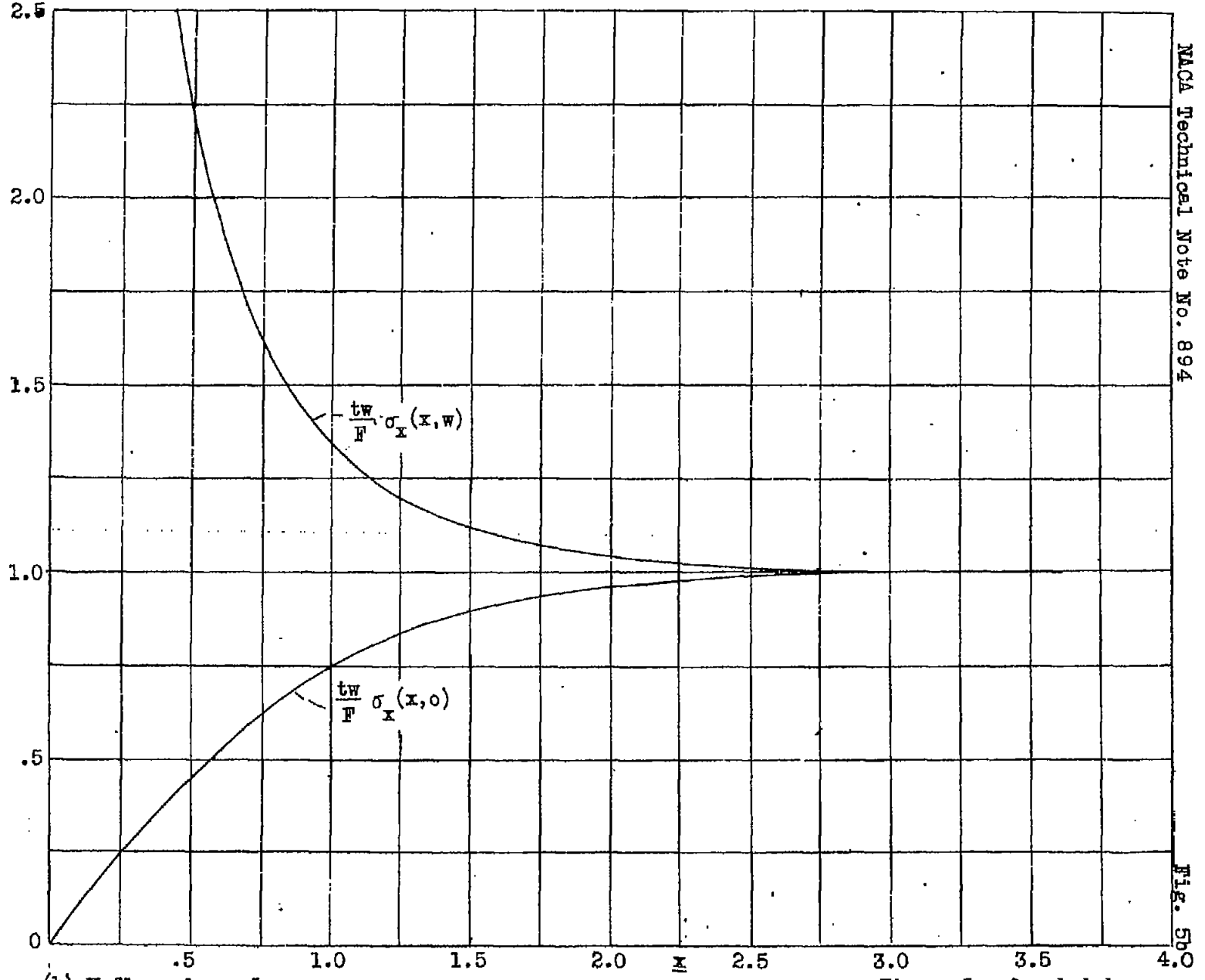

(b) Unflanged panel

Figure 5.- Concluded.

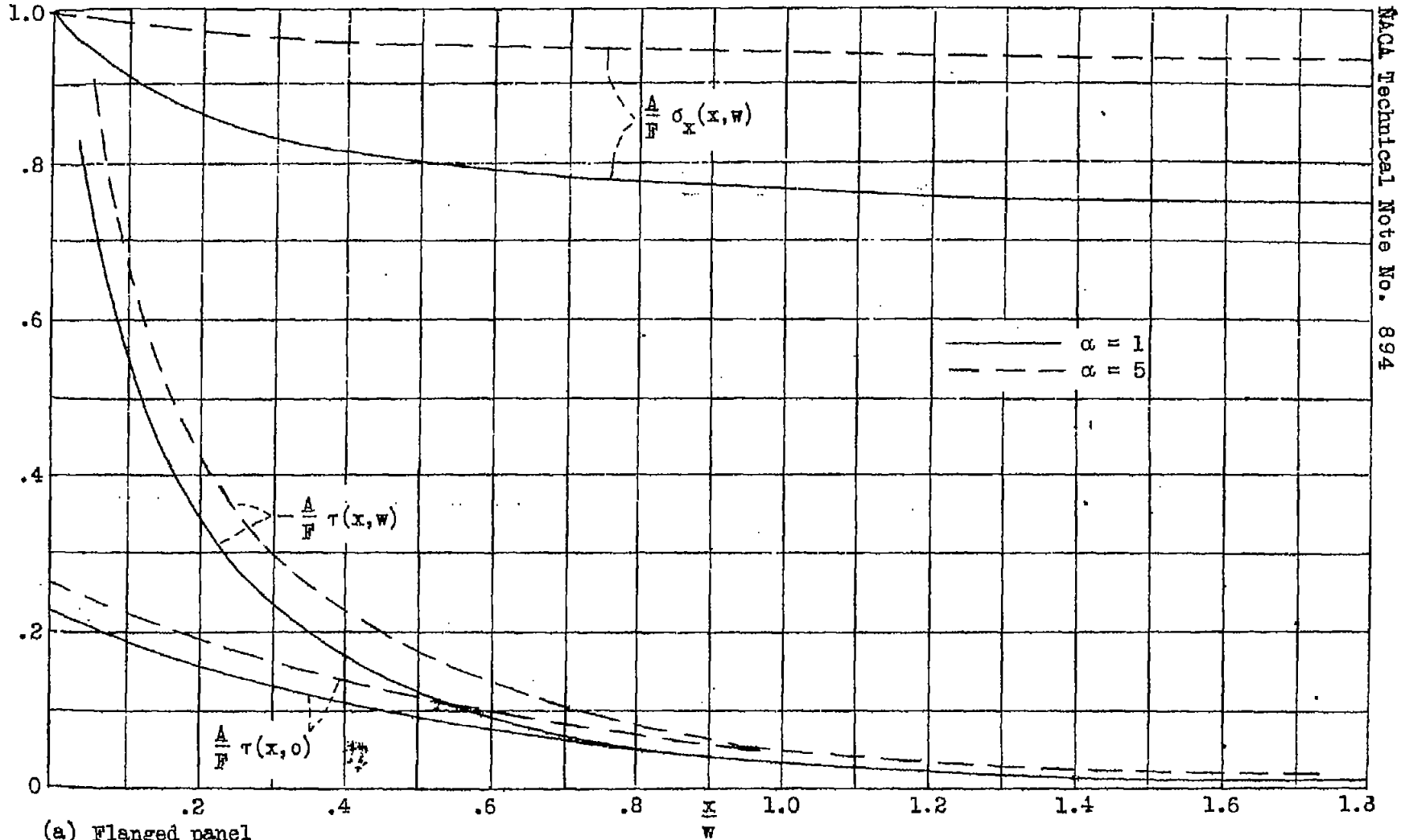

(a) Flanged panel

Figure 6.- Stresses in panel 2.

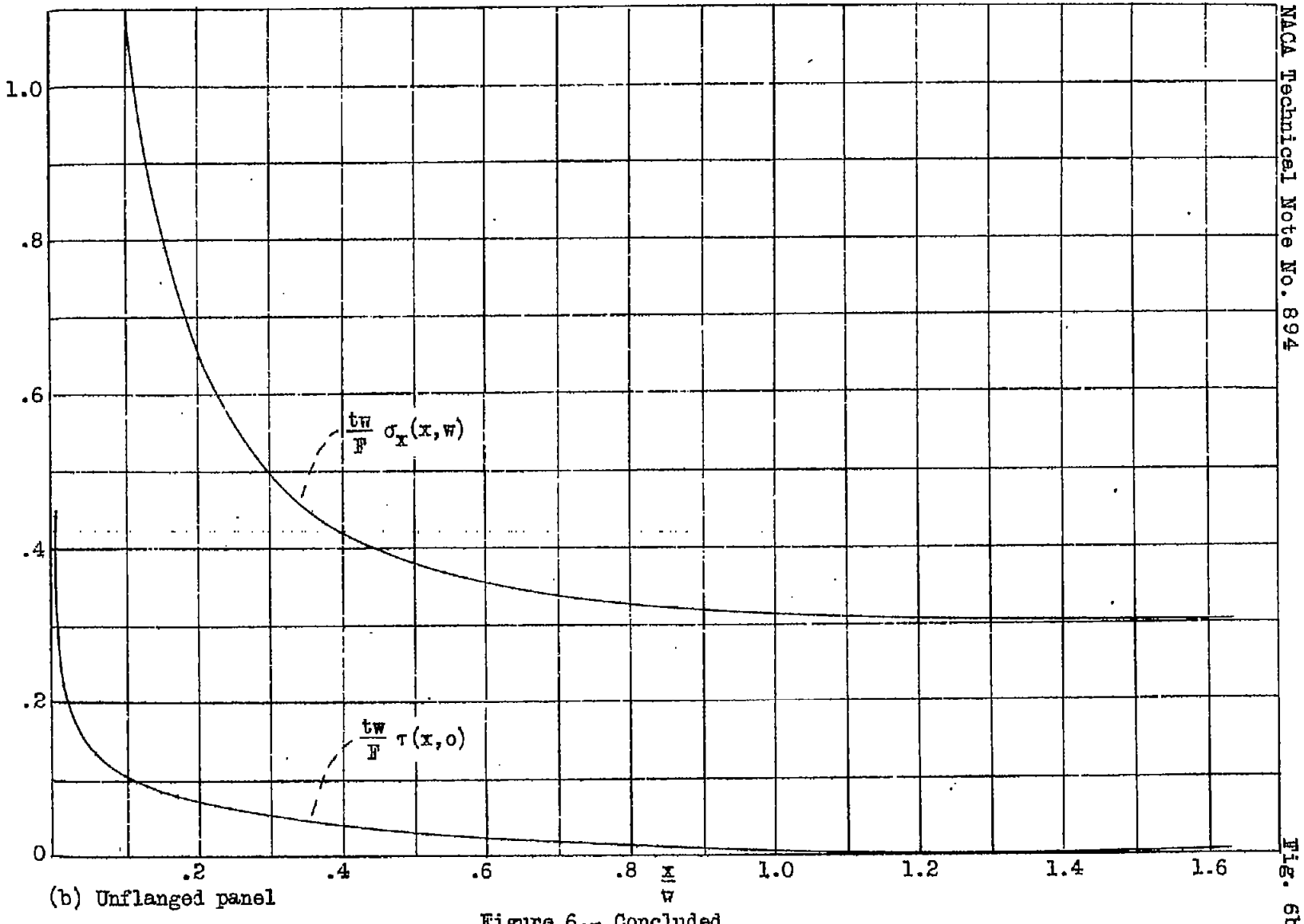

(b) Unflanged panel

Figure 6.- Concluded

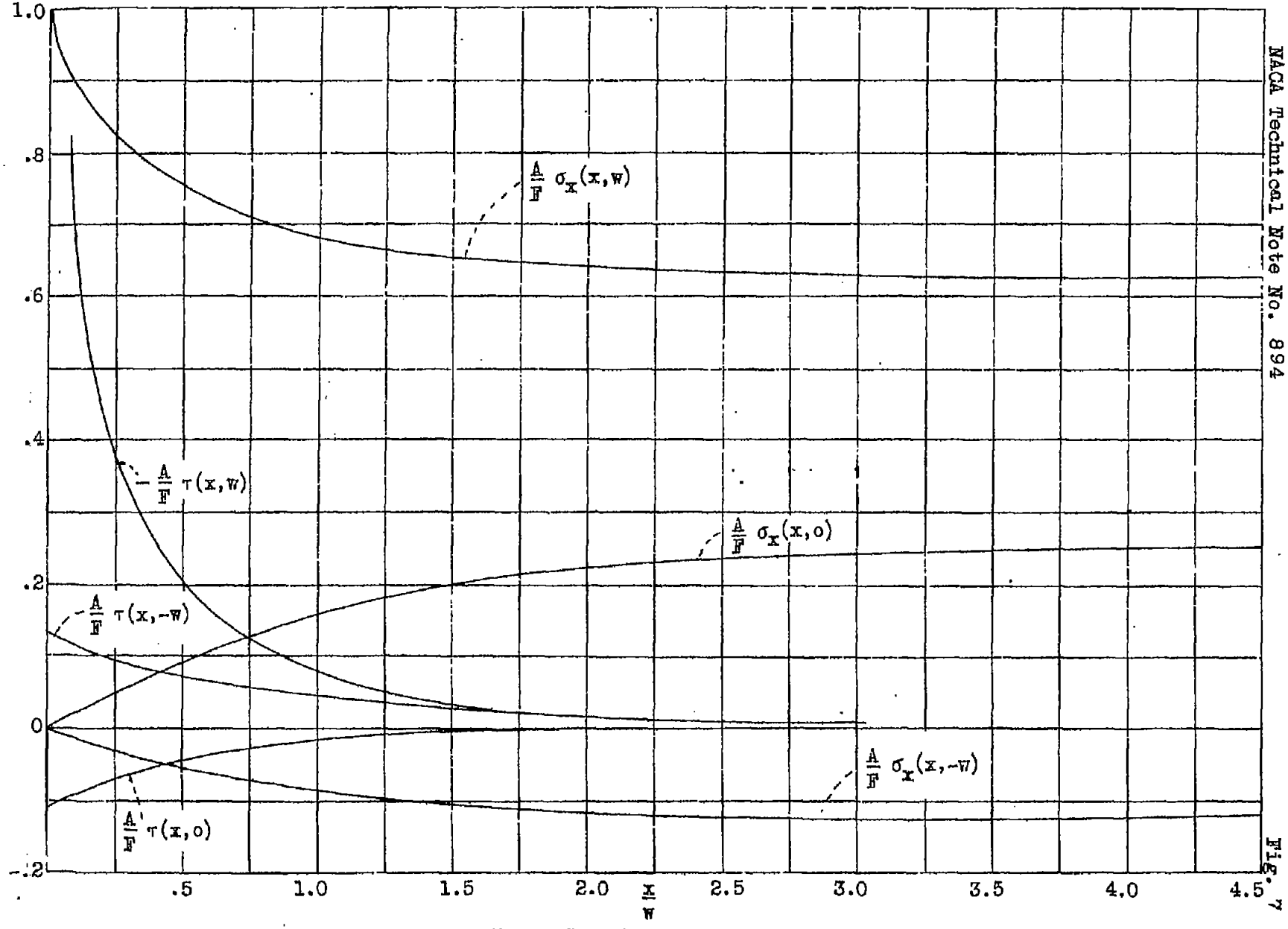

Figure 7.- Stresses in panel 3. $\alpha = 1$.

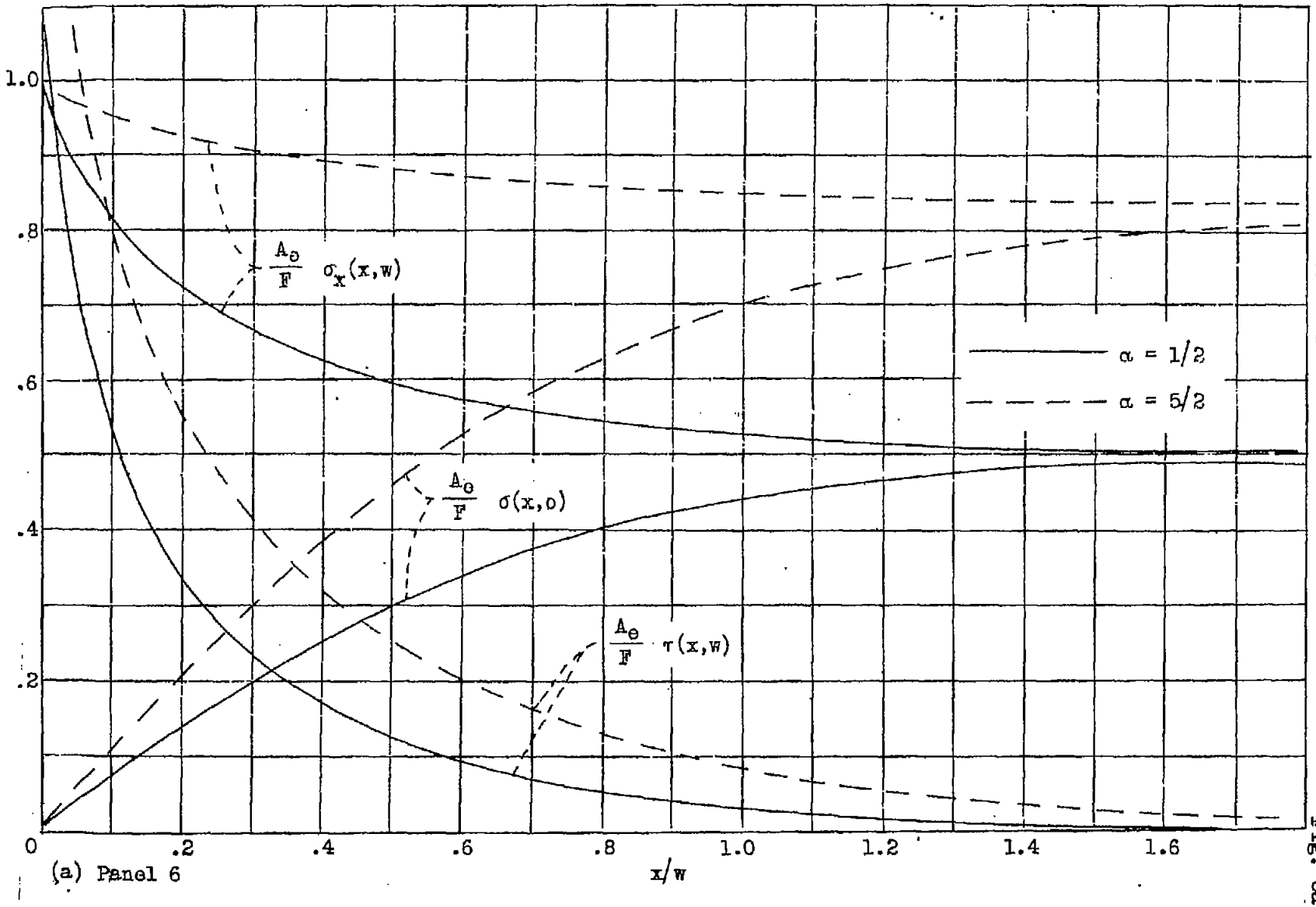

Fig. 8a

Figure 8.- Stresses in panels 6 and 7.

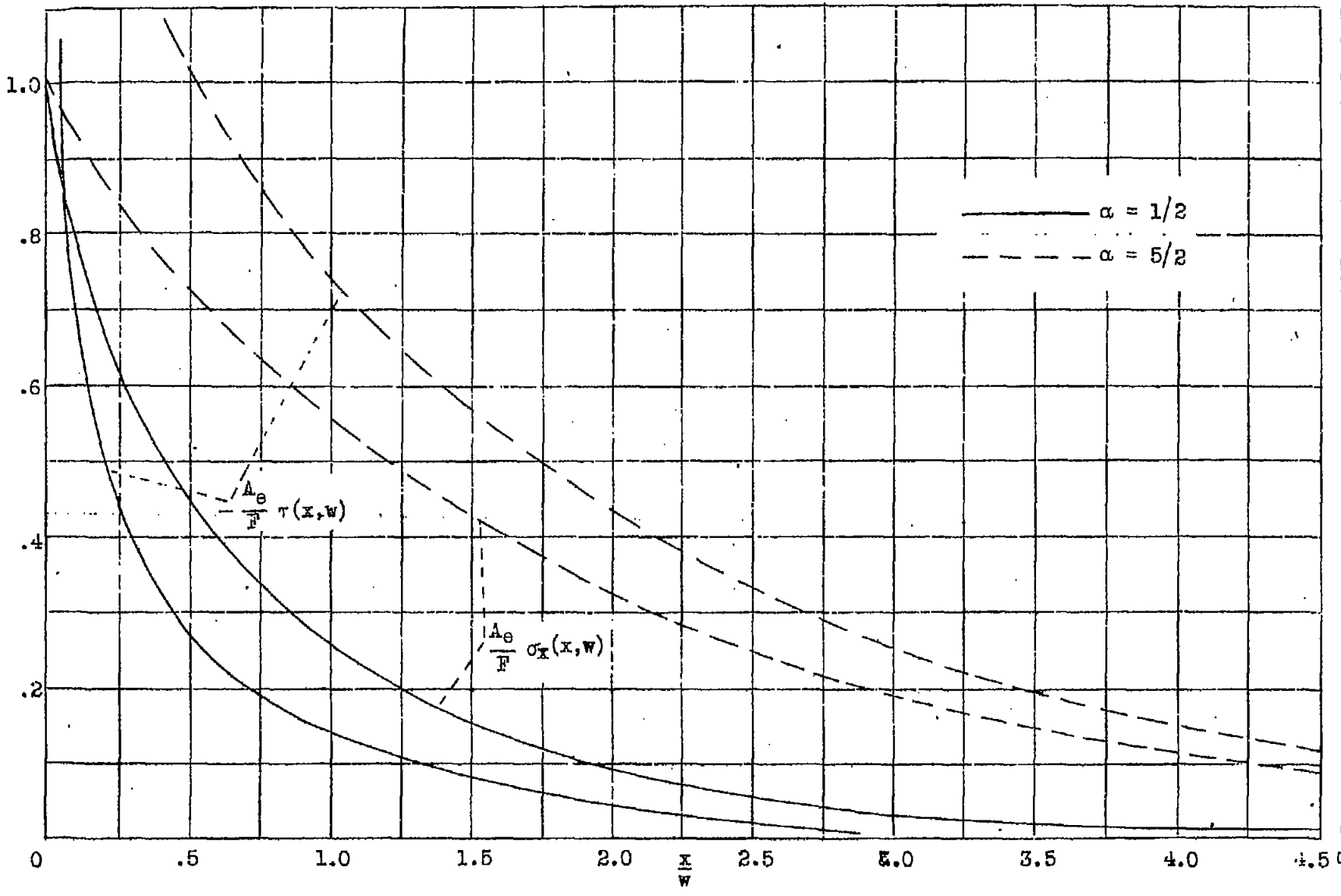

(b) Panel 7.

Figure 8.- Concluded.

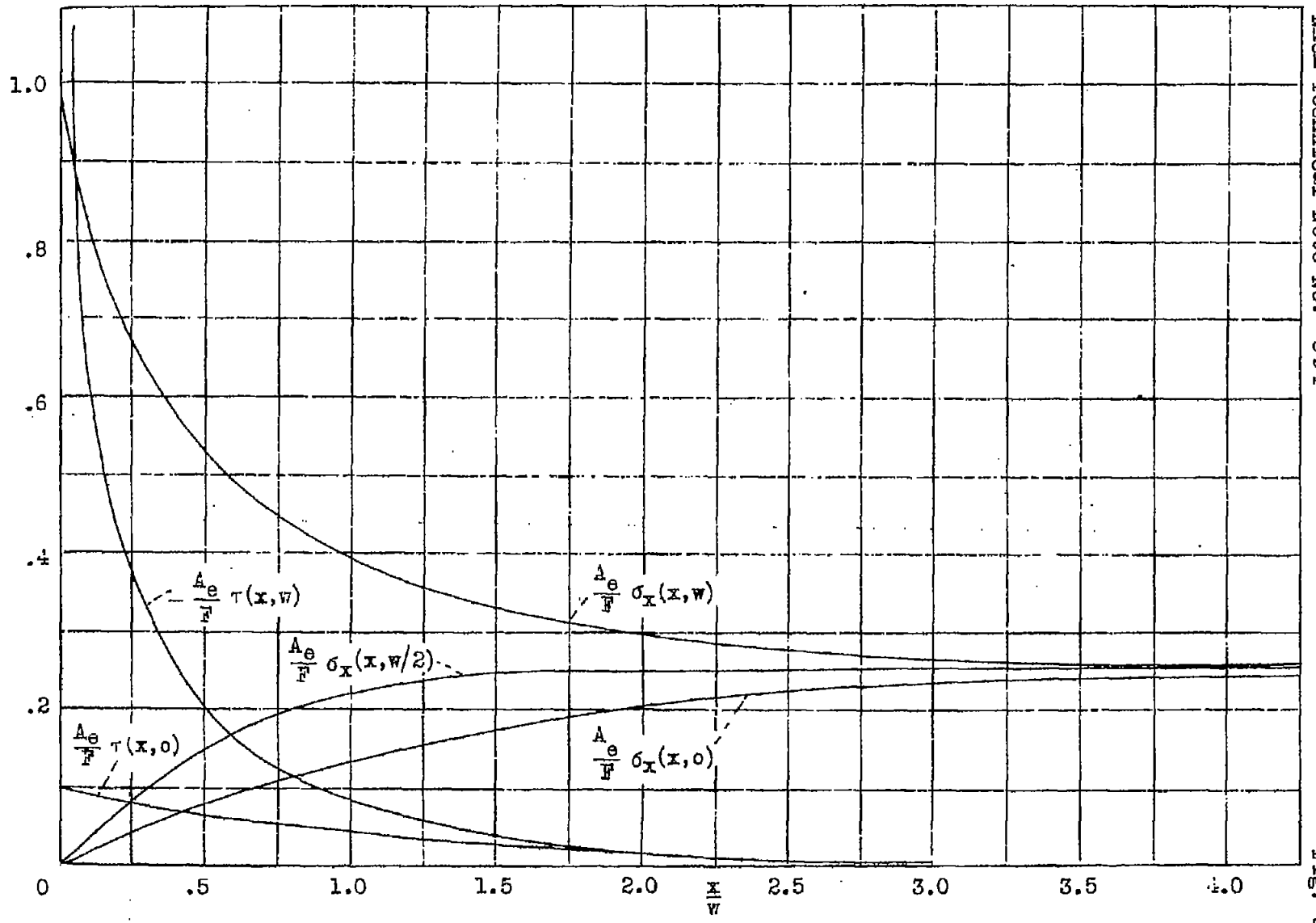

(a) $\alpha = 1/2$.

Figure 9.- Stresses in panel 8.

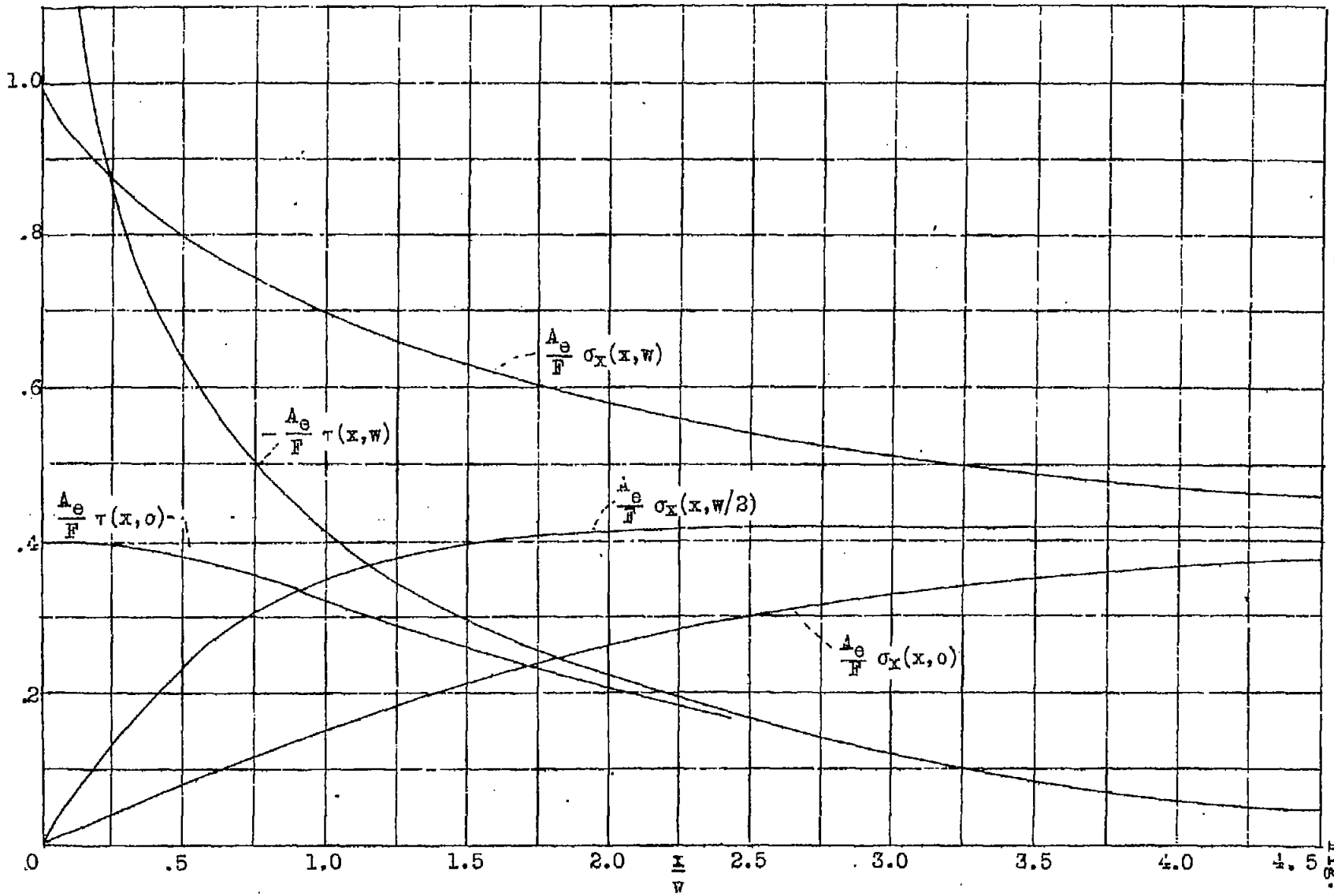

(b) $\alpha = 5/2$.

Figure 9.- Concluded.

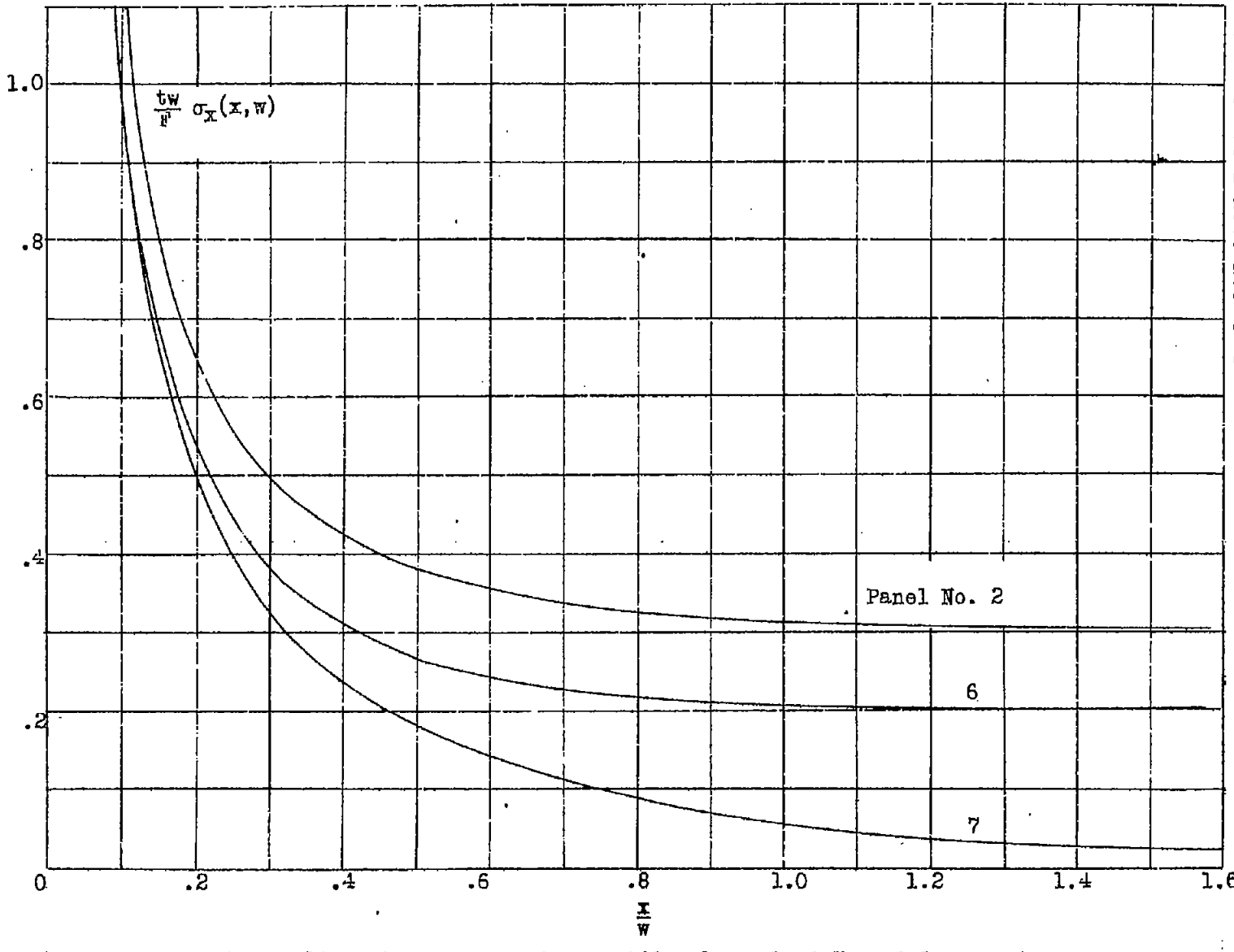

Figure 10.- Edge stresses in unstiffened panels 6,7, and 2. $\alpha = 0$.

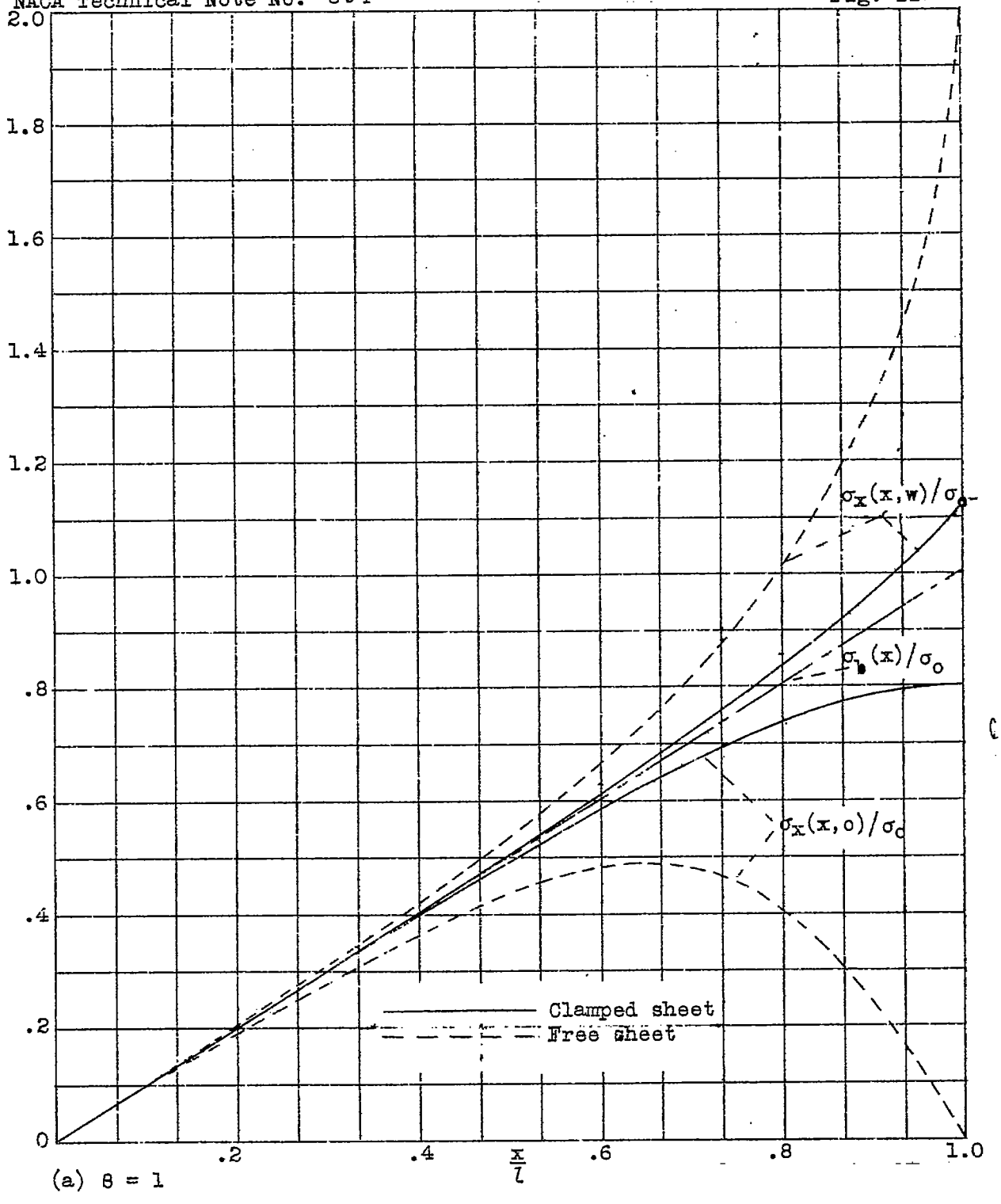

Figure 11.- Stresses in cover sheets of box beams with and without cut-out. $l = 5w$.

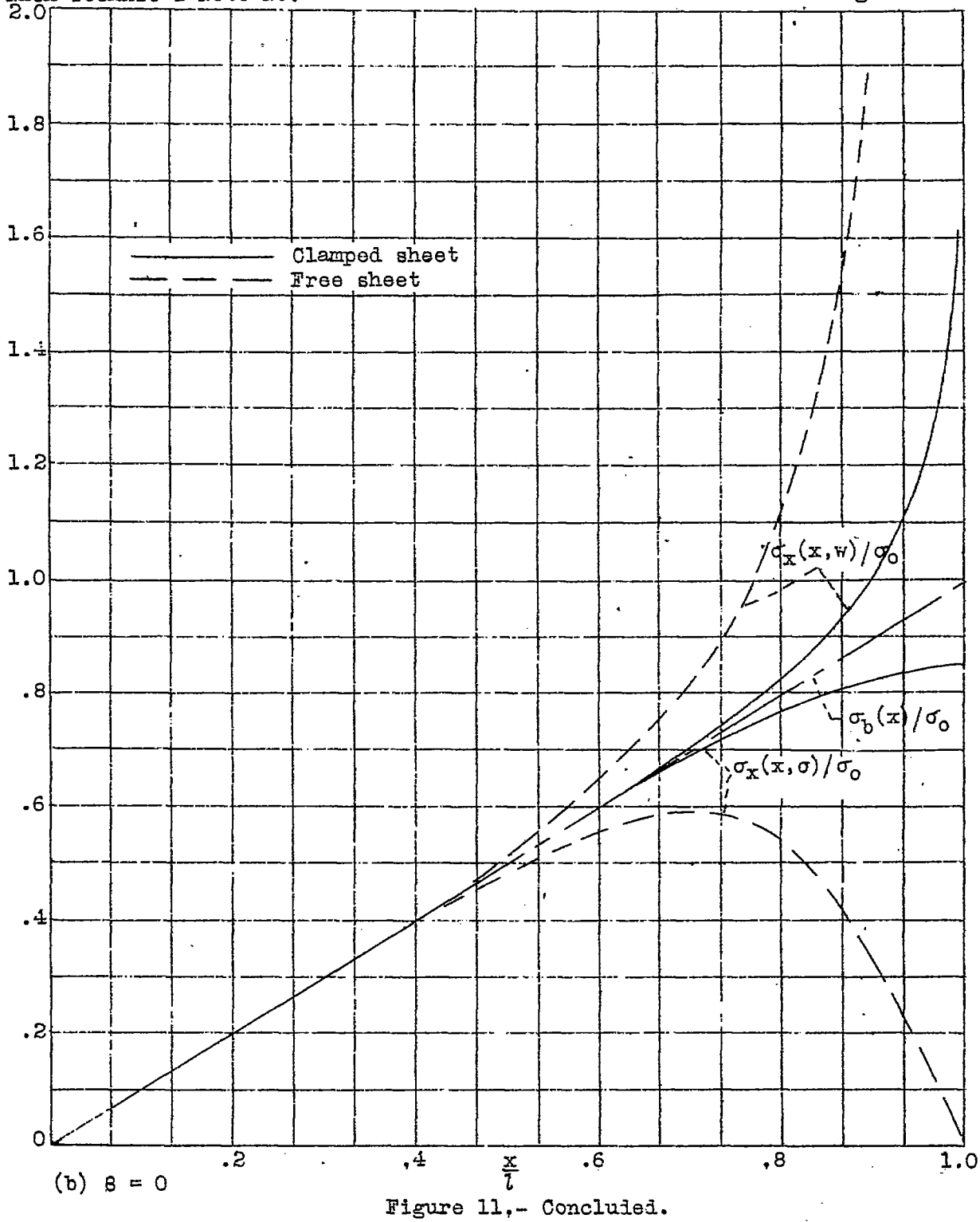

(b) $\beta = 0$

Figure 11.- Concluded.

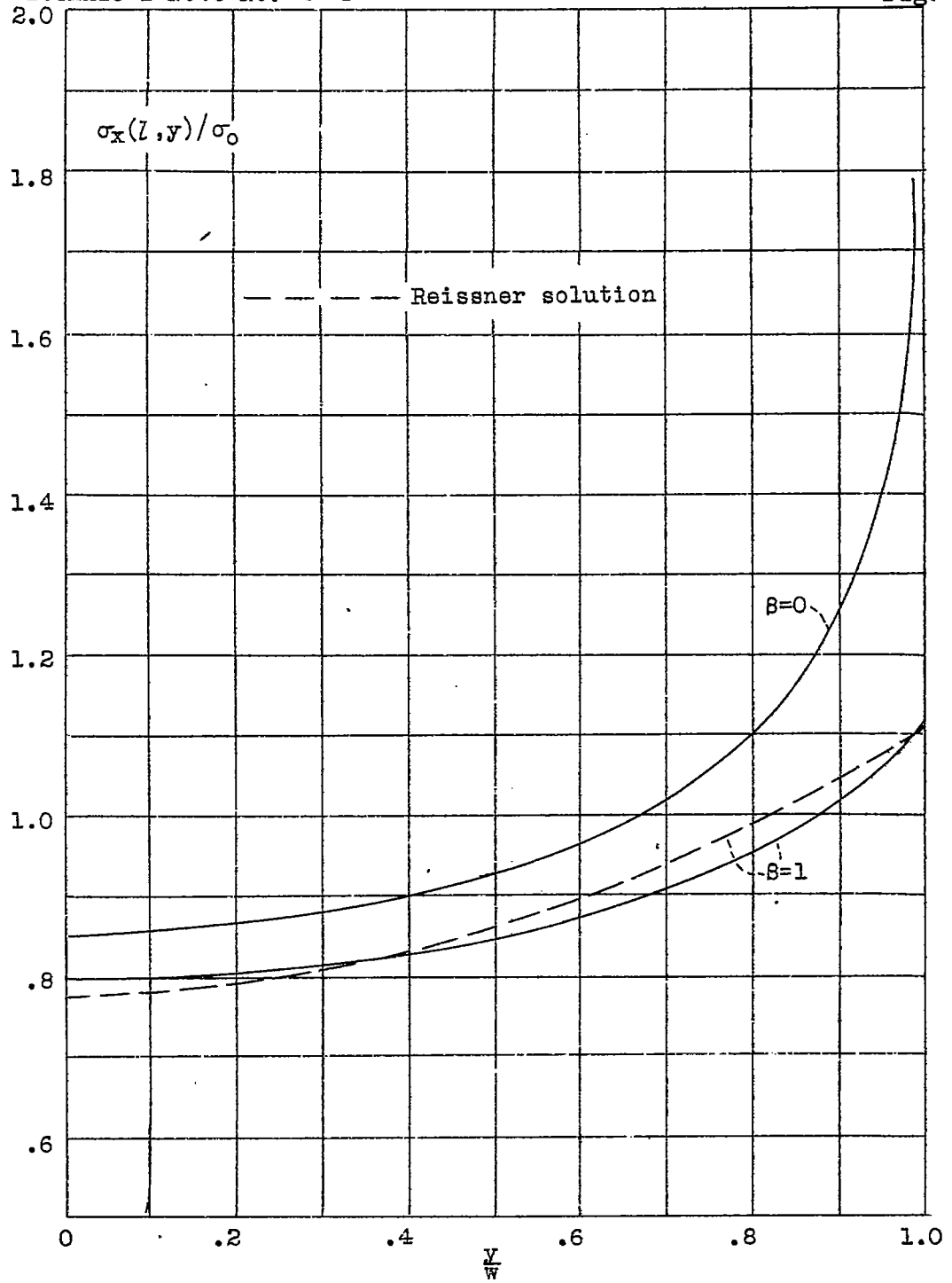

Figure 12.- Transverse distribution of root normal stress for box beam without cut-out. l = 5w.

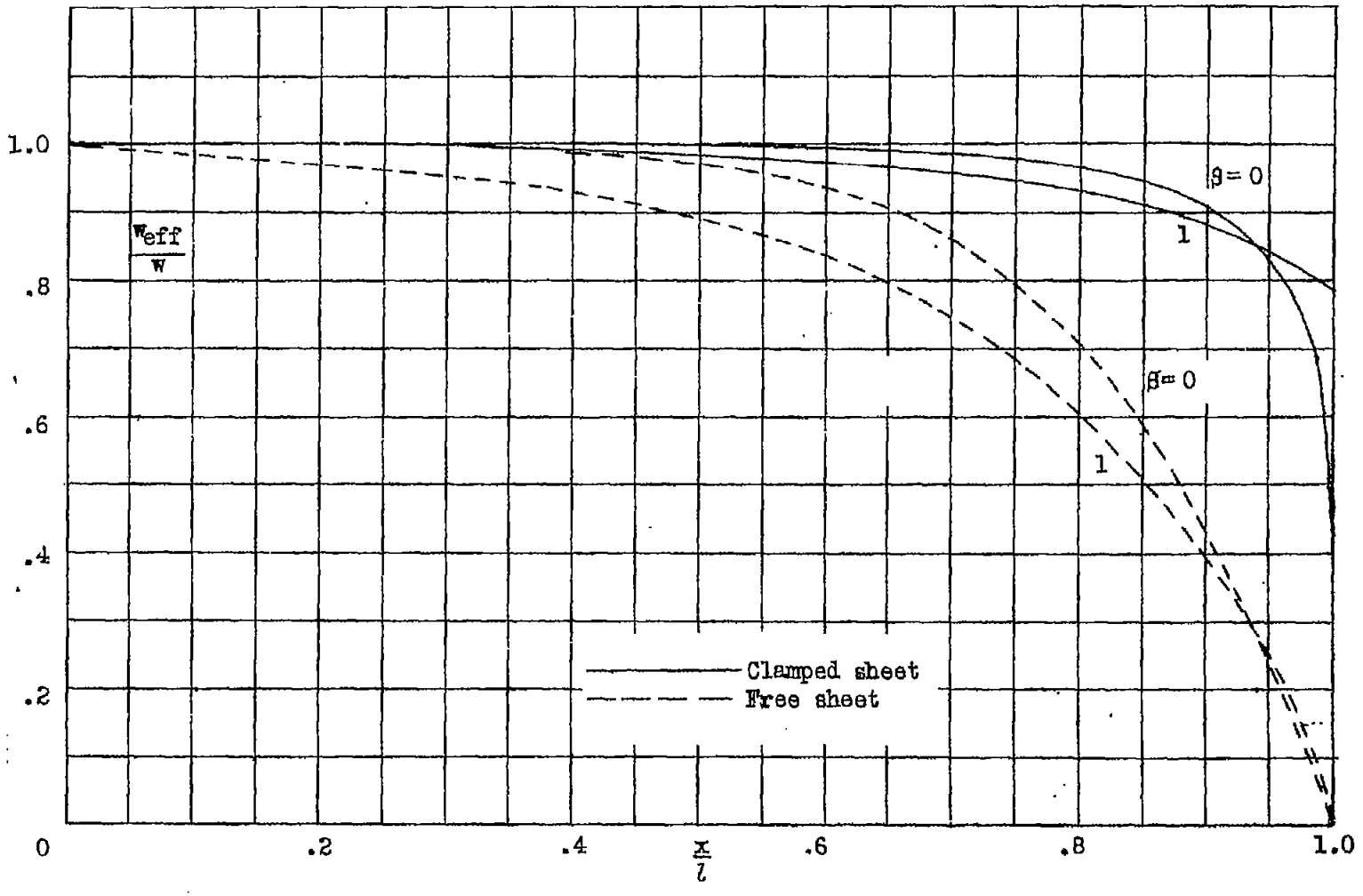

Figure 13.- Spanwise variation of cover-sheet effective width for box beams with and without cut-outs. $l = 5w$.

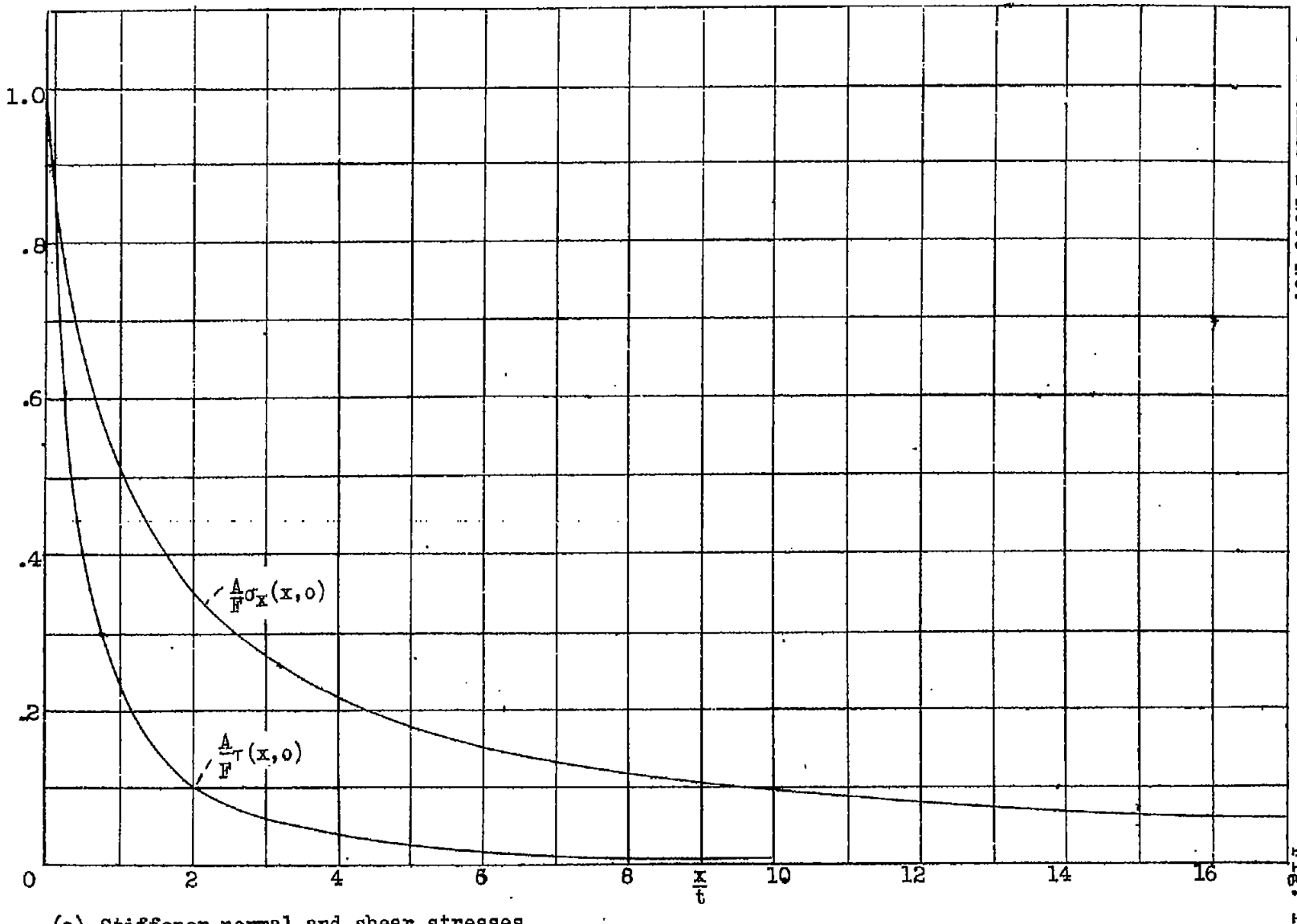

(a) Stiffener normal and shear stresses.

Figure 14.- Stresses in stiffened half-sheets.

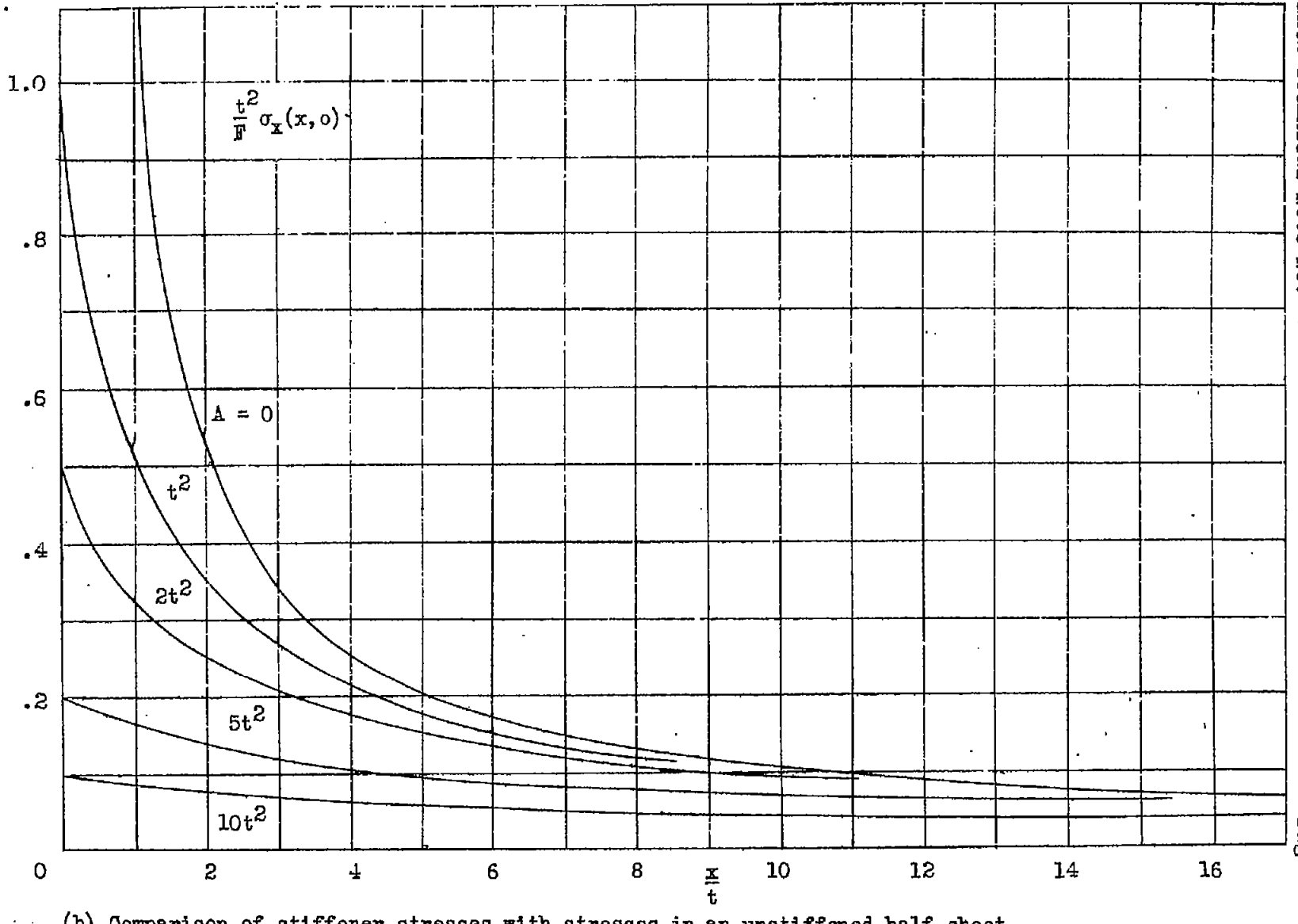

(b) Comparison of stiffener stresses with stresses in an unstiffened half-sheet.

Figure 14.- Concluded.

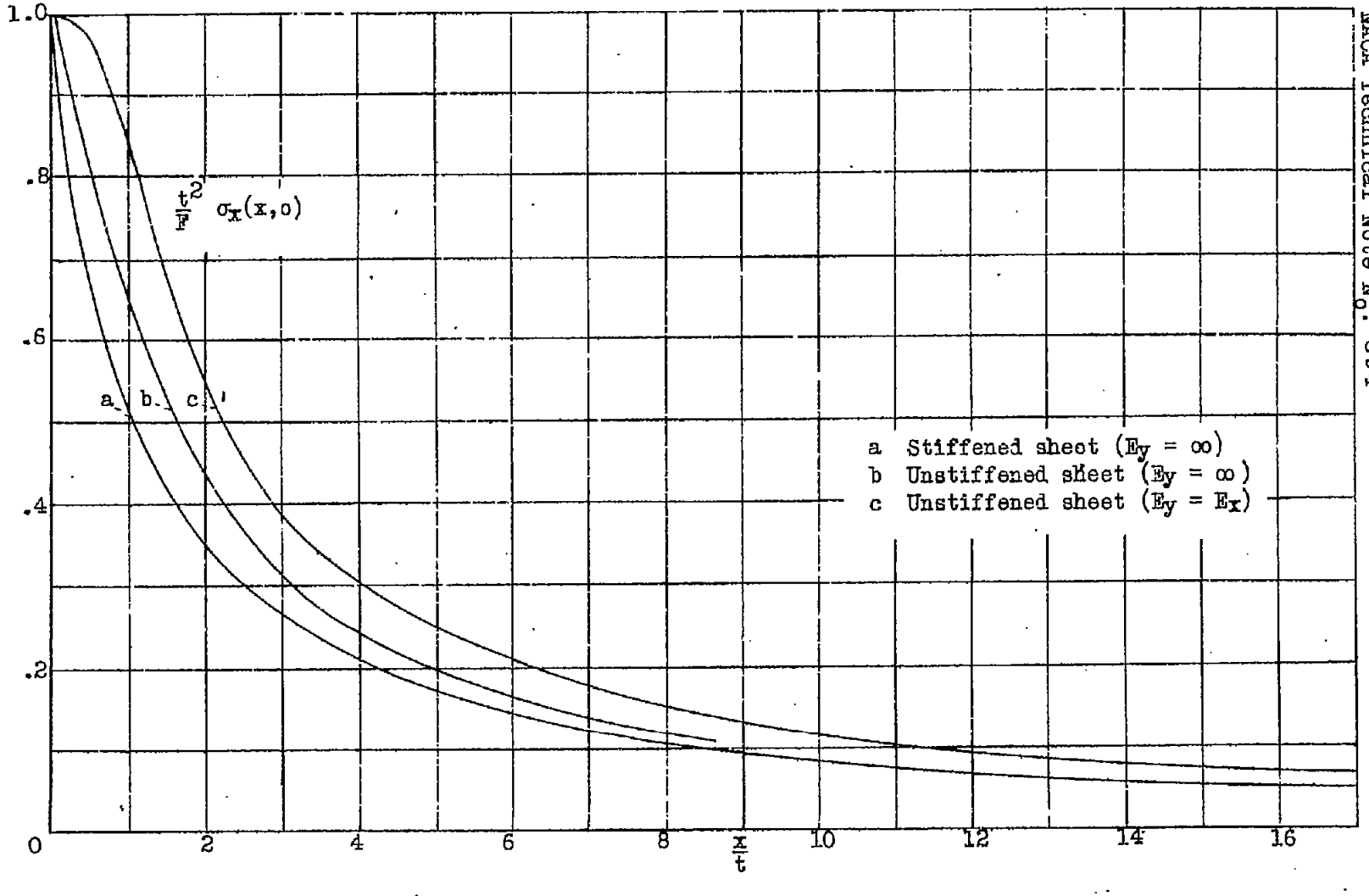

Figure 15.- Comparison of normal stress distributions in stiffened and unstiffened half-sheets.

Fig. 15

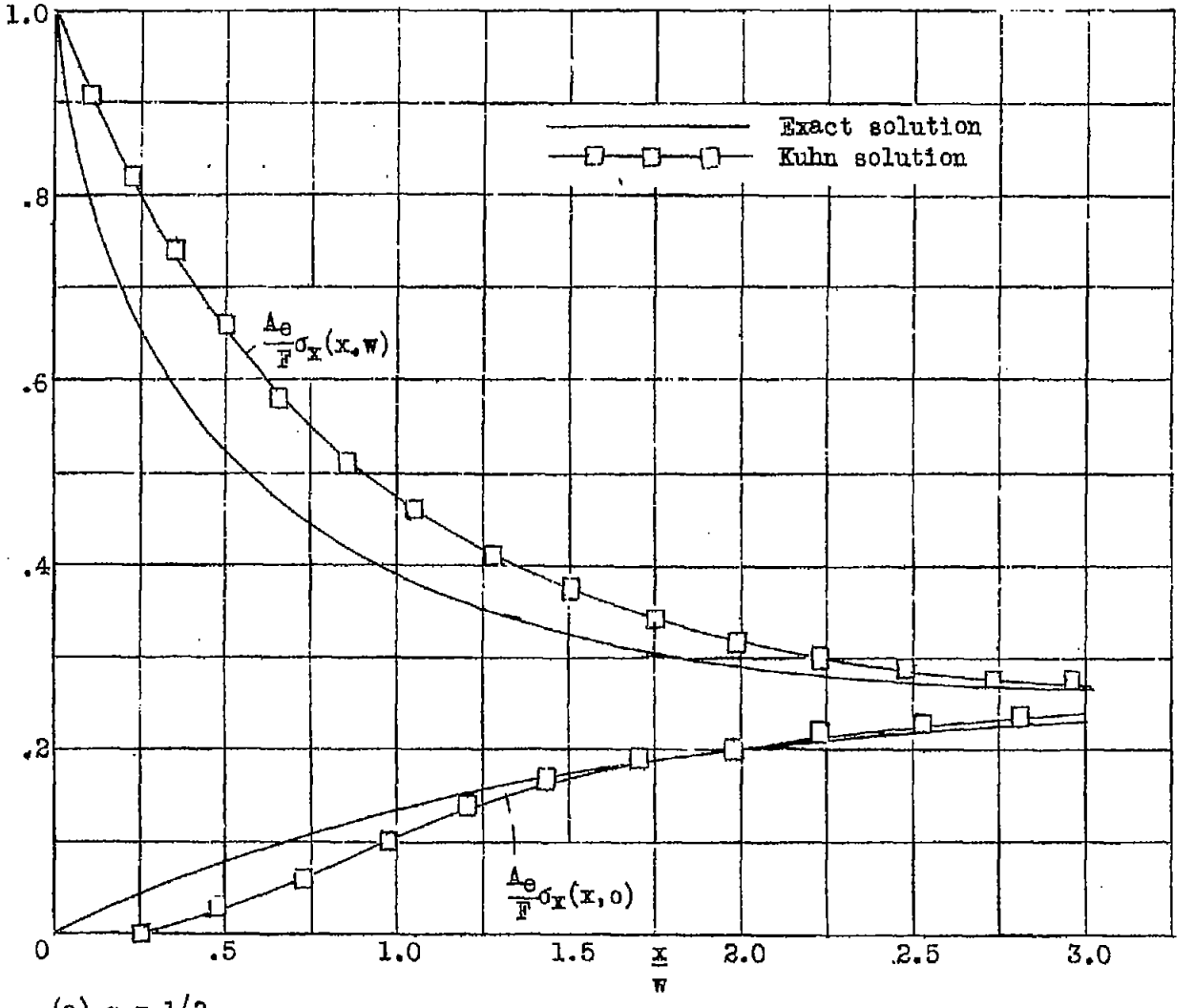

(a) $\alpha = 1/2$.

Figure 16.- Comparison of stress distributions predicted by the exact procedure and by the Kuhn procedure for panel 8.

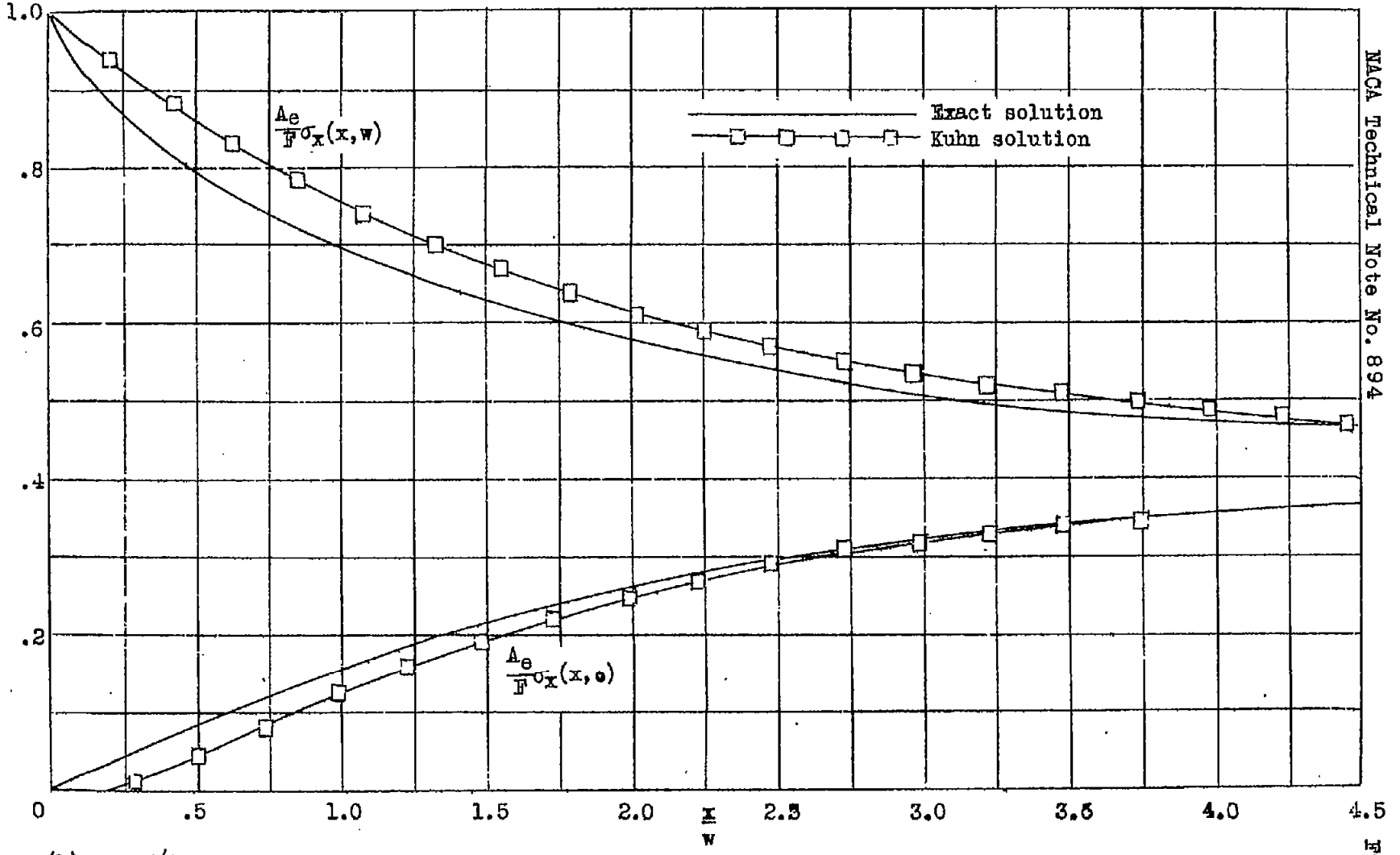

(b) $\alpha = 5/2$.

Figure 16.- Concluded.

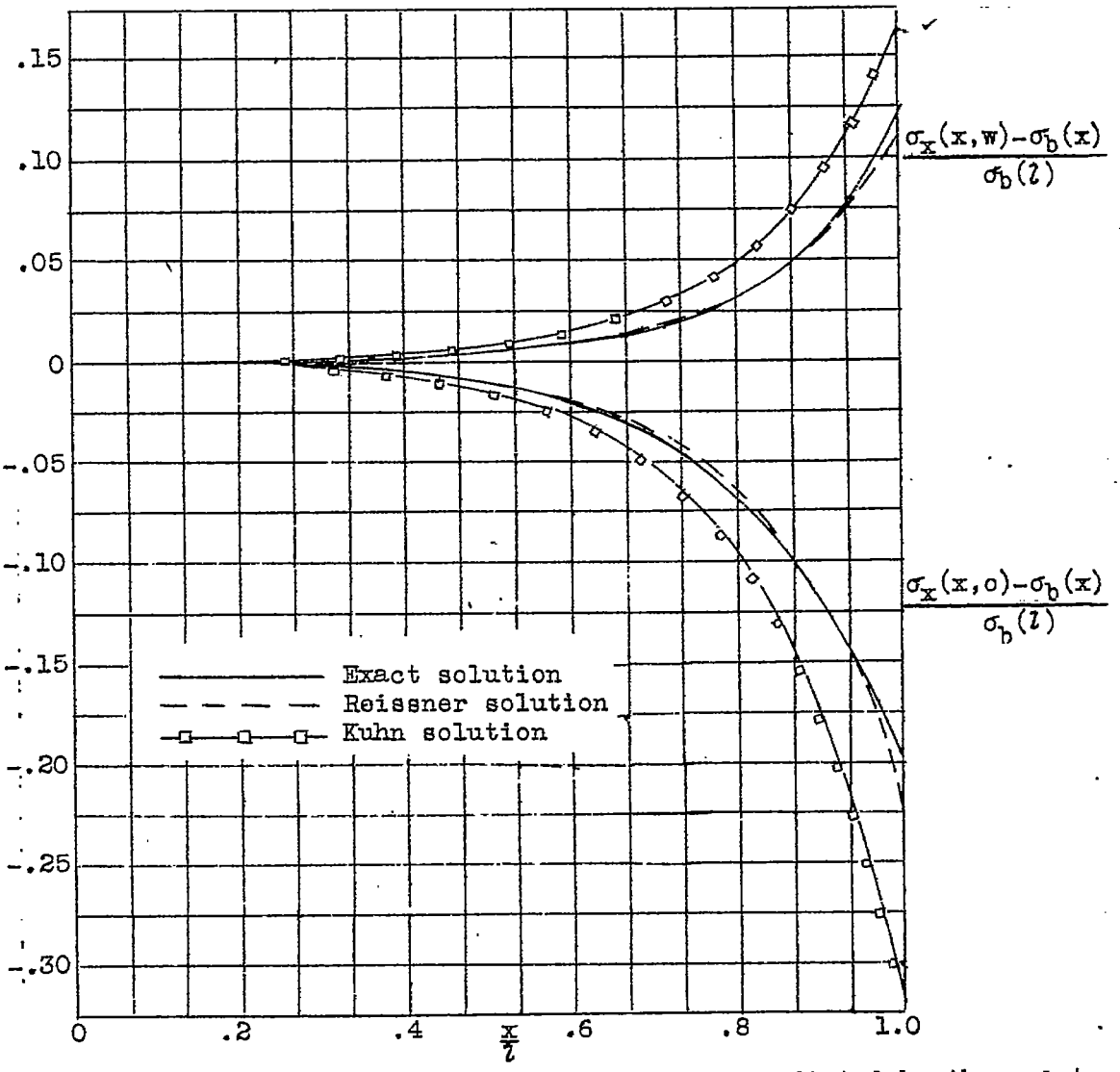

Figure 17.- Comparison of stress distributions predicted by the exact procedure, the Reissner procedure, and the Kuhn procedure for a box beam without cut-out. $\beta = 1$; $l = 5w$.

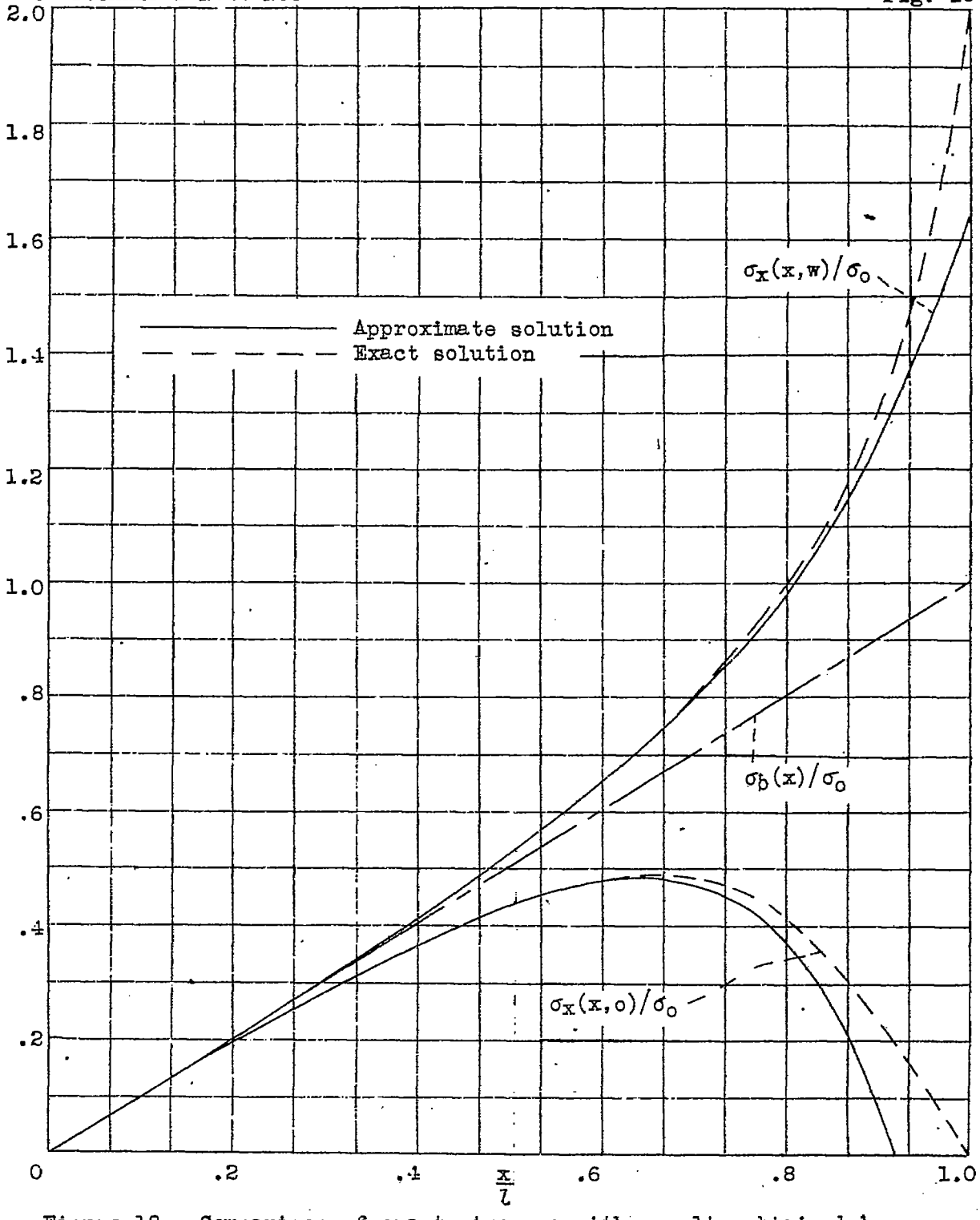

Figure 18.- Comparison of exact stresses with results obtained by retaining only one term of the series in the exact solution for a box beam with cut-out. $\beta = 1$; $l = 5w$.

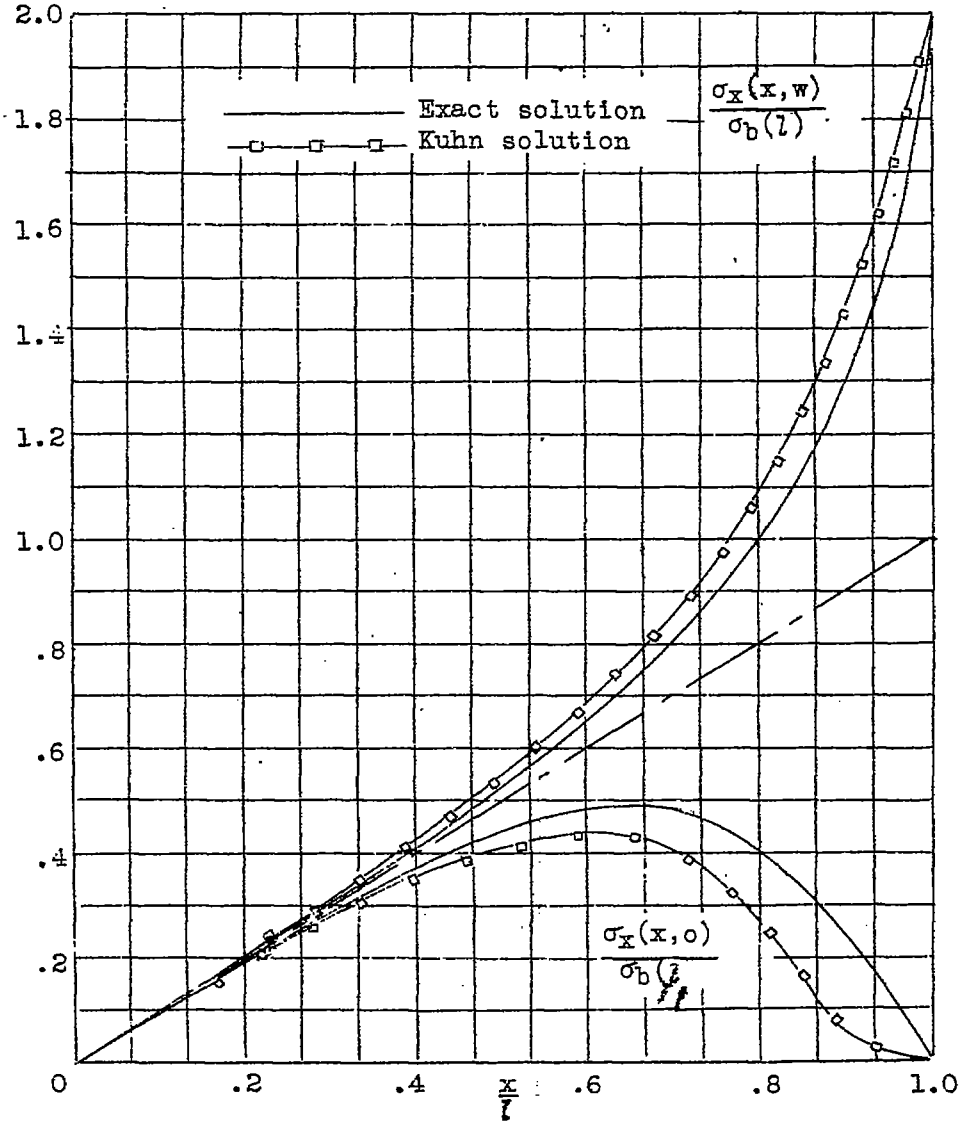

Figure 19.- Comparison of Kuhn solution with exact solution for a box beam with cut-out. $\beta = 1$; $l = 5w$.

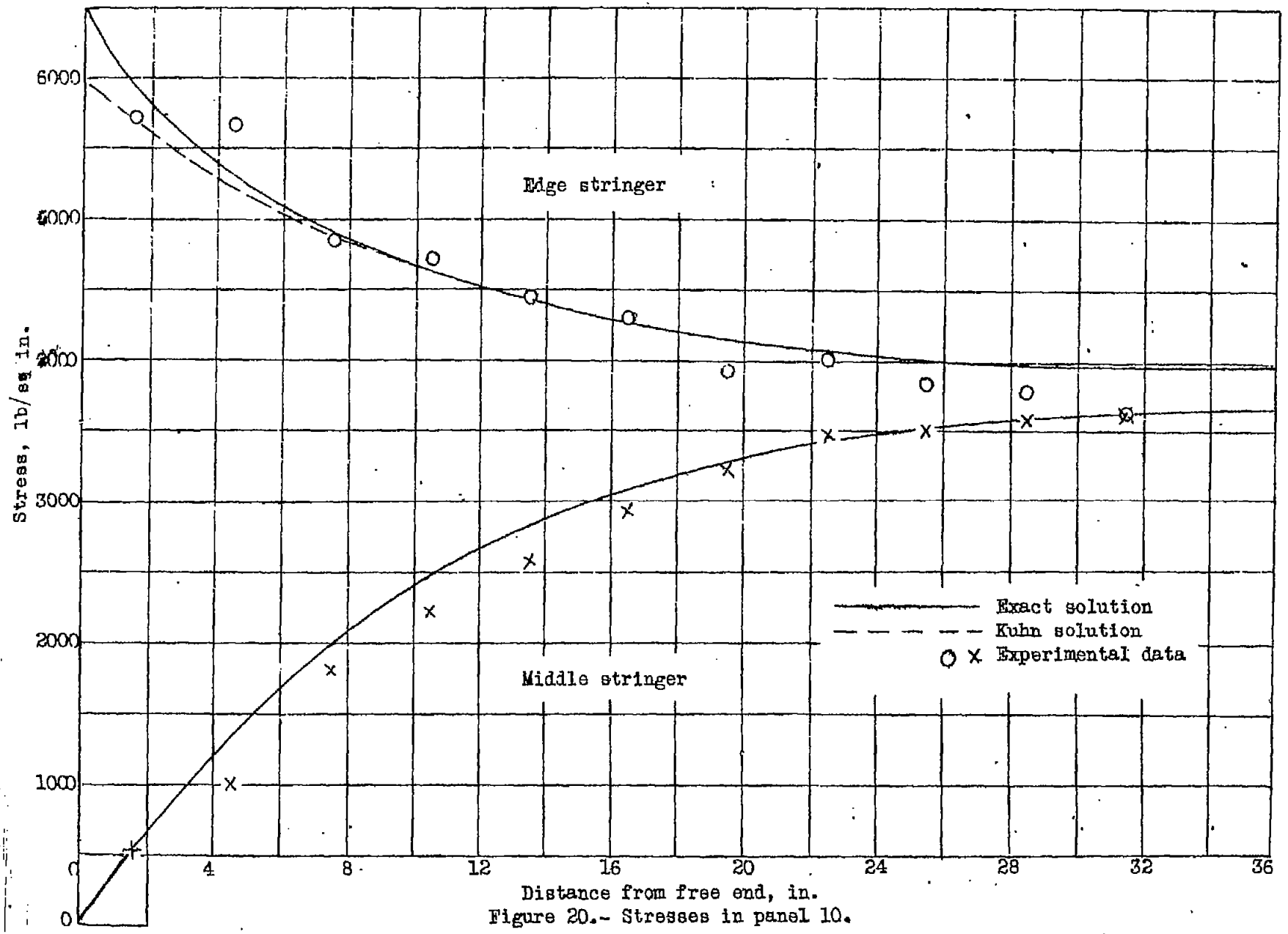

Figure 20.- Stresses in panel 10.